CryoSat Mission and Data Description

•

ESTEC
Noordwijk
The Netherlands

•

2 Jan 2007

•

Change Record

Issue	Date	Page	Description of Change
Draft 1	7 Sep 2001	All	Initial Issue to Project and SAG
Draft 2	9 Nov2001	All	Update following SAG comments
1	16 Nov 2001		Minor corrections prior to AO release
2	15 Dec 2003	All	Thorough revision prior to Data AO release
3	2 Jan 2007	All	Update for the rebuild of CryoSat

Table of Contents

1 Introduction

1.1 Purpose and Readership

The purpose of this document is to provide information about the CryoSat mission and its implementation. The level of detail is intended to be such that potential users, and other scientists, will be in a position to understand the capabilities and limitations of the system as well as the nature of the information it will deliver. We have attempted to structure the document in a way which will be accessible to the intended readership.

Chapter 2, "Mission Objectives", which is a highly condensed extract of the *CryoSat Mission Requirements Document* [Ref. 1] identifies the measurement objectives of the mission, and the corresponding payload complement which has been identified in order to satisfy them.

Chapter 3, "The CryoSat Mission" describes the way in which the orbital lifetime of the space segment of CryoSat has been divided into phases. It also describes the orbital characteristics.

Chapter 4, "CryoSat Space Segment" describes the measurement instruments and the associated infrastructure, which compose the CryoSat space segment, while Chapter 5, "Operations" describes how the mission will be operated.

The ground segment of the mission is described in Chapter 6, "CryoSat Ground Segment", including the generation of scientific data as well as the operational command and control.

Finally, in Chapter 7, "Data Products" and Chapter 8, "Simulated Results", the nature of the data products which will be delivered to users from the CryoSat mission is described.

We expect that the primary readership of this document will be those interested in responding to the CryoSat Announcement of Opportunity.

1.2 Context

The CryoSat mission was selected, in June 1999, as the first mission in the Earth Explorer Opportunity Mission series. During the first half of 2000 many analyses and trade-off's were performed by ESA and its industrial contractors in order to demonstrate the feasibility of the mission and to define the overall concepts. In the following year, until mid-2001, the system design was defined and specified in detail, such that procurement could begin.

In May 2001 the mission was approved by the Earth Observation Programme Board to proceed into the full development phase. Development and testing lasted just over 4 years, and in July 2005 the satellite was shipped to the launch site at Plesetsk in northern Russia.

The launch took place on 8 October 2005 but a failure in the launch vehicle led to a shutdown of the launcher system just prior to separation of the second and third stages, at a height of over 200 km. Subsequently the stack of launcher stages and CryoSat followed a ballistic trajectory which re-entered the atmosphere at about 5 km/sec. This re-entry led to total destruction of the entire stack, with the debris falling some 100 km from the North Pole.

Following the failure authorisation to rebuild the satellite as CryoSat-2 was given by ESA's Earth Observation Programme Board on 24 February 2006. Launch is foreseen in March 2009.

2 Mission Objectives

Despite the upheaval in implementation following the launch failure the CryoSat mission objectives remain unchanged and ESA's Earth Science Advisory Committee (ESAC) confirmed they are more relevant now than when the mission was first selected in 1999. A full description of these mission objectives is provided in the *CryoSat Mission Requirements Document* [Ref. 1] and further information about the scientific exploitation of the mission is provided in the *CryoSat Calibration and Validation Concept* [Ref. 2]. A full description in the open literature has been given by Wingham *et al* (2006) [Ref. 3].

2.1 Measurements and Requirements

The CryoSat mission has been defined in order to determine fluctuations in the mass of the Earth's major land and marine ice fields. Predicting future climate and sea level depends on knowledge of these fluctuations, but present observations are deficient in time and space. Satellite observations are the unique source of these measurements at large space and time-scales. The goals of CryoSat are to measure variations in the thickness of perennial sea and land ice fields to the limit allowed by natural variability, on spatial scales varying over three orders-of-magnitude. The natural variability of sea and land ice depends on fluctuations in the supply of mass by the atmosphere and ocean, and snow and ice density. CryoSat measurement requirements are determined from estimates of these fluctuations.

The measurement requirements of the CryoSat system have been formulated in terms of the uncertainty in the measurement of perennial ice thickness change due to all contributing elements, including satellite performance, ground processing *etc.* They are expressed in units of cm yr^{-1} over certain specific averaging areas.

Over sea ice the averaging area of interest is 10^5 km^2 and a minimum latitude of 50° is assumed; the required system measurement uncertainty is 1.6 cm yr^{-1}.

Over ice-sheet margins an averaging area of 10^4 km^2 and a minimum latitude of 72° is assumed, being sufficient to cover the margins of Antarctica; the required system measurement uncertainty is 3.3 cm yr^{-1}.

Over the interiors of the ice-sheets the averaging area is 13.8 x10^6 km^2 (the surface area of Antarctica) and a minimum latitude of 63° is assumed which will include all of Antarctica and most of Greenland; the required system measurement uncertainty in this case is 0.7 cm yr^{-1}.

The CryoSat system is required to perform measurements over three full years in order to establish secular trends. A summary of these requirements is provided in Table 2.1–1. Mission requirements expressed in this way cannot be used to specify the performance of a satellite system. They must be broken down into lower level requirements on the space and ground segment, during which a number of assumptions have to be made. This requirement traceability into performance requirements on the space and ground segment is provided in the *CryoSat Mission Requirements Document* [Ref. 1].

2.2 The Measurement System

Much progress has been made in the determination of mass fluxes, in some special cases, by the use of radar altimeter data from ERS-1 and ERS-2. In order to extend these results to regions extensively covered by sea-ice and to the margins of the ice sheets, respectively, it is necessary to improve the spatial resolution of the altimeter measurement system.

Table 2.1–1 CryoSat measurement requirements, extracted from (Ref. 1).

Surface	Area	Minimum Latitude	Measurement Requirement
Sea Ice	10^5 km^2	50°	1.6 cm yr^{-1}
Ice Sheets	10^4 km^2	72°	3.3 cm yr^{-1}
Ice Sheets	13.8×10^6 km^2	63°	0.7 cm yr^{-1}

The required measurement technique for CryoSat is thus a high spatial resolution radar altimeter. The addition of a synthetic aperture and interferometry to conventional altimeters, such as the EnviSat RA-2 or Poseidon instruments, provides an altimeter which will meet the science requirements. This approach and the resulting performance are unique to CryoSat.

The primary payload of CryoSat is a radar altimeter with these additional capabilities. It is fully described in Section 4.1. This radar is capable of operating in a number of modes, optimised for measurements over different surfaces. A conventional, pulse-width limited, low-resolution mode will provide the measurements over the central regions of the ice sheets, to continue the ERS and EnviSat measurement series. This mode will also be used over oceans where possible (operations concepts and constraints are described in Section 5). The SAR mode will enable an enhancement of the spatial resolution along-track, and this mode will be used over sea-ice to enable measurements over relatively narrow leads of open water which would be indistinguishable in low-resolution mode. Over the topographic surfaces of the ice-sheet margins this SAR mode will be enhanced by interferometric operation across-track so that the arrival angle of the echoes may be measured.

The radar altimeter is supplemented by some other payload elements which are necessary in order to achieve the mission goals. The orientation of the interferometric baseline needs to be very accurately measured in-flight: small errors in knowledge of the roll-angle translate into substantial errors in the elevation of off-nadir points. Thus the payload includes a set of star trackers rigidly attached to the interferometer. These enable the absolute determination of the orientation of the baseline to be established in the celestial reference frame.

As with any altimeter satellite the accurate determination of the orbit is essential to allow the transformation of the measured range into a determination of surface elevation. This Precise Orbit Determination (POD) requires modelling of the forces acting on the satellite as well as a dense set of measurements of the position or velocity of the satellite. The primary means of making these measurements is with the DORIS receiver which makes measurements of the relative velocity to an extensive network of ground beacons. This system has been flown on a number of existing satellites and is a fully operational system. These velocity measurements will be supplemented by measurements of range from ground-based Satellite Laser Ranging (SLR) stations to the laser retroreflector on board. Finally, the low-resolution altimeter measurements over oceans, particularly at orbit cross-overs, will provide an additional measurement type.

3 The CryoSat Mission

3.1 Mission Phases

3.1.1 Launch and Early Orbit Phase

The new CryoSat-2 spacecraft will be launched by a Rockot launcher: the same type used for the original CryoSat. This decision has been made following an exhaustive review of the previous failure and associated improvements in the launcher preparation.

At the start of the CryoSat mission the satellite will be in the Launch and Early Orbit Phase (LEOP). This begins, before the launch itself, with the switch-over from ground-supplied power to the satellite internal batteries and includes the launch, separation, attitude acquisition and initial switch-on. The nominal planning is that this phase will take less than 24 hours; however, contingency planning allows up to a week of intensive support from a network of extra ground stations.

Launch will take place from Plesetsk, some 800 km north of Moscow, using a Rockot launch vehicle. This consists of the booster stages of an SS-19 missile and versatile, re-startable upper stage, the Breeze-KM. Figure 3.1–1 shows the launch of GRACE on 17 Mar 2002 using this launch vehicle – the CryoSat launch will be very similar except that it will occur in the early evening. This Figure also shows an artists impression of the fairing release during the powered flight. A photograph of the CryoSat launch is shown in Figure 3.1–2. As this launch took place in darkness no detailed view of the launcher (which is launched from inside a vertical tube) was possible so a time-lapse exposure was made.

Figure 3.1–1 Left: the launch of GRACE on 17 Mar 2002 using a Rockot launcher. Right: an artists impression of the release of the fairing during the second-stage flight. The Breeze-KM upper stage is within the black cylinder between the satellite and the second stage.

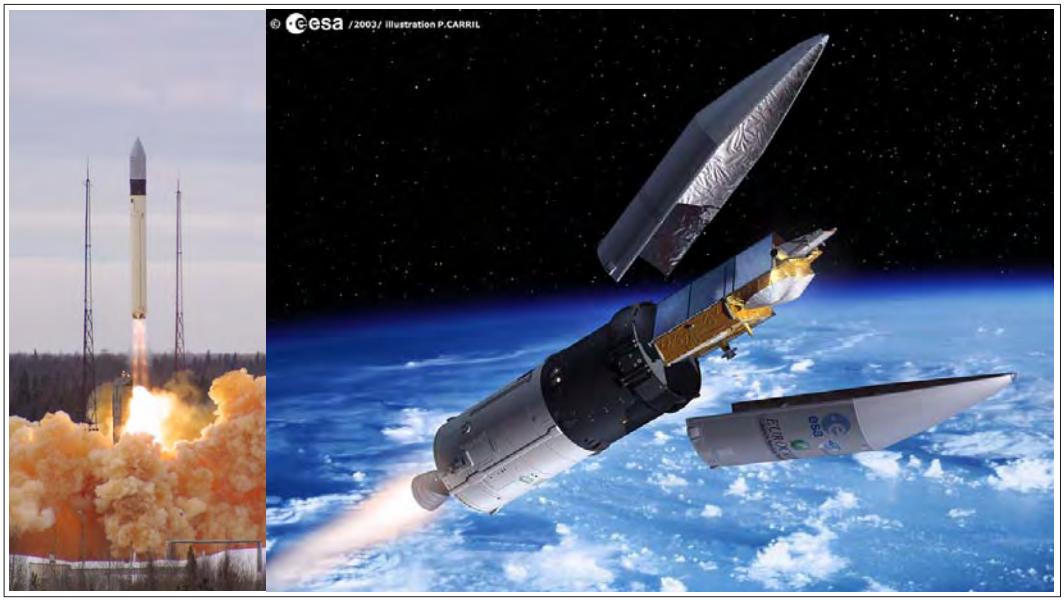

Figure 3.1–2 Photograph of the CryoSat launch on 8 Oct 2005. This launch took place in darkness so only a time-exposure is available. The failure occurred 300 seconds after launch, well after this exposure ended.

The satellite will be launched into an orbit plane which has local solar time of 1800 at the equator (loosely called the "dawn-dusk" plane) in order to maximise the available power during the LEOP. This is illustrated in Figure 3.1–3, which also shows the launch and injection sequence. CryoSat will separate from the upper stage as it comes into visibility of the Kiruna ground station, where both of the available antennas (as well as the Svalbard station) will be used for initial acquisition.

The sequence of operations following separation is based on the periods of visibility by the supporting ground stations. As the attitude control subsystem (see Section 4.8, "Attitude and Orbit Control") converges towards a stable coarse pointing mode other subsystems are switched into full operation to support the satellite autonomy. The star trackers and the DORIS receiver are switched on during LEOP as they are necessary for the (automatic) transition to fine pointing mode. At the end of the LEOP, everything on board, except the main radar altimeter will be switched on and fully operational, with the satellite in its operational pointing mode.

Orbit corrections will be performed in the few days following launch to correct for the launcher dispersion errors and acquire the nominal orbit (see Section 3.3). These corrections are asynchronous to the other operations and are constrained by the need to acquire

Figure 3.1–3 CryoSat will be launched into the "dawn-dusk" plane in which the satellite is constantly illuminated by the sun. At CryoSat's altitude this is true even at the solstice. Following the launch and initial boost phase the composite of satellite and upper stage coast for half a revolution before a second burn into the final injection orbit. Separation occurs after almost a complete revolution as the satellite comes into visibility of the Kiruna ground station.

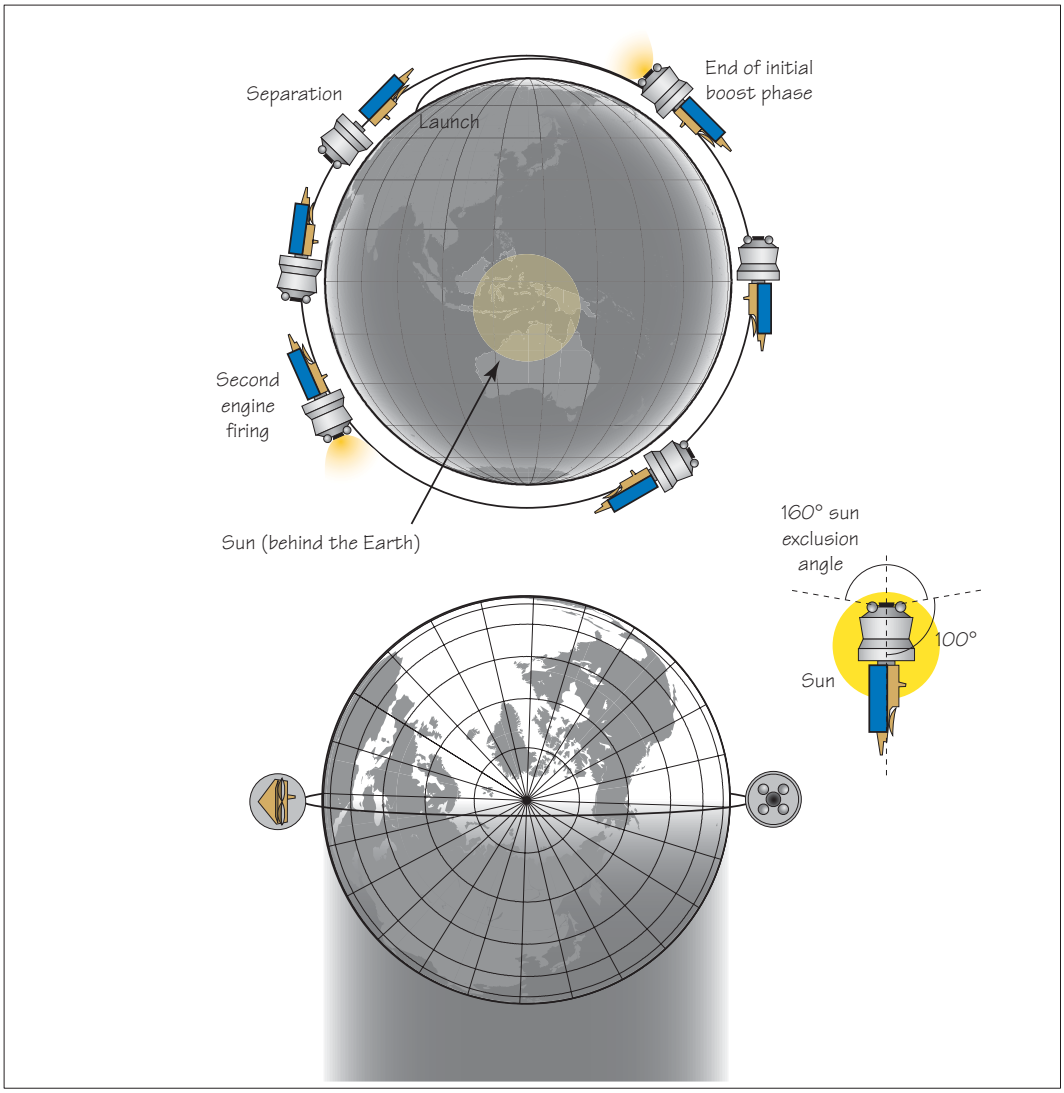

sufficient measurements to compute the actual orbit and the need to optimise the manoeuvres towards the nominal orbit.

3.1.2 Commissioning Phase

The Commissioning Phase follows the LEOP and ends with the Commissioning Review, which is the formal event which marks the transition to a fully operational mission and the general availability of data products from the mission. This Commissioning Review is expected to be about 6 months after the launch. Note that at this stage however, in contrast to some missions, validation of all products is unlikely to have been completed (due to seasonal constraints which we describe below) and appropriate caveats will be attached.

The Commissioning Phase has a number of sub-phases, which run partially in parallel and have links and dependencies amongst their constituent activities.

In the *Platform Verification* sub-phase the functional and performance verification of the satellite services (such as power, on-board data storage and downlink, and pointing) will be performed.

The *Payload Verification* sub-phase is devoted to the in-orbit CryoSat measurement system as a whole. The objective here is to verify that everything is working correctly, determine its performance and to make all required adjustments and tunings to the operating parameters. We intend to put a high priority on this sub-phase because changes in the measurement system will potentially invalidate earlier measurements from inclusion in any long-term time-series. This is not the case for changes in the ground-based processors as these may be retrospectively be applied through re-processing.

The *Payload Data Segment (PDS) Verification* sub-phase encompasses the activities required for functional and performance verification of the PDS (including payload planning, data processing, archiving, distribution and monitoring) in terms of functionality, throughput, data distribution *etc*. The actual values in the products may be incorrect, but the format, structure, identification and other attributes are reliable. At the end of this sub-phase the data products themselves are in a condition where they may be verified scientifically.

The next sub-phase, *Product Calibration*, is where the objective is to test the contents of the data products for correctness. This sub-phase is largely concerned with products at Level 1b[1], and the activities will generally lead to adjustment of parameters (or even some algorithms) used in the processors. This process is known, in the CryoSat context, as *calibration*.

The final sub-phase is *Product Validation*. Here the objective is to ensure the correctness, and identify the confidence limit (that is to say the errors), of the Level 2 products. These products contain parameters expressed in geophysically meaningful units, such as surface elevation. Determining the errors in these parameters, and eventually adjusting the Level 2 data processors, requires quite extensive independent data collection, largely in inconvenient places. In some cases the nature of the measurements required also puts constraints on when the data may be acquired. As a result this sub-phase may extend well beyond the Commissioning Phase and into the operational phase of the mission.

More detailed information about the calibration and validation objectives is provided in the *CryoSat Calibration and Validation Concept* [Ref. 2].

3.1.3 Science (or Exploitation) Phase

The Science[2] Phase will occupy the majority of the mission. During this phase the satellite, payload and ground segment will operate nominally, as described in this document.

3.1.4 Other Phases

Within the definition of the mission operations it is recognised that there will be other phases necessary for special situations. In the event of a major on-board emergency the payload will be switched off and the satellite will automatically enter a *Safe Mode*, in

1. Level 1b is a CEOS definition meaning “data with the same general structure as that produced by the instrument, converted to engineering units and calibrated”.

2. Historically the CryoSat project has referred to the main phase of the mission as the Science Phase, while the normal practice in Earth Observation missions is to call this the Exploitation Phase. Both terms, which are synonymous, may be encountered in CryoSat documentation.

which it can survive for a long period. At the end of the mission lifetime the satellite will enter the *Disposal Phase* – the exact handling of this phase will be determined at the time.

3.2 Availability of Measurements

3.2.1 Lifetime

Satellite *lifetime* is a duration used for sizing consumables, margins required for system ageing and life-testing of critical components. CryoSat has been designed to be able to make measurements over three full annual cycles. Therefore the specified lifetime is 3 years, excluding the Commissioning Phase. For the purpose of specifying the overall design life of the satellite, the Commissioning Phase has been defined as lasting for six months. The CryoSat-2 spacecraft has also been provisioned such that a 5 year lifetime (after Commissioning) is possible, although the calculations of reliability do not take this into account.

3.2.2 Availability

A recoverable failure, or *outage*, such as a software error which can be overcome by patching the flight software, leads to the system being unavailable for a time. A non-recoverable failure which leads to mission degradation or loss is handled as a reliability issue, covered in the next section. Therefore, for CryoSat, availability is defined as the probability that the space segment and the link to the ground segment provides the required data service to the ground segment, excluding the effects of non-recoverable failures. It is the fraction of the lifetime which is available for measurements.

All sources of unavailability are considered, such as major anomalies leading to Safe Mode, planned and unplanned orbital excursions, atmospheric effects and single event upsets due to cosmic ray effects. In computing the availability budgets the estimated outage periods include an allowance for the time taken for the spacecraft to become visible to the ground station.

The satellite is designed to provide an in-orbit availability of greater than 95% over the lifetime, after acquisition of the operational orbit and commissioning.

3.2.3 Reliability

Reliability is defined as the probability that the spacecraft will carry out its specified mission for the specified period. The reliability of the CryoSat spacecraft for the 3.5 year operational period is specified to be greater than 0.7.

Most elements of CryoSat are duplicated, that is to say they are *redundant*, which improves reliability. Thus the satellite is largely free of *single point failures*, defined as a single failure which causes the service to be permanently discontinued. This is because the satellite is mostly composed of equipment designed and qualified for other satellite missions (*i.e. recurrent* hardware) and such equipment is often internally redundant. There are some exceptions however, the most notable of which is the primary radar, the SIRAL instrument. The SIRAL has little internal redundancy; redundancy would have to be achieved by duplication of the equipment and this approach was too costly for the limited budget available to the CryoSat mission.

3.3 Orbits

3.3.1 CryoSat Orbit

The selected orbit for CryoSat is a compromise. The altitude is a compromise between air drag on one hand and radar link-budget and launcher capability on the other, while the inclination is a compromise between coverage of very high latitude regions and density of cross-overs. The selection of orbital parameters for the mission has been made by the CryoSat Science Advisory Group (C-SAG) and may be summarised as:

- Type: near-circular, polar, low-earth orbit
- Mean altitude: 717.242 km
- Inclination: 92.00°
- Repeat period: 369 days (5344 revolutions); 30 day sub-cycle
- Inter-track spacing: 7.5 km at the equator
- Orbit control: ±5 km (see also Section 3.3.3)
- Longitude of equator crossing: TBD (to be determined)

The osculating Keplerian elements, with respect to the J2000.0 inertial frame, are:

- Semi-Major axis $a = 7095.348557673$ km
- Eccentricity $e = 0.001406846$
- Inclination $i = 92.000678420°$
- Right Ascension of Ascending Node $\Omega = 129.997076727°$
- Argument of Perigee $\omega = 115.619512345°$
- True Anomaly $M = 283.899507188°$

The nominal ground track has not yet been fully defined. It will be based on the orbital injection by the launch vehicle, for which the mission analysis has not yet been finalised. After injection the actual orbit will be determined and then the reference orbit defined such as to optimise the required orbital manoeuvres.

An example of the ground coverage provided by this orbit is shown in Figure 3.3–1. Only a subcycle of 30 days is plotted in this figure as the full 369-day cycle provides such dense coverage that the coverage would appear to be continuous.

The variation in the number of cross-overs per 10^4 km^2 for a 1-year repeat orbit, at inclinations of 92°, 93° and 94°, for a latitude range of 60° to 90° is shown in Figure 3.3–2. The numbers were calculated at 10^2 km^2 resolution and averaged upwards: this is why there is an apparent drop in the number at the inclination limit. The discreteness effects in the curves are real, and are connected with the fact that cross overs occur along lines of latitude whose density (number per unit latitude) increases with latitude. Clearly, then, the selected inclination of 92° is a compromise between reducing the loss of sea ice coverage at the North Pole, and maintaining the measurement requirement in southern Greenland.

The operations of the payload are described in Chapter 5, “Operations”.

3.3.2 Non-Sun-Synchronism

The CryoSat orbit is not sun-synchronous and consequently the orbital plane will rotate with respect to the sun direction. The nodal plane regresses at a rate of about 0.25° per day (in an inertial frame). It makes half a revolution with respect to the earth-sun line in 244 days (just over 8 months), sampling all local solar times. This means that the satellite faces great variations in solar illumination and there are periods when it flies along the dawn-dusk line and is in constant sunlight (this is the plane into which CryoSat will be launched). At other periods it flies in the noon-midnight plane and undergoes eclipses.

Figure 3.3–1 Nominal ground track for one sub-cycle of the CryoSat orbit.

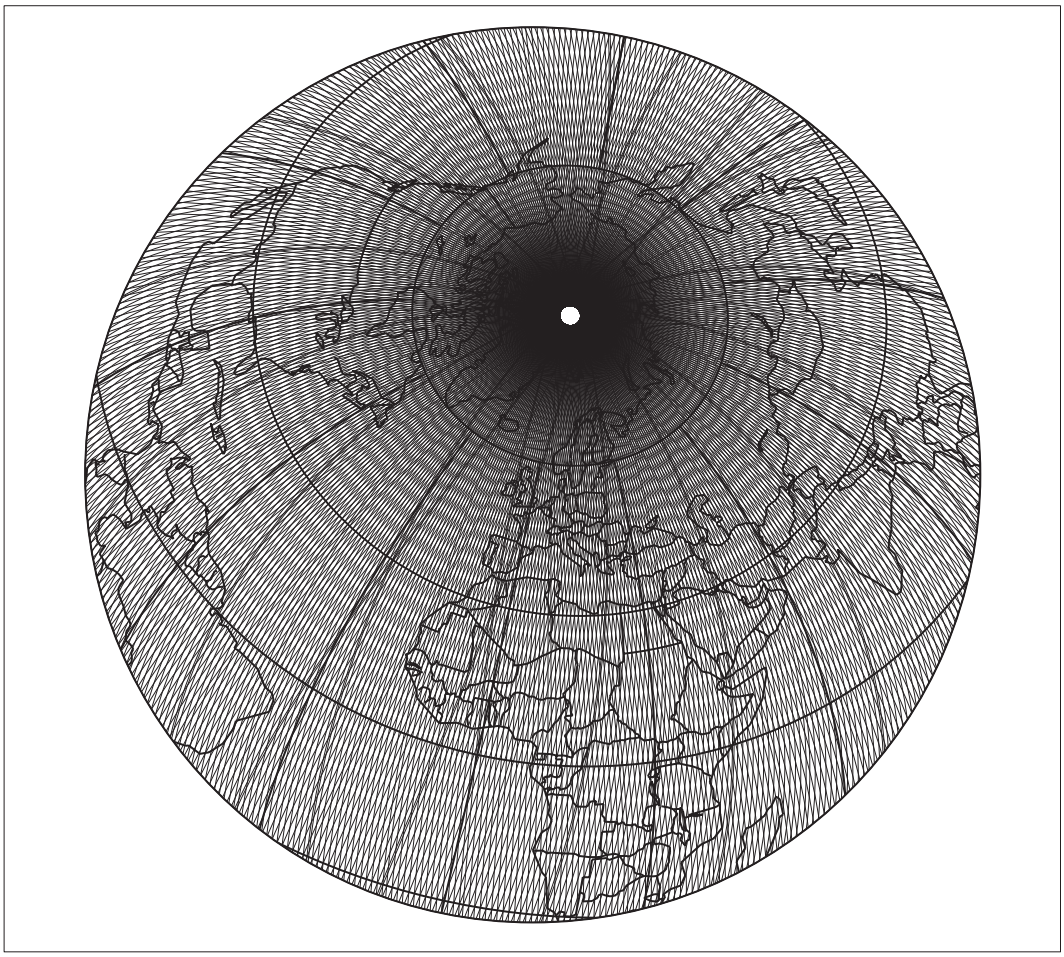

This is illustrated in Figure 3.3–3.

The consequences of this for the satellite design are profound, having particular impact in the domains of electrical power generation and storage, and in thermal control. It also has an influence on the configuration of the attitude sensors. The consequences which *may* influence the scientific exploitation of the mission include:

- orbit inclination variation (see Section 3.3.3, "Orbit Maintenance");
- solar radiation pressure modelling in precise orbit determination;
- varying thermal environment on the scientific instruments;
- combination of sun and moon blinding for the star-trackers (see Section 4.3, "Star Tracker").

3.3.3 Orbit Maintenance

In order to meet the science goals of the mission a relatively relaxed orbit control dead-band of ±5 km was specified. However, as we describe in Section 5, "Operations" mission planning is based on the reference orbit and a geographical mask. The along-track deviation from the reference orbit is proportional to the across track deviation with an amplification factor of 14.5 (the number of orbits per day). In order to keep the along-track

Figure 3.3–2 The variation in the number of cross-overs per 10^4 km^2 for a 1-year repeat orbit, at inclinations of 92˚, 93˚ and 94˚, for a latitude range of 60˚ to 90˚

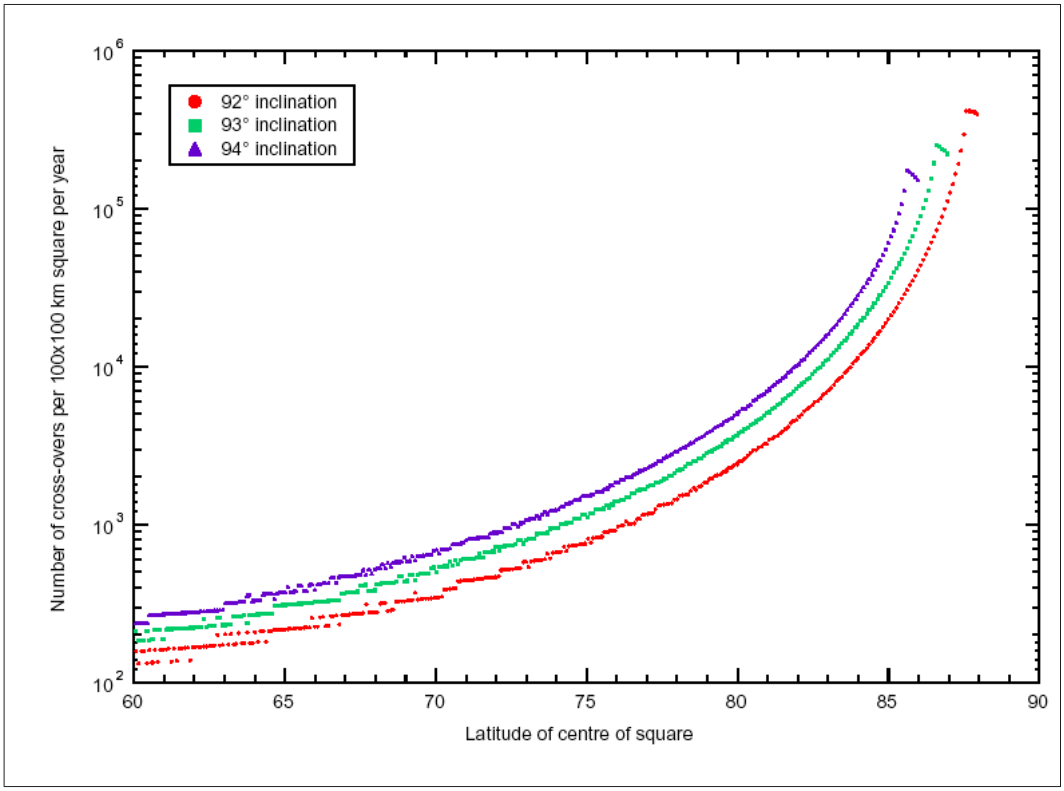

deviation reasonably small we have decided to maintain a ±1 km dead-band across-track, at the equator (the definition at higher latitudes is complicated by inclination drift).

The actual ground track error is given by the sum of different perturbations acting on the spacecraft, due to:

- air-drag;
- Sun and Moon attraction;
- solar radiation pressure;
- high-order (>2) harmonics in Earth's gravitational field.

Of these effects the largest influence is air-drag, and this is correlated to the solar activity, being higher in periods of high solar activity due to the increased atmospheric density at the given orbit altitude. The principle effect is a reduction in the semi-major axis amounting to some tens of metres per month. As the semi-major axis decays the orbital period changes, and this degrades the synchronism between the orbital period and the Earth's rotation period which produces the repeating ground track.

If uncontrolled, the ground-track error resulting from air-drag would typically have the form shown in the left panel of Figure 3.3–4. The right panel of this Figure shows the effect of combining all the effects, but note that apart from air-drag these effects depend on the assumed starting conditions, particularly the assumed local solar time of the orbital plane.

In order to overcome the effect of decay of the semi-major axis the satellite regularly performs orbit maintenance manoeuvres, in which thrusters are used to increase the semi-major axis. The strategy adopted is to raise the orbit above the nominal altitude by a small amount so that the ground track drifts westwards. Ideally the effect of the air-drag has

Figure 3.3–3 Illustration of the eclipse duration for the CryoSat orbit. The assumed launch date, for the purposes of the plot, is 1 March 2003, but this is largely irrelevant. The units of the vertical scale were established for satellite design purposes, but are proportional to eclipse duration per orbit. At maximum extent the eclipse duration is almost half the orbit

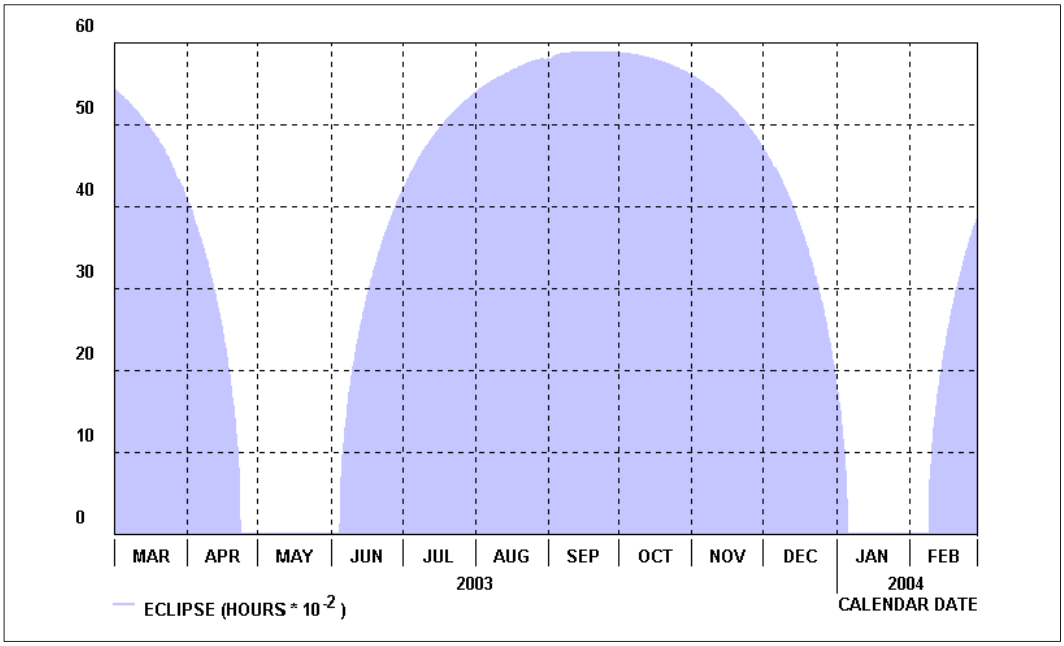

Figure 3.3–4 Typical trend of uncontrolled ground track error for CryoSat, taking account of air-drag only in the left panel, and all contributions in the right panel

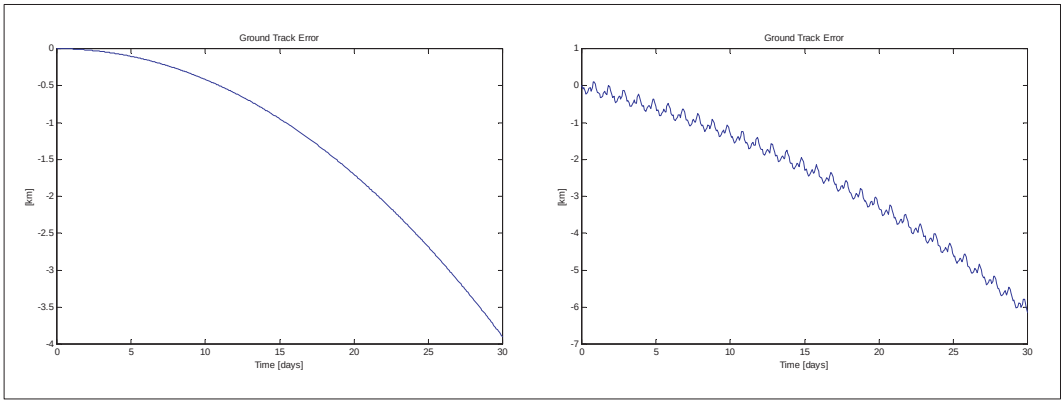

been accurately predicted so that the semi-major axis decays to the nominal value just as the ground-track error reaches the western end of the dead-band. As the orbit continues to decay below the reference altitude the ground track starts to move eastwards again, and when it reaches the eastern boundary another orbit maintenance manoeuvre will be performed. An actual example of this behaviour, from ERS-2 during May 2000, is shown in the red trace of Figure 3.3–5.

At higher latitudes the inclination also has an effect on the ground track error and this is shown in the other traces in Figure 3.3–5. In particular the high-latitude traces are constrained to one edge of the dead-band throughout most of the month because of an inclination error compared to the reference inclination. At the end of the month an out-of-

Figure 3.3–5 The evolution of the ERS-2 ground track error during May 2000, within the dead-band of ±1 km. The red line shows the error at the equator, and blue and cyan lines show the error at 60° latitude. In-plane manoeuvres (to increase the semi-major axis) were made on 2 May, 19 May and 31 May, and an out-of-plane manoeuvre (to increase the inclination) was made on 30 May.

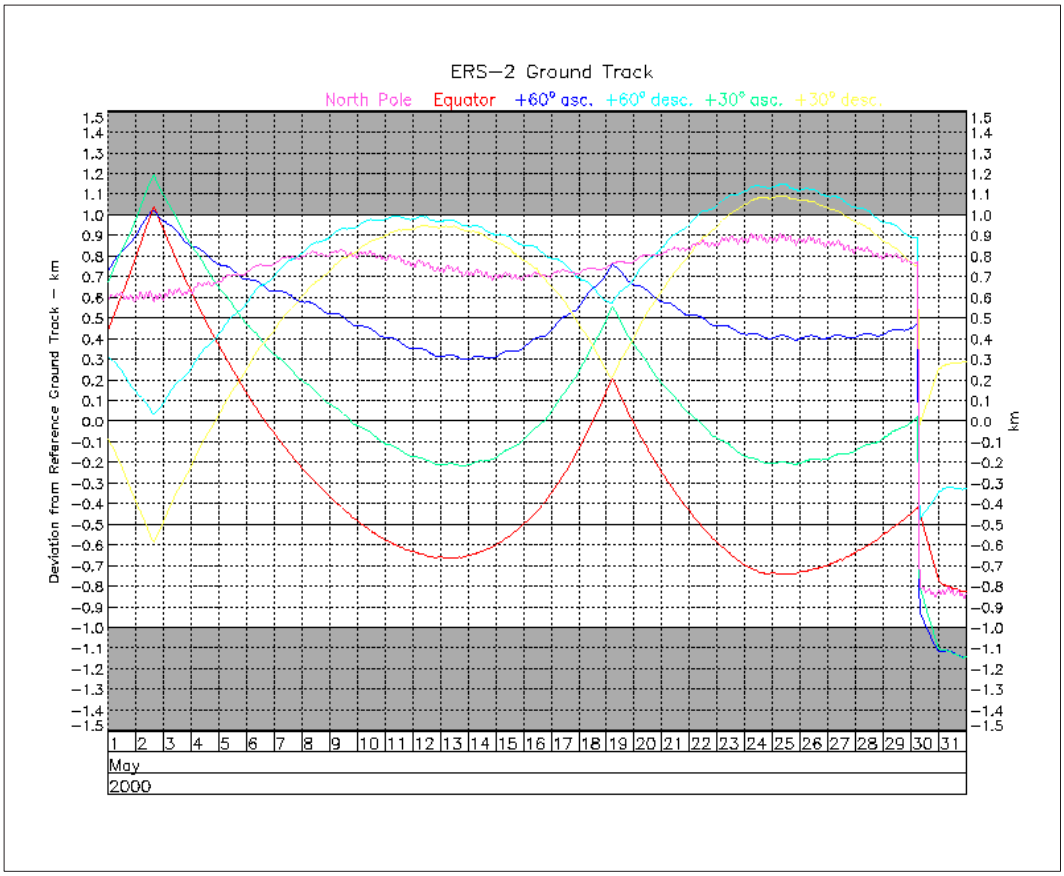

plane manoeuvre to correct the inclination was performed and the effect of this can be clearly seen in the ground track error traces.

Inclination adjustment, by out-of-plane manoeuvre, is more demanding than increasing semi-major axis by in-plane manoeuvre: the manoeuvre of 2 May required two thrusts with a total along-track velocity change (Δv) of 0.046 ms^{-1}. The manoeuvre of 30 May required a cross-track Δv of 1.875 ms^{-1} combined with an along-track Δv of 0.051 ms^{-1}.

An important influence on inclination drift is the gravitational attraction of the Sun. Like all sun-synchronous satellites, ERS-2 suffers a constant inclination drift due to the quasi-constant angle between the orbital plane and the sun. CryoSat, in contrast, has a constantly rotating orbital plane and therefore inclination changes are not uni-directional. An example of the uncorrected inclination drift of the CryoSat orbit, with arbitrary initial conditions, is shown in Figure 3.3–6. The maximum error, 0.045°, corresponds to a ground track error of 5 km at the maximum latitude (less at lower latitudes: the ground track error due to inclination change is essentially a sinusoidal variation with a minimum at the equator).

The selection of the ±5 km dead-band for the CryoSat orbit, and the restriction of the ±1 km dead-band to the equator crossing, has been made with the intention of avoiding the costly out-of-plane manoeuvres required to correct inclination. The satellite propellant

Figure 3.3–6 Evolution of orbital inclination during a 3.5 years in the Science Phase orbit, if no control is performed, with an arbitrary starting date.

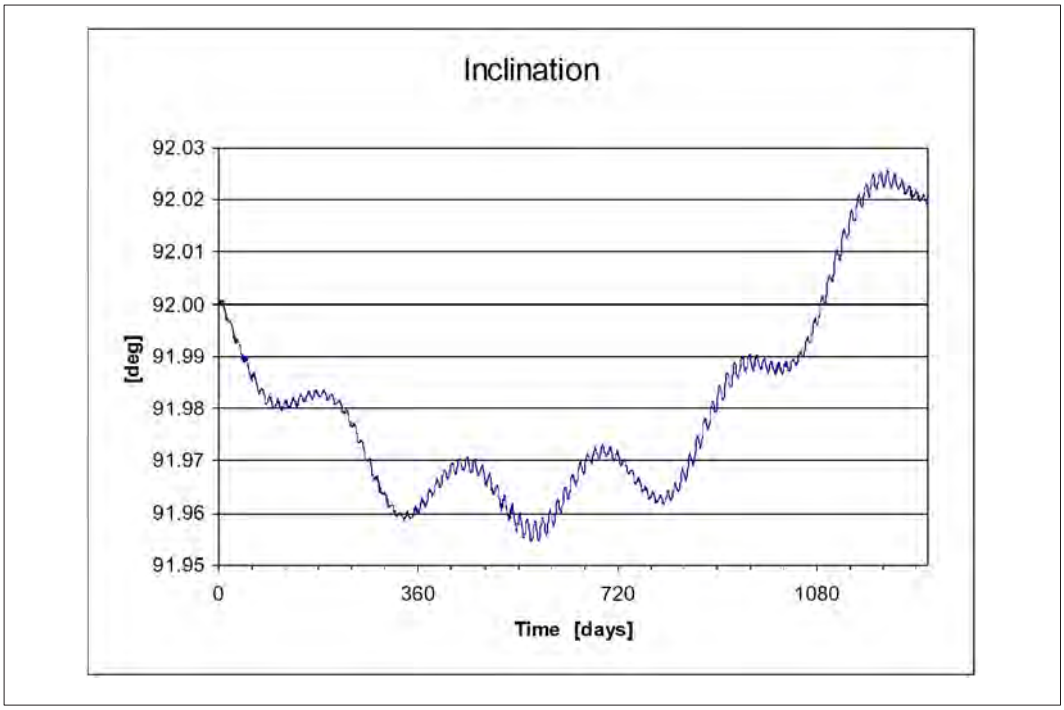

budget (see Section 3.4, "Overall Δv Budget") does not include the necessary provision, although it does show margin.

3.3.4 Precise Orbit Determination

The estimated accuracy of the precise orbit determination for CryoSat, primarily based on DORIS measurements, is 5 cm RMS for the radial component. This has been estimated based on the performances of other DORIS systems. The on-board, real-time estimates are estimated as <30 cm RMS radially and <1 m RMS for three axes.

3.3.5 Orbital Manoeuvres

Based on the 3σ dispersion in the semi-major axis of the launch vehicle the Δv required to acquire reference orbit is over 7.7 ms^{-1}. Due to the low thrust of the CryoSat orbit control thrusters (40 mN), being based on cold, low-pressure gas, it will take a significant time to accelerate through such a Δv; in fact almost 2 days of continuous thrust will be needed. This is significantly more than the orbital period and so the orbit change has to be performed as a continuous spiral manoeuvre, rather than a Hohmann transfer. A detailed analysis has shown that the required Δv for this spiral manoeuvre is essentially the same as the more efficient Hohmann transfer, if control of the orbital parameters is restricted to semi-major axis and eccentricity during the manoeuvre.

3.4 Overall Δv Budget

The total Δv, or equivalently, the amount of propellant, necessary for controlling the CryoSat orbit during the mission lifetime is calculated by summing the contribution of the following contributions:

- initial orbit acquisition;
- collision avoidance manoeuvres;
- orbit maintenance for ground track control (see Section 3.3.3).

Additional propellant is needed for attitude control of the satellite, both to correct any residual attitude rates after separation from the launcher and for control during routine operations (see Section 4.8, "Attitude and Orbit Control").

Finally, some propellant cannot be effectively used due to gas leakage and inaccessibility through the pressure regulator at the low final tank pressure.

The total Δv and propellant budget is presented in Table 3.4–1.

Table 3.4–1 Nominal propellant budget for CryoSat; the budget shows a margin of 12% for the nominal life and a margin of <1% for 5.5 years. The budget includes 4 orbit changes.

Mission Phase	ΔV (m/s)	Propellant Mass (kg)	Comment
Orbit Control			
- Initial orbit acquisition (Rockot)	8.28		
- Orbit maintenance	1.80		2.83 m/s for 5.5 years. Air density increase due to solar cycle taken into account.
- Space debris collision avoidance	1.48		
- Orbit changes	12.13		
- Attitude control during orbit control	0.33		0.35 m/s for 5.5 years
Subtotal	24.03	24.94	
Attitude Control			
- Attitude slews for re-orientation		0.24	
- Initial rate damping & attitude acquisition		0.09	
- Coarse Pointing (Safe Mode)		1.36	2.04 kg for 5.5 years
- Fine Pointing (nominal operations)		3.43	5.39 for 5.5 years
Subtotal		5.12	
Leakage and Residual			
- Overall external leakage		1.00	1.57 kg for 5.5 years
- Residual EOL propellant mass outside guaranteed performance		1.62	
- EOL non-usable propellant		0.20	
Subtotal		2.81	
Propellant mass		32.87 (37.17 for 5.5 years)	Satellite Mass: 743.5 kg Specific Impulse: 72 s Tank Capacity: 37.4 kg

3.5 Ground Contact

CryoSat will be operated from a single ground station; possible locations were studied during the early definition studies and the site selected was the ESA facility at Salmijärvi, near Kiruna. The coverage mask of this station played a major part in that decision and CryoSat will be visible from this ground station during, typically, 11 out of the 14 orbits per day. During the other orbits, sometimes called *blind orbits*, CryoSat will have no contact and has to store all scientific data on board, and be autonomous for its operations. The extent of the coverage mask is shown in Figure 3.5–1.

Figure 3.5–1 CryoSat orbits during 2 days, showing the passes visible from the ground station at Kiruna.

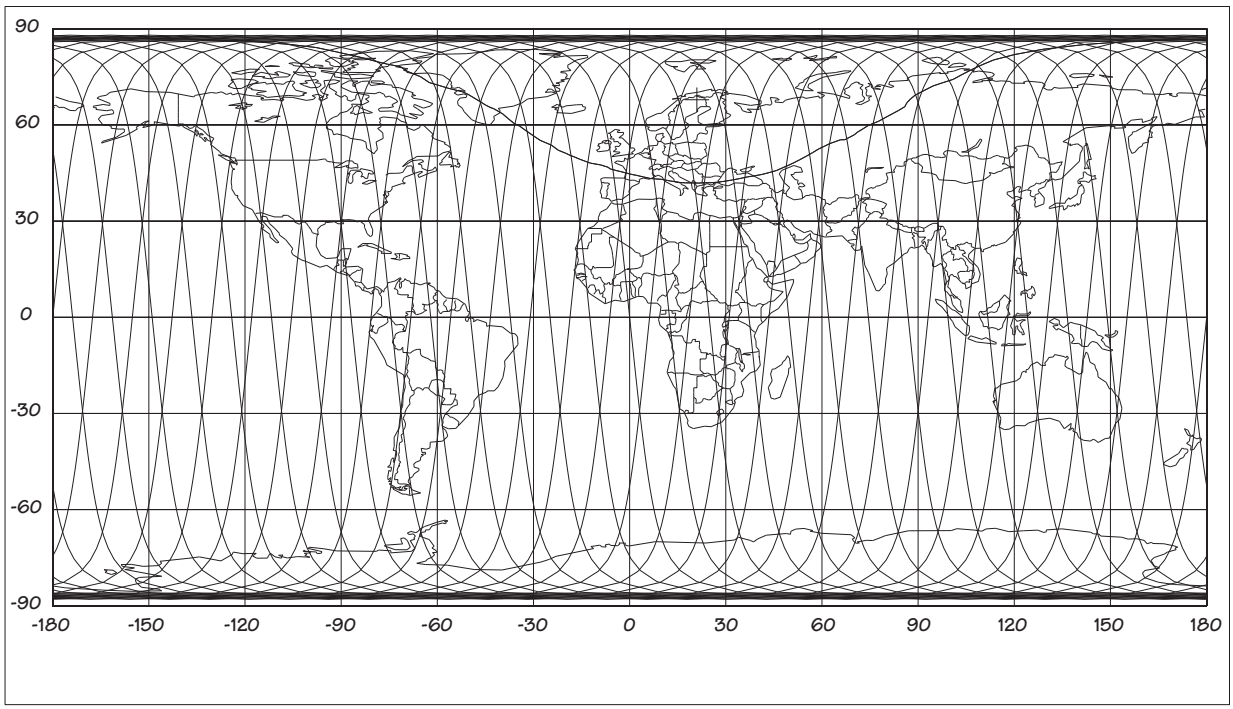

4 CryoSat Space Segment

CryoSat has been designed with the intention of avoiding the development of new equipment wherever possible. Such new development is too costly and takes too much time to be feasible within the CryoSat constraints. This approach has been followed for both the payload and for the satellite itself although some new development for the main payload, the SIRAL, has been unavoidable.

4.1 The SIRAL Instrument

The SIRAL radar altimeter is derived from a conventional pulsewidth-limited altimeter design; it is a single frequency Ku-band radar altimeter using the *full deramp* range compression technique. In addition to conventional operation it features additional design characteristics, which enable it to provide data which can be more elaborately processed on ground. A high Pulse Repetition Frequency (PRF), ensuring a coherent sampling along-track, allows azimuth processing to provide along-track resolution enhancement. The addition of interferometry, with two antennas and two receive chains, resolves across-rack slope over ice sheets.

These capabilities form the basis for the instruments name: SIRAL is an acronym for SAR/Interferometric Radar Altimeter.

The additional features required to achieve these capabilities include pulse-to-pulse phase coherence and a second complete receiver chain, including a second antenna. These features make this instrument unique. Nevertheless its design benefits from the heritage of technology and experience gained from the development of the Poseidon 2 altimeter on the Jason mission.

For the CryoSat-2 satellite the SIRAL instrument has been made fully redundant (that is, all items which could credibly fail are duplicated). In the original design the instrument was non-redundant (although there were some redundant features built in) and while this enabled the spacecraft to meet its calculated reliability requirement, it did leave the measurement system vulnerable to loss due to a single (albeit unlikely) failure. The redundancy removes this possibility and completes the full redundancy of the entire satellite.

4.1.1 Configuration

The instrument is split into three major subsystems. Two of these consist of one or more discrete electronics boxes:

- the Digital Processing Unit, which provides all of the digital electronic functions of the altimeter;
- the Radio Frequency Unit, which contains all of the analogue electronics, mainly in the intermediate and radio frequency range;

The third subsystem is the Antenna Subsystem, consisting of two Cassegrain antennas mounted side-by-side, forming an interferometer across-track. Both antennas are identical but one is used both to transmit and receive whereas the other is only used to receive echoes. The Cassegrain design offers particular advantages for the SIRAL as the resulting waveguide lengths are much shorter than those required for the more common, front-fed, design.

The primary, elliptical, reflectors are approximately 1.15 m by 1.4 m. The use of elliptical antennas, rather than the more conventional circular pattern, is based on several criteria:

- it enables a larger antenna area to be accommodated within the limited diameter of the launch vehicle fairing, thus increasing the echo power received in the instrument;
- the requirements on beamwidth, and thus antenna dimension, in the along-track and across-track direction are derived from different criteria, as the instrument depends on SAR processing for along-track resolution and interferometry for across-track angular discrimination;
- in conventional altimeter mode, over ocean surfaces, the theoretical form of the echo (described by *Brown*, 1977 [Ref. 7]) may be modified to account for the asymmetrical antenna pattern.

The antenna subsystem is supported on an "optical bench": a structure of great thermo-elastic stability, needed to meet the interferometric performance requirement of the instrument. The interferometer requires knowledge of the orientation of the antenna phase centres to 30 arcsec in roll. It is manufactured from a composite sandwich of thin carbon-fibre reinforced plastic (CFRP) face-skins with a honeycomb core also made of CFRP. This composite is selected because CFRP has a very low coefficient of thermal expansion. Despite the material selection the optical bench will be isolated from its environment as far as possible, using thermal isolation (multi-layer insulation), and will also be equipped with temperature sensors in order to be able to monitor its thermal gradients in-flight, should problems with its stability be suspected. Figure 4.1–1 shows the antenna bench with the

Figure 4.1–1 The SIRAL antenna in the anechoic test chamber during RF testing. The thermal protection, a single layer of germanium-coated mylar, covering the antenna apertures is in place but the Star Trackers have not been fitted at this time.

antenna apertures covered with a single layer thermal shield to further isolate the antennas from the environment.

In order to precisely measure the orientation of this antenna bench a set of Star Trackers (described in Section 4.3, "Star Tracker") is mounted directly on the structure. The bench is isolated from the thermo-elastic deformation of the rest of the satellite by means of quasi-isostatic mechanical mounting.

The stability of the RF waveguides between the electronic equipment and the antennas also contributes to the overall interferometric performance and therefore the waveguides exposed to high thermal variations are made of invar and are fitted with temperature sensors.

A perspective drawing of the satellite, showing the SIRAL equipment, is shown in Figure 4.1–2. This does not show any of the external surfaces of the satellite. The yellow cones in this image are not physical but indicate fields of view of the star trackers and thrusters.

Figure 4.1–2 View of the CryoSat-2 satellite showing the SIRAL instrument at the "nose", to the right of the picture. Two electronics boxes and the antenna subsystem can be seen. Also mounted on the antenna support plate are the star trackers, and, at the end, an earth-facing radiator plate linked by 6 heat-pipes.

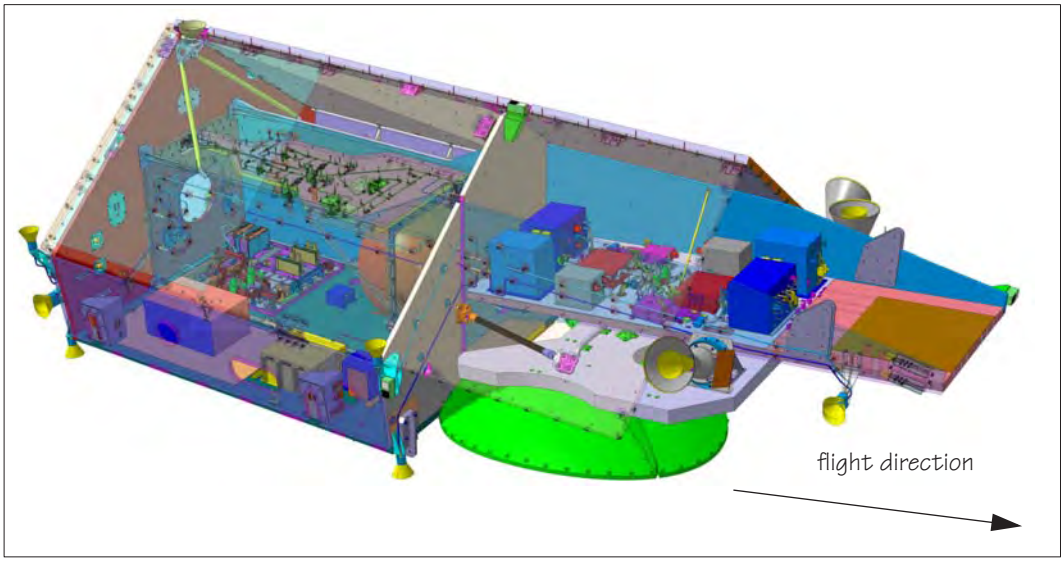

A further drawing, with more detail of the installation of the SIRAL units, and the Star Trackers, is shown in Figure 4.1–3. This shows the redundant electronic units in different colours. In nominal operation the units in red are used with the left-hand antenna (in the direction of flight) being used for transmit and receive while the right-hand antenna is used for receive-only. If a nominal unit fails the equipment will be reconfigured to the redundant units (shown in blue) and in this case the right-hand antenna is used for transmit and receive while the left-hand antenna becomes receive-only.

This swapping of the antenna functions during reconfiguration is taken into account in the ground processing of the science data.

Figure 4.1–3 A perspective view of the nose of the CryoSat satellite, showing the installation of the SIRAL units. The three Star Tracker baffles are also visible. The primary units are in red and the redundant units in blue

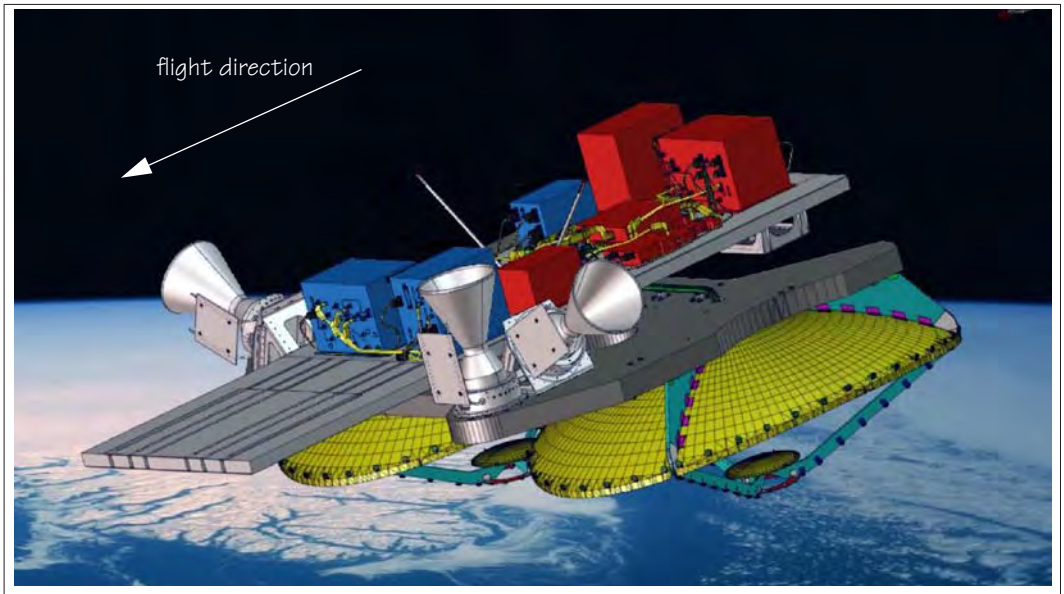

4.1.2 Operating Modes

The SIRAL is capable of operating in three main measurement modes, described below. Further details about the approach to processing the measurement made in these modes is provided in the *CryoSat Data Processing Concept*, [Ref. 4].

- *Low-resolution mode (LRM)*: This mode is similar to the operation of conventional pulsewidth-limited altimeters and uses a single receive channel. The PRF is low and the echoes are transmitted to the ground segment in the spectral domain after on-board averaging. The data rate is therefore low. This mode will be used over ice sheet interiors, where the slopes of the surface are small. It will also be used over ocean.
- *SAR mode*: In this mode, which also uses a single receive channel, the along-track horizontal resolution of the altimeter is enhanced by exploiting the Doppler properties of the echoes as they cross the antenna beamwidth, by on-ground processing. The result is equivalent to decomposing the main antenna beam into a set of 64 narrower synthetic beams along track. The footprints of the different sub-beams over a flat surface are adjacent rectangular areas ~250m wide along track and as large as the antenna footprint across-track (up to 15 km). Consequently, a larger number of independent measurements are available over a given area and this property is used to enhance the accuracy of the measurements over sea ice. In order to ensure the coherence between echoes from successive pulses, the PRF is about 10 times higher than for LRM and the instrument operates in burst mode. The echoes are transmitted to the ground segment in the time domain, prior to any averaging. Therefore the data rate is significantly higher than for LRM.
- *SAR-Interferometric mode (SARIn)*: This mode is used mainly over the margins of the ice sheets, where the surface slopes are high. The combination of SAR and interferometry makes it possible to accurately determine the arrival direction of the echoes both along and across the satellite track, by comparing the phase of one receive channel with respect to the other. This directivity is required to derive the height of the surface from the range measurement of the radar. In this mode both receive channels are

active and the corresponding echoes are transmitted to the ground in the time domain. The data rate is about twice as high as for SAR mode. In order to cope with abrupt height variations, the range-tracking concept for this mode has to be particularly robust. In SIRAL, this is ensured by using narrow-band tracking pulses, transmitted in-between successive wide-band measurement bursts.

Table 4.1–1 summarises the key instrument parameters for each mode. Some of these are further discussed in Section 4.1.4, "Operating Characteristics".

Table 4.1–1 Key instrument parameters for the SIRAL in each mode.

	LRM	SAR	SARIn
Receive chain[1]	left	left	left and right
Centre frequency	13.575 GHz		
Bandwidth	350 MHz		
Transmit power	25 W		
Noise figure	1.9 dB at duplexer output		
Antenna gain	42 dB		
Antenna 3 dB beamwidth (along-track)	1.0766°		
Antenna 3 dB beamwidth (across-track)	1.2016°		
Interferometer baseline	-	-	1.172 m
Samples per echo[2]	128	128	512
Sample interval	0.47 m		
Range window	60 m	60 m	240 m
PRF	1970 Hz	17.8 kHz	17.8 KHz
Transmit pulse length	49 µss		
Useful echo length	44.8 µs	44.8 µs	44.8 µs
Burst length	-	3.6 ms	3.6 ms
Pulses per burst	-	64	64
Burst repetition interval	-	11.7 ms	46.7 ms
Azimuth looks (46.7 ms)	91	240	60
Tracking pulse bandwidth	350 MHz	350 MHz	40 MHz
Samples per tracking echo	128		
Tracking sample interval	0.47 m	0.47 m	3.75 m
Size of tracking window	60 m	60 m	480 m
Averaged tracking pulses (46.7 ms)	92	32	24
Data rate	51 kbps	11.3 Mbps	2 x 11.3 Mbps
Power consumption	95.5 W	127.5 W	123.5 W
Mass	62 kg		

1. as seen by an observer on the satellite, facing forward with feet towards the Earth. The sense is reversed if the redundant instrument is used
2. the useful number of samples is less, due to end effects cased by the FIR filtering.

4.1.3 Instrument Design

The block diagram of the altimeter instrument is shown in Figure 4.1–4. This Figure contains much detailed information, not all of which will be specifically described here. As mentioned above, the instrument is a single frequency, pulsewidth-limited radar using the

full deramp principle. The electronic subsystems, identified in Figure 4.1–4, are further described in the following subsections. The electronic units (and embedded software) are unchanged from the original CryoSat design.

Figure 4.1–4 Block diagram of the SIRAL Radar Altimeter. The two major electronic subsystems of the instrument are identified, as well as internal detail described in the text. The Nominal/Redundant waveguide switches (immediately to the left of the labelled Calibration coupler) are controlled by ground commands routed directly from the satellite (not via the instrument). Powering of both nominal and redundant units simultaneously is blocked.

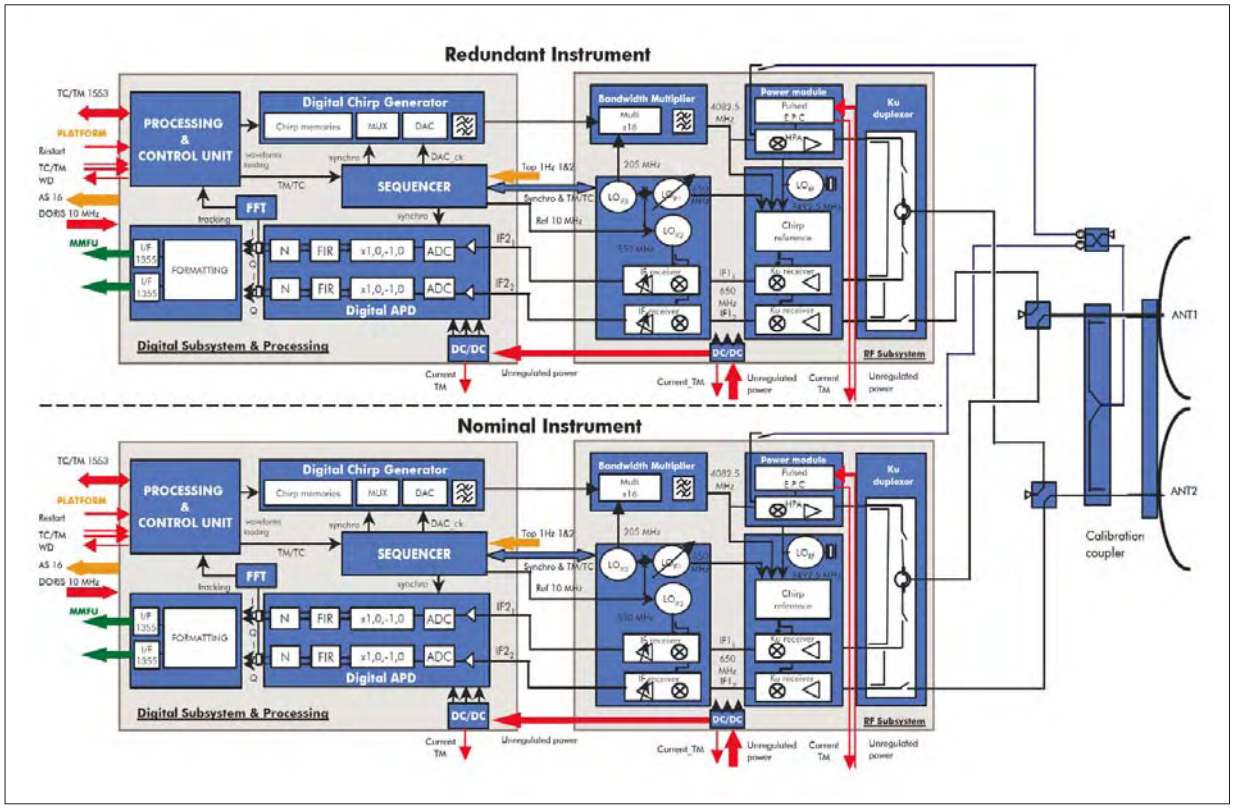

4.1.3.1 *Digital Processing Unit*

The Digital Processing Unit is responsible for the control of the instrument, as well as the communication interfaces with the main satellite computer for telecommands and housekeeping telemetry (see Section 4.6, "Control and Data Handling"). A sequencer, driven by the reference 10 MHz clock from the DORIS, controls all of the instrument timing, including the echo delay timing.

A digital chirp[3] generator, controlled by the sequencer, generates the modulated radar pulse for transmission. It operates at 160 Msamples/sec and requires subsequent bandwidth multiplication by a factor 16, in the RF Unit, to achieve the required output bandwidth of 350 MHz. Digital chirp generation ensures the signal coherency from pulse to pulse. It is also used to compensate for the distortions of the transmitter by pre-distorting the digital waveform stored in the device.

3. A chirp radar signal is a linear frequency modulated pulse which, upon reception, may be compressed in time to yield an intrinsic time resolution equal to the inverse of its bandwidth. Radar altimeters use a large bandwidth to achieve high resolution in the time domain.

On echo reception the digital signal processing section digitises the incoming video signal, performs digital filtering, and formats the echoes as scientific telemetry. The digital filters provide well controlled characteristics and phase stability.

Fourier transformation is performed on some echoes to generate the echo waveforms needed to drive the software tracking loops. These enable the instrument to autonomously adjust its timing and gain in order to optimise its measurements over all surfaces.

4.1.3.2 *Radio Frequency Unit*

The Radio Frequency Unit receivers the chirp signal from the digital unit and multiplies its bandwidth by a factor 16 using analogue circuitry. Signal amplification for transmission is achieved by a solid state power amplifier, with an RF peak power output of 25 W. This is a new development and a breadboard of this was the first specific CryoSat hardware to be manufactured – a photograph of the unit prior to testing is shown in Figure 4.1–5.

Figure 4.1–5 Breadboard model of the solid-state power amplifier for the CryoSat SIRAL. It consists of four identical amplifier modules and a waveguide power-combiner structure, to the right in the picture.

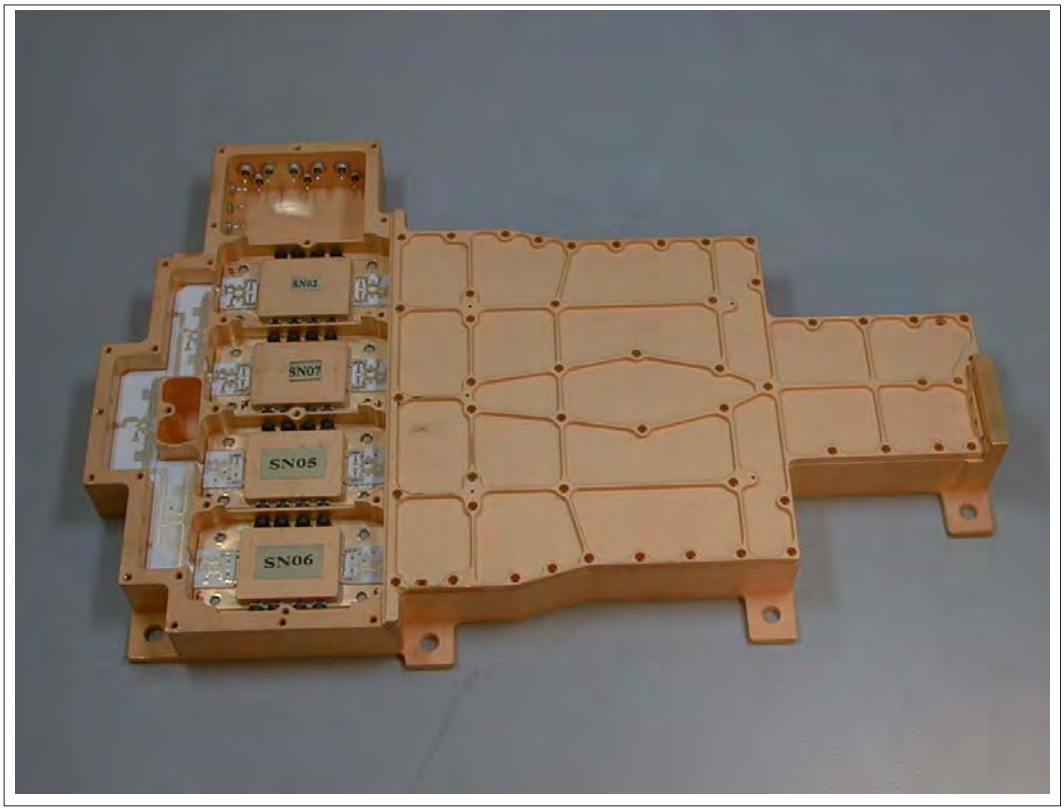

The duplexer is an arrangement of RF switches and couplers which route the radar and calibration pulses between the transmitter, the antennas and the receiver. The waveguide switches (and, in detail, the waveguide lengths) are arranged so that the radar operation and internal delay characteristics are identical irrespective of which side is in use.

The waveguide switches used for redundancy switching are not themselves redundant. Thus switching between nominal and redundant chains is to be avoided as far as possible.

There are two receive chains, one for each antenna, in which signal demodulation by means of the full deramp principle, and gain control is performed. To ensure stability between both receive channels, the down converter oscillators are connected to both channels and digital sampling at the intermediate frequency, 100 MHz, is used. These digitised signals are passed to the two receive parts of the digital unit.

4.1.4 Operating Characteristics

The SIRAL instrument is a pulsed radar but the characteristics of the pulses timing differs between the modes. In the LRM the timing is similar to existing altimeters such as ERS or Jason, in which the transmit and receive pulses are interleaved. This is shown in the top panel of Figure 4.1–6. The interval between transmit pulses is 508 μs while the round-trip time to the surface is typically 4.8 ms. Therefore nine pulses are emitted before the first one returns; there are always nine pulses in transit during this mode. The PRF is sufficiently low that the echoes are decorrelated so that they may be incoherently summed to reduce speckle noise.

Figure 4.1–6 Timing of transmit (E) and receive (R) pulses in each of the three SIRAL modes.

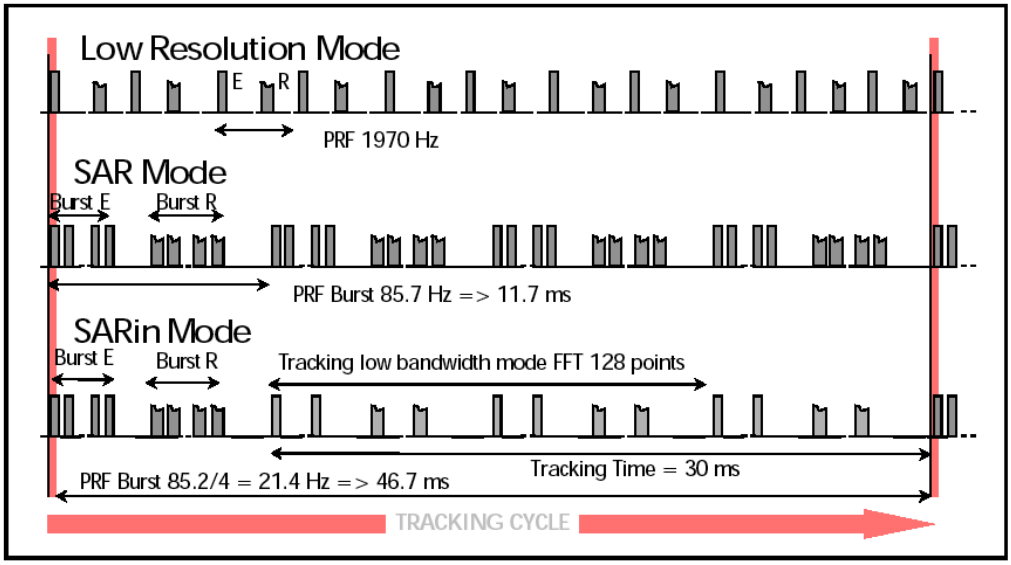

In the SAR mode the pulses are transmitted in bursts of 64 pulses; here the pulses have to be correlated so the PRF within the burst is high. After the burst there is an interval to allow the burst of echoes to return. Each burst will be processed to yield 64 doppler beams along-track, each of width 250 m. Four bursts make up a tracking cycle, which is a fundamental interval common to all the modes, enabling a periodic and synchronous operation of the tracking software. In fact the satellite orbital speed is such that it covers 250 m in the 4-burst tracking cycle, thus the 4 bursts in the cycle oversample the surface. Over specular surfaces this oversampling is likely to be necessary as off-normal incidence reflections will have little energy.

SARIn mode is intended for use over topographic terrain which is less specular. Therefore oversampling of the echoes is unnecessary and consequently there is one measurement burst during the tracking cycle. In order to ensure that the instrument is able to follow the expected rapid variations in the echo delay time and shape the tracking loop is main-

tained during the remainder of the tracking cycle with a low-bandwidth chirp which has a correspondingly large range-window.

In the LRM and SAR modes the range-window recorded is 60 m; as the range resolution is about 0.47 m (it is related to the inverse of the chirp bandwidth) this leads to 128 samples of measurement data. In the SARIn mode the range window is increased to 240 m due to the slope variations at the ice sheet margins, so that 512 sampled data are needed.

In the high resolution SAR and SARIn modes the echo samples are available in the measurement data coded as the complex time-domain signal for each echo (*ie* I and Q samples). In LRM however the data are converted to waveforms representing the echo power, and averaged on-board, similar to a conventional altimeter.

4.1.5 Redundancy Considerations

Since switching between nominal and redundant chains is discouraged the instruments will be cross-calibrated prior to launch by presenting common signals to the antennas and switching between the radars. The radars will also be individually calibrated prelaunch. The two radars have independent characterisation data (the so-called *radar data base*) used on-board and on-ground. For example, the pre-distortion of the digital chirp to compensate for distortions in the radar (mainly from the radio frequency unit and solid state power amplifier) will be individually tailored for each unit.

The science data telemetered will be identical to the original SIRAL, save that an additional bit will be added to identify whether the nominal or redundant radar is in operation. This will be used in ground processing to enable the correct selection of radar data base.

Any in-orbit reconfiguration from the nominal to redundant configuration will invoke the the following procedure.

- the nominal radar is powered down by tele-command from ground;
- analysis of telemetry to confirm that the nominal radar is switched off;
- waveguide switches are commanded from ground to connect the calibration coupler and antenna sub-system to the redundant radar;
- analysis of telemetry data to confirm the waveguide switching has been successful;
- by tele-command the redundant radar is powered up and an analysis of telemetry follows to determine the success of this operation;
- operations continue following a commissioning of the redundant radar.

4.1.6 Performance

The performance of the SIRAL has not been specified in terms of height noise, which is frequently used to characterise such instruments. This is because such specifications make the assumption that the instrument is operating over an ocean surface, in which case the average return echoes can be described analytically. This property is not valid for the ice-covered surfaces which Cryosat is intended to measure.

Nevertheless, it is possible to estimate the height noise of the SIRAL instrument over ocean surfaces. This is given in Table 4.1–1 as a function of assumed significant wave-height.

Table 4.1–1 Estimated height noise performance of SIRAL over an ocean surface, for different values of significant waveheight, SWH. The values have been estimated as the standard deviations of 1-second averages, for retracked waveforms.

SWH (m)	Height Noise (cm)
2	1.6
4	1.8
8	2.7

4.2 DORIS

4.2.1 The DORIS System and Operation

The DORIS receiver carried on-board CryoSat is part of a an overall system which is able to provide tracking measurements for precise orbit determination, and time-transfer. The DORIS system comprises a network of more than 50 ground beacons, a number of receivers on several satellites in orbit and in development, and ground-segment facilities. It is part of the *International DORIS Service*, the IDS, which also offers the possibility of precise localisation of user-beacons.

DORIS is an up-link radio frequency tracking system based on the Doppler principle. Each beacon in the ground network broadcasts stable two frequencies, at S-band and VHF (2036.25 MHz and 401.25 MHz respectively). Every 10 seconds the receiver on-board measures the Doppler shift of these signals using the on-board ultra-stable oscillator (with stability of $5x10^{-13}$ over 10 to 100 seconds) as a reference; essentially this enables the line-of-sight velocity to be determined. The use of two frequencies allows the ionospheric effects to be compensated and this also enables the ionospheric total electron content to be estimated. The set of radial velocities from the dense network of precisely located beacons is rich set of tracking data.

The network of beacons is shown in Figure 4.2–1.This Figure also shows the coverage mask for each beacon, corresponding to the zone where CryoSat is at an elevation of more than 15° above the horizon at the station. Although this network offers full coverage of the Arctic, the coverage in the Antarctic is not quite complete. Other regions are also incomplete and this does not significantly degrade the POD performance currently achieved with DORIS. The CryoSat DORIS receiver is capable of acquiring and processing the signals from two beacons simultaneously.

The effect of the incomplete DORIS coverage in Antarctica is currently under study in the framework of the *CryoSat Orbit and Altimetry Group*[4], particularly with respect to the long term stability of the *z*-component of the orbit.

The DORIS system includes the possibility of encoding information on the uplinked signals, and two privileged *master beacons*, at Toulouse and Kourou, provide such uplink services. Data uplinked from these stations (which is updated weekly and used by all DORIS instruments in orbit) include the coordinates of the stations, earth rotation parameters *etc*.

4. A subgroup of the CryoSat *Calibration, Validation and Retrieval Team* (CVRT) which was established following the Cal/Val Announcement of Opportunity.

Figure 4.2–1 The global network of DORIS beacons. The red dots mark the positions of beacons, and the visibility circles shown represent the coverage limit for the CryoSat altitude and an elevation angle of 15°.

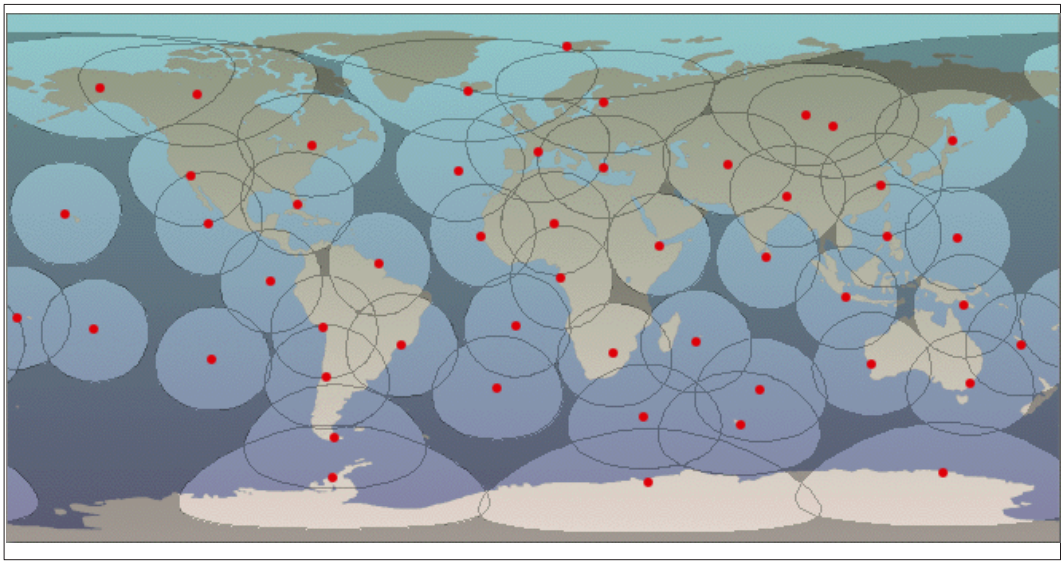

4.2.2 On-board Services

Included in the uplinked messages from the master beacons are time signals which enable the synchronisation of the DORIS internal time reference using the International Atomic Time (*Temps Atomique Internationale*, TAI) system. This time reference is used as the central time reference on board CryoSat. The accuracy with which DORIS is able to provide the on board reference time is 5 μs (1σ) with respect to TAI, although, in general, the *resolution* of the time stamps in the data packets is only 1 ms.

First introduced on SPOT-4, the on-board DORIS instrument includes a software package which processes the beacon signals in order to provide real-time estimates of the orbital state vector. The estimated accuracy of these real-time values are:

- < 1 m (RMS) 3-axis position;
- < 30 cm (RMS) radial component.

This service, sometimes called the DORIS *Navigator*, is used by the on-board systems for satellite navigation, and it is also provided in the telemetry so that good quality orbital parameters will be available before the POD can be produced.

A final on-board service offered by DORIS is the provision of the reference frequency to the SIRAL instrument, which does not have its own ultra-stable oscillator. The frequency of the DORIS oscillator is continuously monitored as part of the POD service, and this measurement will be taken into account in the processing of the SIRAL data.

4.2.3 DORIS Hardware

The hardware implementation of DORIS on CryoSat-2 has changed compared to the original CryoSat, now being the new generation of DORIS receiver to be flown on Jason-2. Although the hardware accommodation is significantly different (one internally-redundant unit replacing the 5 separate boxes of the previous version) the performance and stability are expected to be equivalent to those of the previous equipment.

4.3 Star Tracker

4.3.1 Function and Operation

The Star Tracker is the principal means of determining the orientation of the SIRAL interferometric baseline. It is also the principal 3-axes attitude measurement sensor in the nominal operating mode. It is a lightweight, low power consuming, fully autonomous device capable of delivering high-accuracy inertial attitude measurements in order to satisfy the high pointing knowledge requirement of CryoSat.

A set of three autonomous Star Trackers are accommodated such that the sun and moon can each blind only one head at any time; the baffles around the camera heads mounted on the SIRAL antenna bench are visible in Figure 4.1–2, Figure 4.1–3 and Figure 4.5–1 below. This multiple configuration makes the sensor system one-failure tolerant, except for the occurrence[5] of simultaneous sun and moon blinding of the remaining two heads, to which the system software is tolerant (although the Attitude Control System will revert to Coarse Pointing Mode).

All three Star Trackers are mounted (using brackets made of CFRP and titanium, which have near-zero thermal expansion coefficients) on the SIRAL antenna bench order to maximise the structural stability between the star sensors and the antennas frame.

The camera head of one of these Star Trackers is shown in Figure 4.3–1. Behind the optics is a CCD of 1024 × 1024 pixels, with a field of view of 22° × 22°. With the baffle (shown in Figure 4.3–2) the exclusion angle for the sun is 30° while for the earth or moon it is 25°. The optical axes of the three star trackers are all in the plane parallel to the plane containing the electrical axes of the two SIRAL antennas, and thus parallel to the local vertical. Within this plane the central star tracker points towards the zenith, while the other two point at 65° to either side, keeping the earth horizon outside the exclusion angle.

The Star Trackers are fully autonomous, with no need for ground update of star maps. In its Acquisition Mode, which takes 2 – 3 seconds, the Star Tracker calculates a coarse attitude by matching triangle patterns of stars with patterns stored in its catalogue. After two consecutive successful initial acquisitions it autonomously jumps to Attitude Update Mode in which it uses information from the last attitude update (or initial acquisition) to calculate a precise attitude. This can occur at a rate of up to 1.7 Hz. To cope with possible sun-blinding situations, two camera heads are operated in parallel at full speed at all times.

4.3.2 Performance

The performance of the star tracker has been evaluated by means of a combination of analysis, laboratory measurements and tests using the real night sky. The attitude measurement errors are dependent on the following contributions:

- sensitivity;

5. each one of the star trackers will have a period of about 2 months during a 16 month cycle when it will be sun-blinded during part of the orbit. During those 2 months there will be periods of 2 days during which for a period of about 7 minutes each orbit the moon is in the field of view of the remaining star tracker. If the failed star tracker is one of the 65° camera heads then the moon will be 5 days old (or the equivalent age on the "other side" of new moon), while if the 0° head has failed it will be about 11 days old. The brightness of the moon is quite different in these cases and it is not clear at present what the effect on the star tracker will be.


Moon age 5.3 days


Moon age 10.6 days

Figure 4.3–1 Photograph of one of the three CryoSat Star Tracker camera heads.

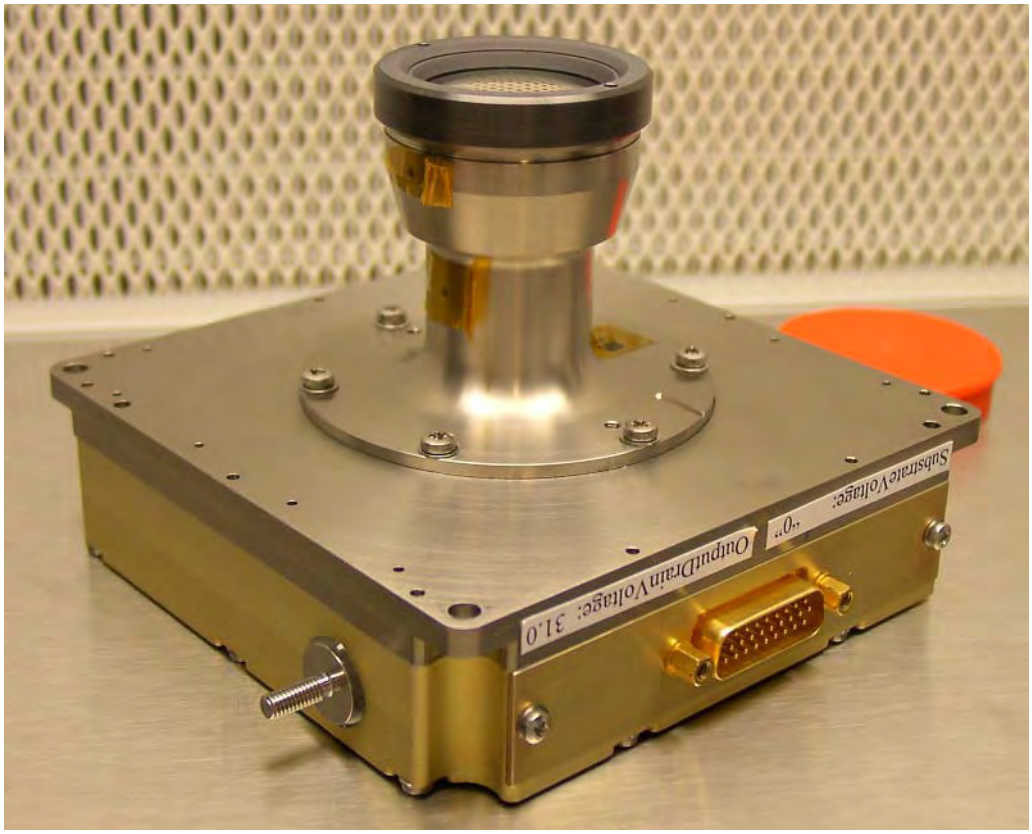

- camera electrical noise;
- Noise Equivalent Angle for a single star;
- chromatic aberration;
- residual errors after calibration of optics;
- centroiding error;
- effect of vacuum.

The Star Tracker algorithm is optimised to use rather faint stars, around magnitude 5. These stars, which are barely visible to the naked eye except at dark sites, are far more numerous than the brighter stars and provide many triangles for use in the pattern matching process in all directions of the sky.

The effect of cosmic rays, and other charged particle radiation, is to dump electrical charge in a pixel in the CCD which might be mistaken for a star. This is avoided by the software, which searches adjacent pixels around each bright spot to search for the diffraction pattern which distinguishes stellar images from single-pixel cosmic ray effects.

Taking account of these contributions, and also the distribution of stars in the field of view, the estimated performance is:

- pitch and yaw axis: $< 2''$ (1σ);
- roll axis: $< 10''$ (1σ).

These axis definitions are in the camera frame of reference, not the satellite frame of reference. Roll (rotation around the optical axis) is less well determined by the algorithm.

Figure 4.3–2 The light baffle for the CryoSat Star Tracker. This photograph was taken during a night sky test with one of the CryoSat TSar Trackers, which was protected in a clean environment. The baffle itself was manufactured as a flight unit was slightly damaged during handling and thereafter only used for testing.

Figure 4.3–3 shows the performance measured during a night sky test, during which the camera head unit was mounted on a thermo-mechanically stable stand pointing to the zenith. Attitudes were acquired for about 30 minutes. The data were corrected for astronomical aberration and compensated for earth rotation (including precession and nutation) to transform them to an earth centred, earth fixed coordinate system.

These results can be summarised as the following 1σ values:

- RA: 0.96 arc sec (*c.f.* analysis: < 2 arcsec)
- Dec: 1.08 arcsec (*c.f.* analysis: < 2 arcsec)
- Roll: 4.91 arcsec (*c.f.* analysis: < 10 arcsec)

4.4 Laser Retroreflector

The Laser Retro-Reflector (LRR) is a passive optical device for ground-based measurement of the satellite orbit by means of Satellite Laser Ranging (SLR) stations. Such LRR's are used on all radar altimeter satellites, and several others as well. The CryoSat LRR will be based on existing LRR's which have flown on many Russian and other satellites, including Meteor-1, 2 and 3, Etalon-1 and 2, GFZ-1 and WESTPAC. It is not the same design as the LRR's which have been used on ERS-1 and 2 and on EnviSat.

Technical and optical parameters for a single corner cube reflector within the overall LRR array are given in Table 4.4–1. These individual corner cubes are recurrent, but the hous-

Figure 4.3–3 Results of a night sky test on the CryoSat Star Tracker (unit FM2), performed 2 Oct 2003.

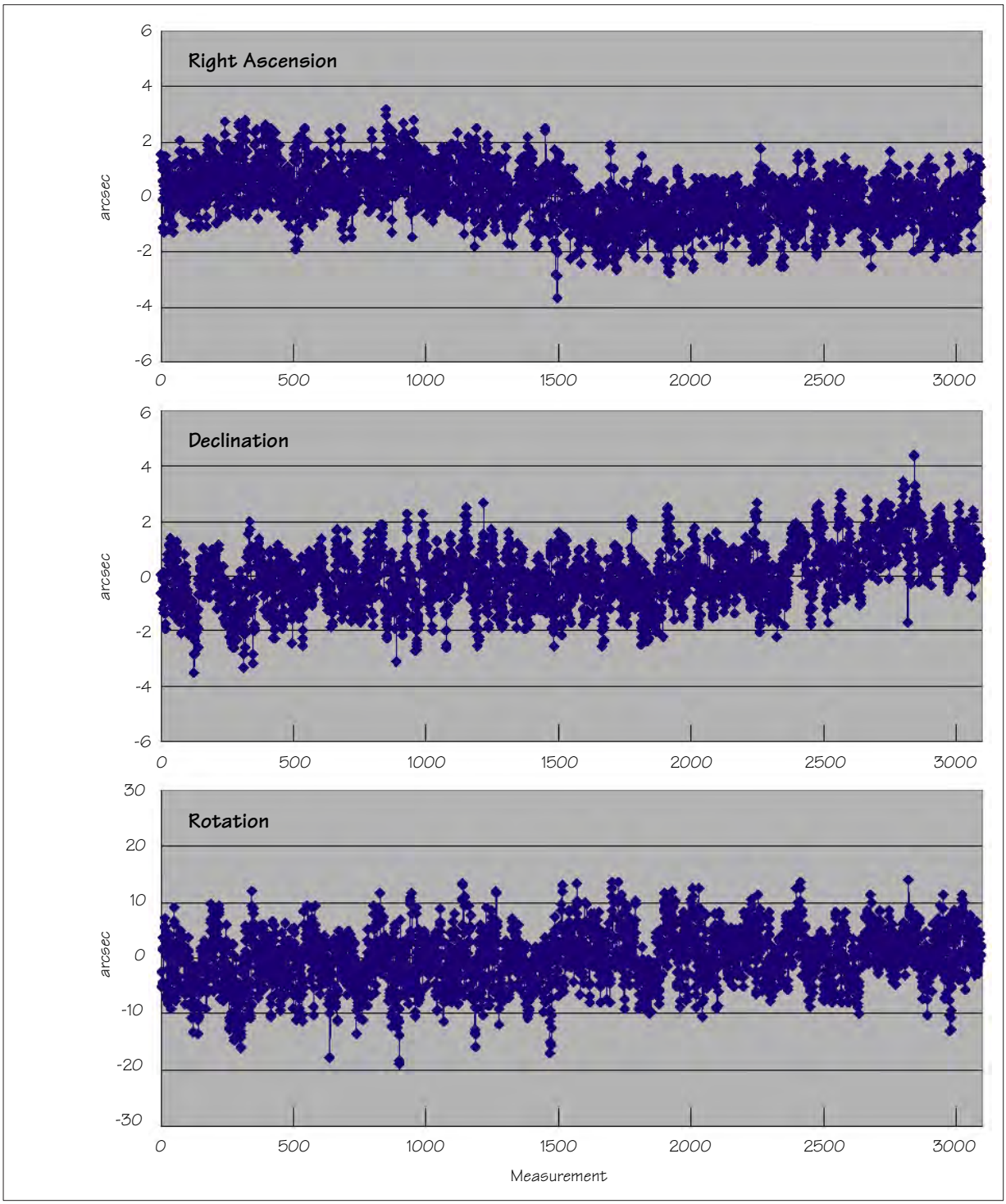

ing to form the LRR array is a new design. This new design is needed to take account of the orbital altitude of CryoSat, which influences both the geometry and the number of cubes needed to provide enough cross-sectional area to satisfy the link budget. The corner cubes within an LRR also have to be customised to compensate for the aberration of light

due to the satellite velocity. If this compensation, achieved by slightly changing the angles of the corner cube faces from orthogonality, is not performed, then the laser light will be reflected by exactly 180° and will return to a point further along the satellite track.This displacement is typically of order a hundred metres away from the SLR station, such that the returned laser light is severely attenuated.

Table 4.4–1 Parameters of a single corner cube reflector

Parameter	Value
Free aperture diameter	28.2 mm
Prism material	Fused quartz
Geometrical area of the input aperture	~6 cm^2
Reflective surface coating	Aluminium
Reflective pattern width	5 … 6 "
Wavelength range	310 … 1450 nm
Transmittance	0.55 … 0.78[1]

1. Depending on the wavelength

The design of the array, containing 7 individual cubes, is shown in Figure 4.4–1 and a photograph is shown in Figure 4.4–2.

Figure 4.4–1 Design of the LRR array

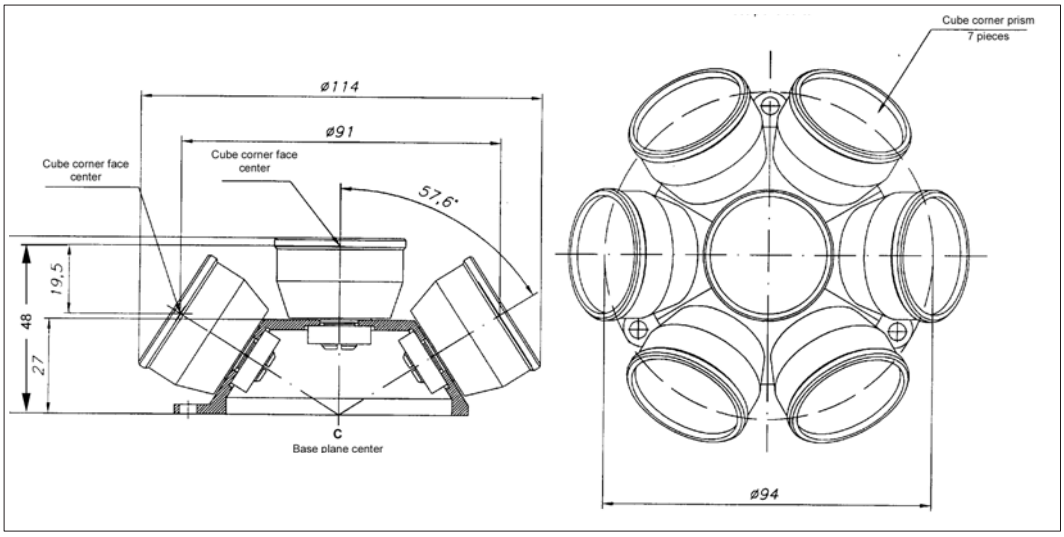

The LRR is accommodated on the nadir plate of the satellite with full visibility towards the earth. Its field of view is ±57.6 °, providing measurements at spacecraft elevation angles greater than 20° for all azimuths. The orientation of the corner cubes optimises the link budget for measurements at these low elevations. In view of the high measurement precision the LRR will be accommodated as close as possible to the satellite centre of gravity to avoid any measurement inaccuracies caused by satellite attitude motion.

Initial calculations for the LRR, provided in Table 4.4–1, identify the optical cross-section (assuming atmospheric transparency grater than 0.7) and a correction to be added to the measured values in order to reduce them to the base plane centre shown in Figure 4.4–1.

Figure 4.4–2 The CryoSat Laser Retroreflector Array

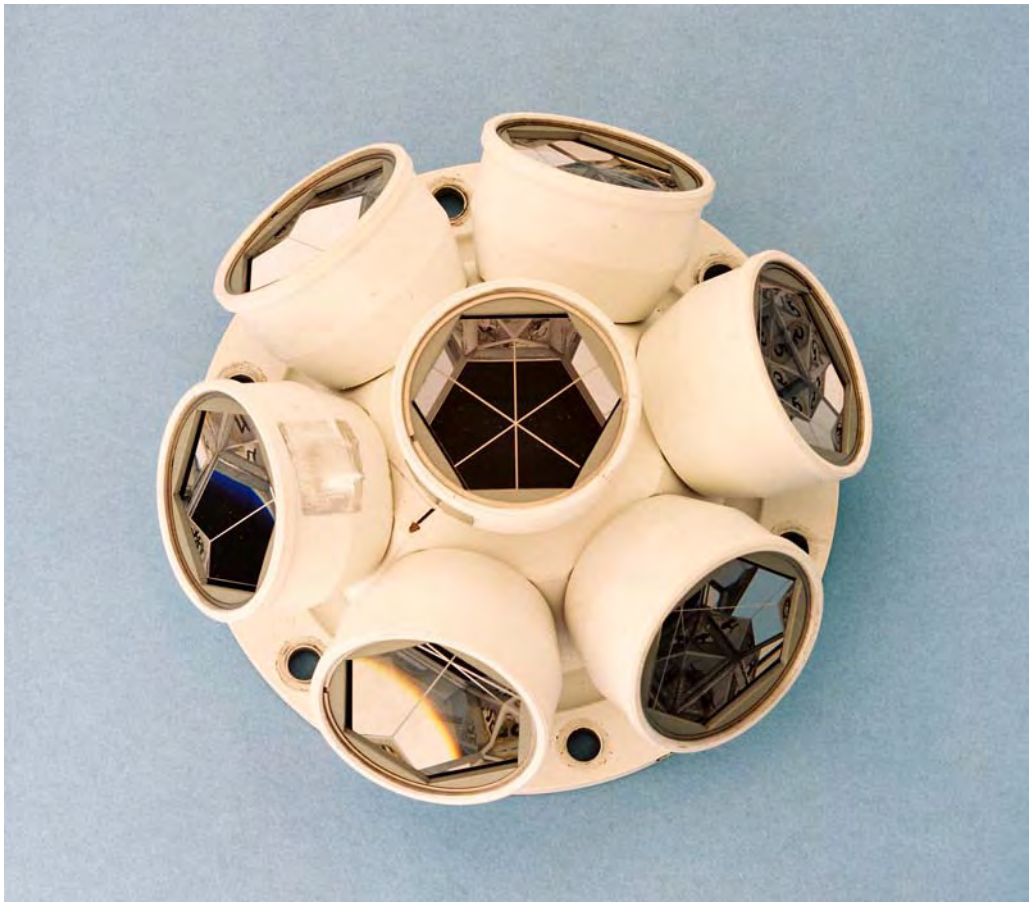

Table 4.4–1 Geometrical and other parameters for the LRR

Elevation at SLR (deg)	Elevation at Satellite (deg)	LRR cross-section ($m^2 \cdot 10^6$)	RMS target error (mm)	Correction value (mm)
90	0.0	1.37	0.6	20.1
80	9.0	1.02	2.4	19.0
70	17.9	0.78	3.3	15.9
60	26.7	0.71	3.0	13.9
50	35.3	0.86	5.9	17.1
40	43.5	1.29	5.6	22.0
30	51.1	1.98	3.6	24.8
20	57.6	2.75	2.3	25.5

Table 4.4–1 also identifies the RMS target error values, which are no more than 6 mm.

4.5 Configuration

A view of the CryoSat configuration was presented earlier, in Figure 4.1–2, and further drawings are presented in Figure 4.5–1 and as a perspective view, in Figure 4.5–2. The satellite has a long rectangular main platform body, above which are mounted two fixed solar arrays in the form of a tent. The lower surface of this structure is permanently earth facing (even in emergencies when the satellite enters Safe Mode). Consequently the antennas used for radio communication as well as the LRR are mounted on this lower surface; an emergency antenna for command and monitoring is also fitted on top of the satellite between the solar arrays. The SIRAL instrument, with its electronic units, large thermal radiator and two antenna mounted on a stable bench structure, is mounted at the front of the satellite. The antennas are covered by a thermally isolating cover, seen in Figure 4.5–2. The Star Tracker camera heads are also mounted on the SIRAL antenna bench. The flight direction is indicated in Figure 4.5–1. The satellite has a small cross section to reduce drag.

CryoSat has a total length of 4.5 m, and width of 2.34 m. The main structural element is a long rectangular tube from the rear to the front of the satellite. The nadir plate is a separate structural element, which is also the primary thermal radiating surface. The “nose-structure” housing the SIRAL is also structurally separate.

The distribution of equipment inside the satellite has been determined by a number of simple design rules. These included: the accommodation of the principal electronic elements on a nadir plate of the body, which is used as a radiator; the location of the SIRAL equipment near to the SIRAL antenna bench to reduce waveguide length; and the location of the cold gas fuel tank at the satellite’s centre of gravity (COG) to eliminate movement of the COG during the lifetime. As a result of this mass distribution, the principal axis of inertia does not coincide with the longitudinal geometrical axis of the satellite. If the satellite flight vector was aligned along the geometrical axis there would be a constant torque, due to the effect of gravity gradient on this principal axis of inertia. Such gravity gradient torques are quite common in satellites and are overcome by opposing torques from the attitude control subsystem. However the CryoSat attitude control subsystem (described in Section 4.8, “Attitude and Orbit Control”) uses the cold gas thrusters to augment its other actuators for attitude control. This uncompensated torque would deplete the supply of fuel; to avoid this the satellite flies in a slightly “nose-down” attitude to align the flight direction with the principal axis of inertia.

Some modifications to the original design have been necessary for CryoSat-2. Several units are new generations of equipment with different mechanical interfaces and there is a new, experimental rate sensor (see Section 4.8.1). Consequently the layout of equipment on the nadir panel had to be modified. The redundant SIRAL could all be accommodated in the nose section. Two additional stiffening struts were introduced and the hole at the aft end has been enlarged to increase the venting after launch. Finally the balance mass has had to be increased to compensate for the additional, redundant SIRAL equipment.

The critical earth-facing antennas, and the LRR, are tilted to align their boresights orthogonal to the flight direction. The Star Tracker camera heads are also mounted, on the SIRAL bench, to take this tilt into account. Finally, the interface to the launcher is achieved through four mounting points on the rear panel.

4.6 Control and Data Handling

In addition to its payload, the CryoSat satellite has other on-board equipment in order to support the mission. We will describe this equipment in this and later Sections. We show, at the level of a block diagram, the whole set of equipment including the payload in Figure 4.6–1. The central control of the whole satellite is implemented by an equipment

Figure 4.5–1 Configuration of the CryoSat satellite. The large SIRAL antennas are elliptical, this is not an artifact of the image. The satellite flies in a "nose-down" attitude, inclined by 6°, in order to avoid excess torques due to gravity gradient effects.

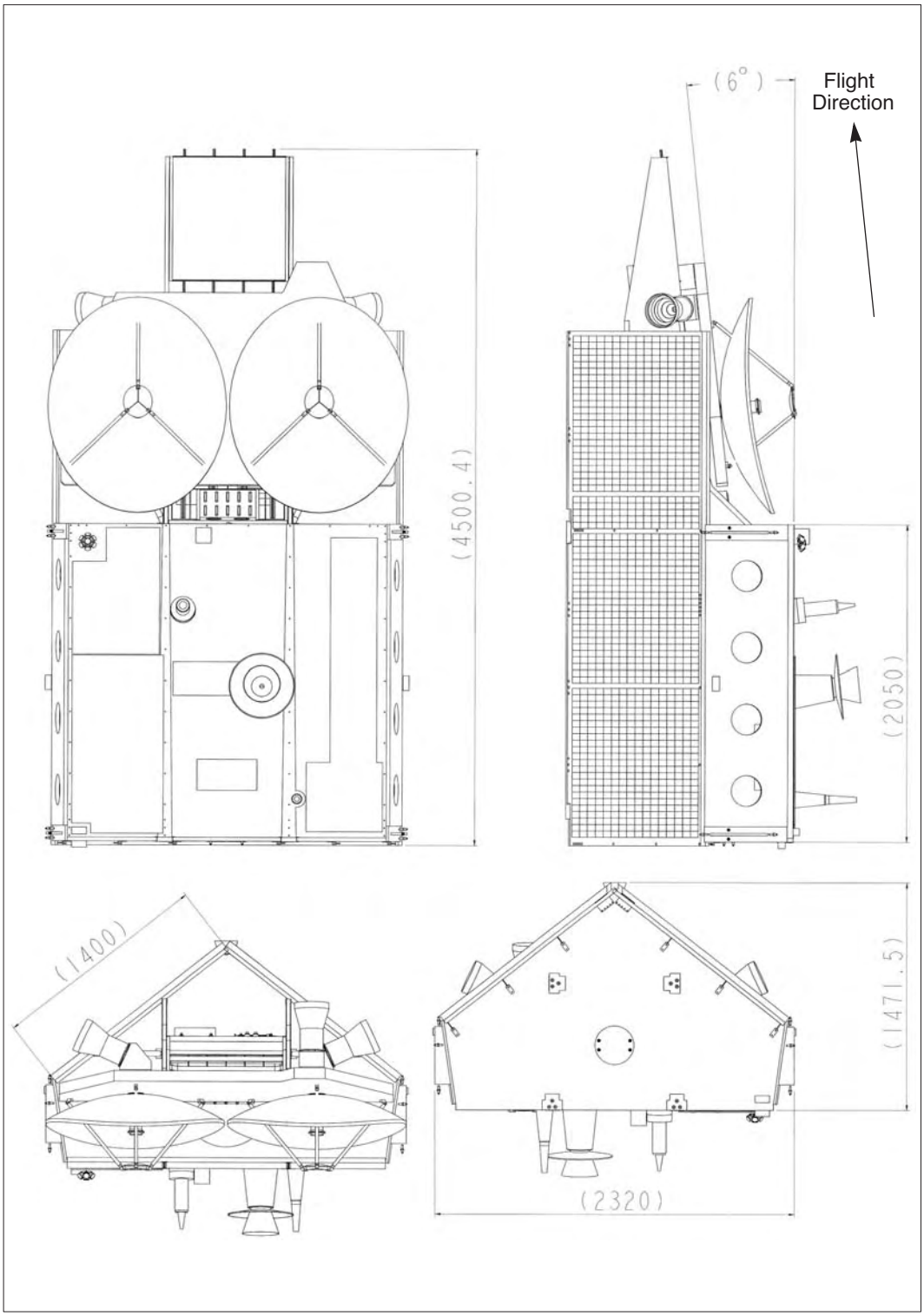

Figure 4.5–2 Perspective view of the CryoSat satellite, showing the thermal covers on the SIRAL antennas.

called the *Control and Data Management Unit*, CDMU, which is part of the *Data Management System*.

This Control and Data Management Unit (CDMU) is the central hub of all on-board operations. It interfaces to all of the satellite equipment in order to monitor their status and to issue commands to them. In order to do this the unit has a range of electrical interfaces: a MIL-Bus-1553 interface is used for the more complex units, such as the SIRAL and DORIS payloads while other units make use of relatively simple serial links. It also has low-level interfaces for the direct acquisition of temperature measurements from thermistors located around the satellite and for the direct control of the attitude control actuators (described in Section 4.8, "Attitude and Orbit Control").

The CDMU runs a number of software tasks concurrently.

- It decodes and interprets incoming telecommands from the ground segment. These commands may be passed for immediate execution by other software processes or by other units. Other commands relate to the management of the master timeline, which contains time-tagged commands for execution later.
- It monitors the status of all the other units on-board the satellite, and, in the event of unexpected situations, controls the fault isolation and recovery.
- It acquires measurements from the attitude sensors and runs the algorithms required to compute any errors in the satellite pointing. It determines the required corrections and generates the commands needed to implement these corrections using the attitude control actuators.
- It monitors temperatures throughout the satellite and commands any required thermal control actions.

This unit contains a high performance processor system based on the ERC32 microprocessor, which is a space version of the SPARC processor. It has 4 Mb of RAM, as well as read-only memory for storing an on-board copy of the flight software. It features a hardware-

Figure 4.6–1 Block diagram of the major elements of the CryoSat satellite, showing the electrical interfaces. The X-Box contains "glue" circuits to resolve small interface inconsistencies resulting from the reuse of existing equipment designs. Redundancy of equipment is indicated.

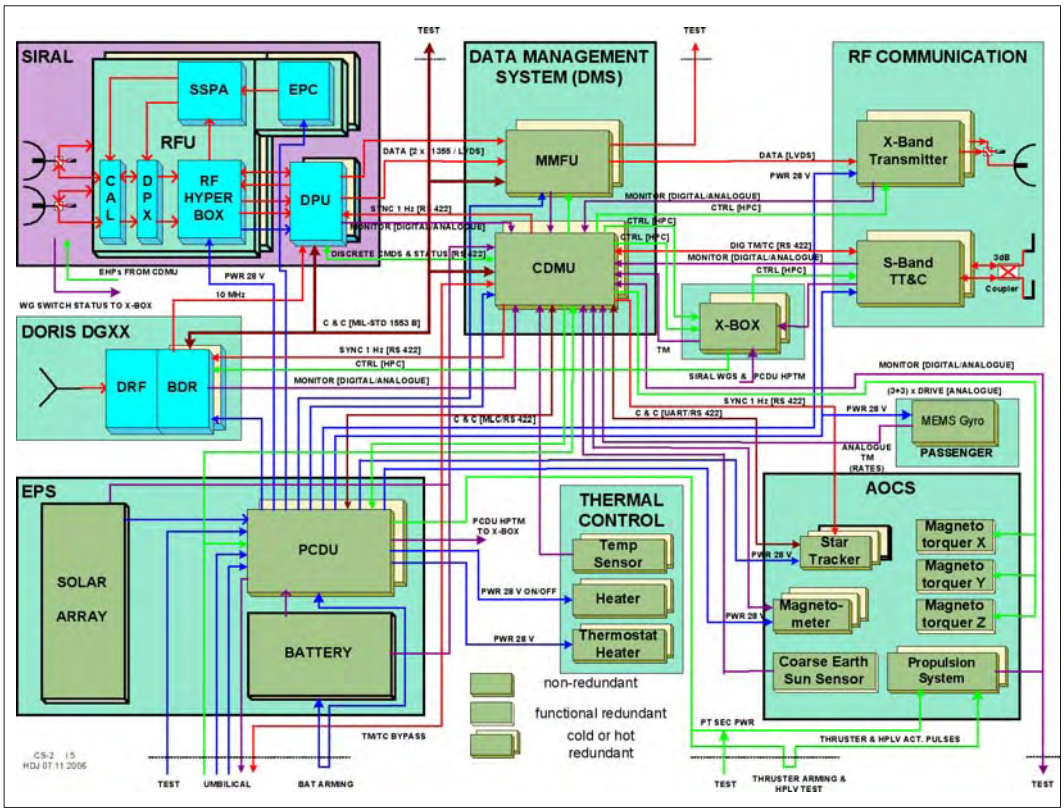

based fault detection system, which is able to start up and switch control to a redundant processor if needed. The many interfaces are handled by a specific hardware module.

In particular it includes the telecommand decoder, which interfaces to the S-band Transponder (described further below) on one side, and the processor on the other. It is possible to command essential functions directly from this telecommand decoder, without software interaction, in emergency situations.

The S-band Transponder, together with S-band antennas, is the physical means by which the CDMU and its telecommand decoder interface to the ground segment. It also enables the ground station to measure the satellite range and range-rate for operational orbit determination. It receives signals (at 2026.7542 MHz) modulated by the telecommand signal and by a ranging tone modulated by codes used for ambiguity resolution. The demodulated telecommands are input to the telecommand decoder. The transponder derives the downlink carrier frequency (2201.0000 MHz) in a fixed ratio of 240/221 to enable coherent Doppler tracking at the ground station. This signal is modulated by the housekeeping telemetry and the coded ranging tone.

Data transfer on this S-band link dedicated to command and control is at the rate of 2 kbps uplink, for commanding, and 8 kbps downlink for housekeeping telemetry. The physical downlink operates at 16 kbps but carries an overhead of error correction coding.

The antennas, a primary antenna on the nadir face, and an emergency patch antenna at the apex of the solar array "tent" provide full spherical coverage.

4.7 Science Data Storage and Downlink

The science data generated by the SIRAL and the other payload elements are stored in the Mass Memory and Formatting Unit, MMFU. This provides a large solid-state memory of 128 Gbits[6] with flexibility in its operations for the storage and dump of data. Data arrive at the MMFU directly from the SIRAL instrument on a pair of fast IEEE 1355 links (for the two high-rate interferometric data channels) and *via* the MIL-Bus-1553 for the low rate data channels. Data are also transferred from the CDMU and the DORIS over the MIL-Bus-1553.

The storage in the MMFU is divided in seven different memory areas, with a granularity of 1 Gbit, each of which is arranged as a circular buffer so that new data will overwrite old. These seven partitions are allocated to the following data storage functions:

1. SIRAL science data on the 1553 bus (LRM and tracker data);
2. SIRAL data on 1355 link 1 (SAR and SARIn channel 1);
3. SIRAL data on 1355 link 2 (SARIn channel 2);
4. science data from the CDMU on 1553 link (DORIS and Star Tracker);
5. housekeeping data from the CDMU;
6. secondary processor (e.g. SIRAL or Star Tracker) memory dump;
7. spare.

The size of these partitions within the overall 128 Gbit limit is established during the initialisation of the equipment. It cannot be reset in flight without loss of all data stored at the time (rather like a computer hard disk). The evaluation of the optimum size for the partitions is currently ongoing, but it is already clear that the sizing of the SIRAL high volume partitions (2 and 3 above) is critical – currently there is uncomfortably little margin.

The MMFU includes a fast data formatter which formats and frames the data, assigning it to a number of virtual data channels, and applying Reed-Solomon error correction codes. These data frames are transferred to the X-band downlink sub-system. Dump of the data while over the ground station is much faster than recording.

The X-band data transmission sub-system has a data downlink rate of 100 Mbps. It operates at a centre frequency of 8100 MHz, which is also one of the EnviSat downlink frequencies. In fact there is no alternative but to overlap frequencies with EnviSat as this satellite, with its 3 broadband downlink channels, is spread all across the available bandwidth. EnviSat and Cryosat are very rarely near the same line of sight from the ground station (in a 6 month simulation there was only one case, lasting a few seconds) as the antenna beam from the ground station is very narrow. Possible interference in such cases will be avoided by operational scheduling.

An isoflux antenna is used to optimise the link budget. This approach is also used on other ESA earth observation missions such as ERS and EnviSat. The antenna is recurrent from the MetOp Programme and is shown in Figure 4.7–1.

The margin in the data downlink is shown in Figure 4.7–2. This shows that for all elevations there is a healthy margin making the system robust against data loss due to unexpectedly high attenuation in the signal path.

6. The smallest memory module available in the current generation of these devices is 128 Gbit (16 Gb) and in order to provide the required memory capacity at end-of-life a second memory module has been installed. However the current design does not allow the usage of this second memory module in parallel to the first. in the event of excessive memory failure (more than can be compensated by the error correction system) the redundant memory module is switched in units of 4 Gbit.

Figure 4.7–1 The X-band antenna used for science data downlink at 100 Mbps. It is stored in a clean container awaiting integration on the satellite. It is inclined at 6° to its base in order to account for the nose-down attitude of the satellite.

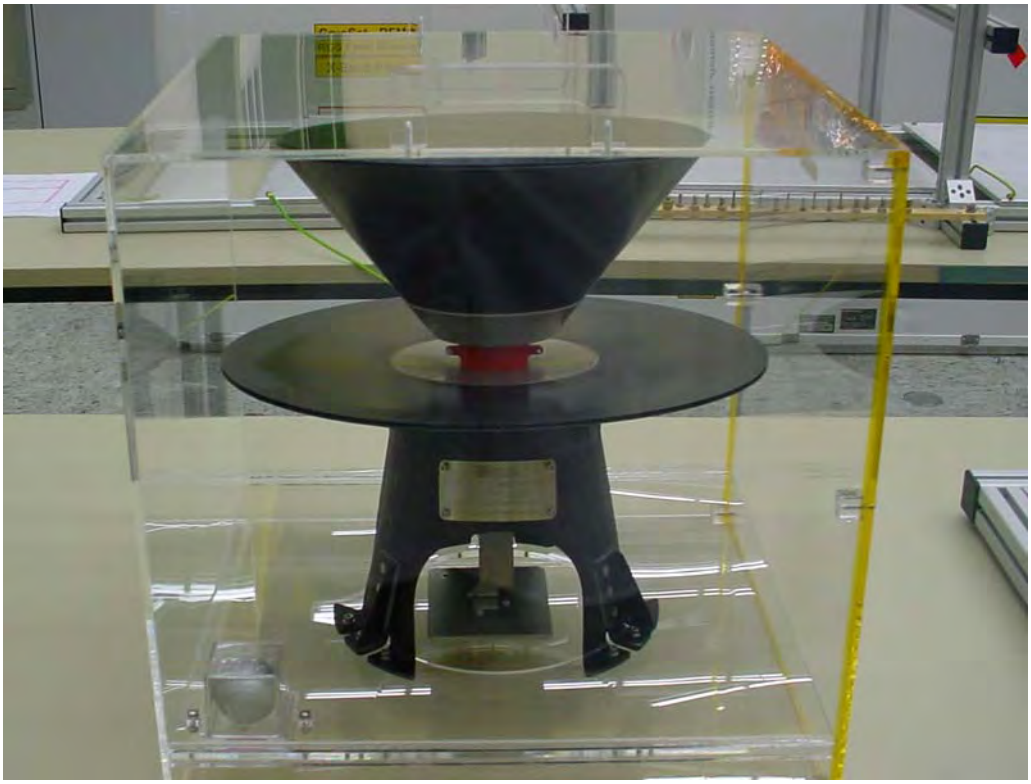

Figure 4.7–2 The margin in the X-band link from CryoSat to the Kiruna station, as a function of elevation angle at the station.

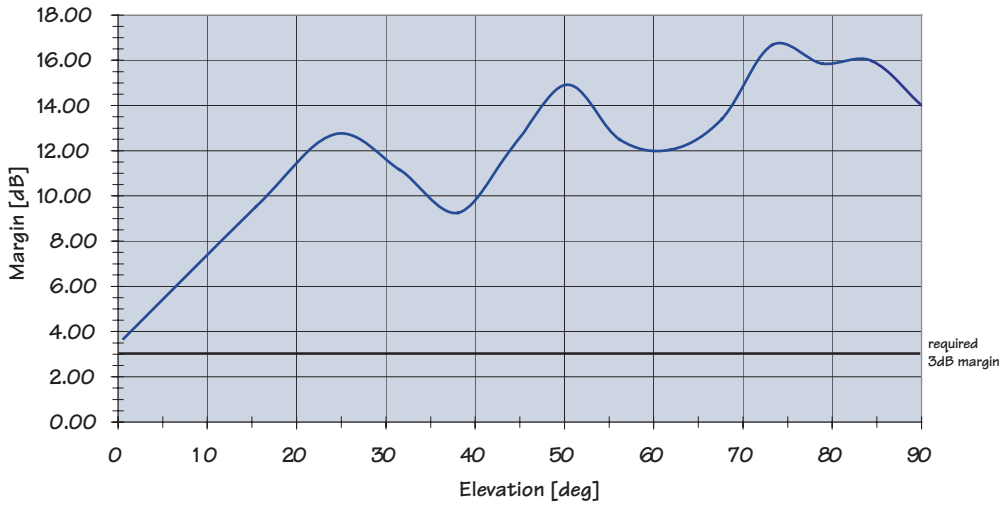

4.8 Attitude and Orbit Control

The Attitude and Orbit Control Subsystem (AOCS) is a combination of hardware and software which are together responsible for ensuring that the satellite is able to acquire and maintain the correct earth-pointing attitude, starting from arbitrary pointing and spin rates, such as those expected on release from the launch vehicle. The subsystem is also responsible for the manoeuvres needed for orbit maintenance and orbital changes, as described in Section 3.3. The modes in which the AOCS may be are:

- Rate Reduction Mode (RRM), in which excess angular rates are reduced (typically this mode follows separation from the launch vehicle).
- Coarse Pointing Mode (CPM), in which the satellite acquires and maintains pointing to within some degrees (typically 15°) of the nominal earth pointing attitude. This mode uses very basic sensors and is used as a fall-back safe mode. Measurements with the SIRAL cannot be made in this mode.
- Fine Pointing Mode (FPM) is the nominal pointing mode, in which the full performance of the AOCS is available.
- Orbit Control Mode (OCM) is used when orbital manoeuvres have to be made.

The main design driver for the AOCS, and in particular for the selection of its equipment, is the high pointing accuracy, knowledge and stability requirement in the nominal earth-pointing phase. We show these requirements, and the estimated performance budget, in Table 4.8–1. Additionally this subsystem has to be able to perform the orbit changes necessary to acquire the nominal orbit following injection from the launcher.

Table 4.8–1 Requirements and budget values for pointing parameters for the interferometric baseline.

Quantity	Control Accuracy	Pointing Knowledge	Stability (over 0.5 s)
Requirement	< 0.2°	<35"	<0.005°
Budget Value	0.1°	27.6 "	<0.001°

The CryoSat AOCS uses measurements from the following sensors.

- **Star Tracker:** a set of 3 star tracker heads (see Section 4.3), which are regarded as part of the payload, autonomously provide high accuracy inertial attitude determination at a rate of 1.7 Hz.
- **DORIS** (see Section 4.2): again part of the scientific payload, provides real time measurements of satellite position, velocity and time. This information is used in the conversion of the inertial attitude measured by the star tracker into earth referenced attitude.
- **Coarse Earth-Sun Sensor** (CESS): a novel sensor, first used on CHAMP. It uses a set of six heads distributed around the satellite, pointing along each of the satellite axes. Each is equipped with two surfaces of known optical properties (*e.g.* white and black), and each surface has a set of three platinum resistance thermometers mounted on it. All of these temperatures are acquired by the main computer (see Section 4.6) which runs an algorithm which is able to compute the direction of the earth and sun, in the satellite reference frame, based on the distribution of temperatures amongst these surfaces of known optical properties. The sensor is simple and robust, yet delivers the measurement accuracy needed for coarse attitude acquisition and for the maintenance of pointing in Coarse Pointing Mode (the "safe mode").

- **Magnetometers**: a set of three axis magnetometers, located at the opposite end of the satellite from the magnetotorquers (see later) are used for magnetotorquer control and as rate sensors.

The measurements from these sensors are processed, according to the mode of the satellite, in order to compare the measured earth-referenced attitude with the attitude required by the pointing law. This law requires pointing the electrical axes (initially assumed to be the same as the mechanical axes) of the SIRAL antennas towards the local normal to the WGS-84 ellipsoid, and rotated in yaw to compensate for earth rotation ("yaw steering"). This axis is rotated by 6° from the satellite's *z*-axis, as discussed in Section 4.5.

In CryoSat there is no dedicated processor for this computation required for the AOCS. It runs in the same processor as the other spacecraft control functions, the CDMU (see Section 4.6). The software computes the required torques in order to close the control loop between the observed attitude and the required law, and commands the operation of the actuators in order to achieve these torques. The available actuators are:

- **Magnetotorquers:** a set of 3 magnetotorquers, aligned along the satellite axes, are provided. These are redundant electrical coils wound around a core of high permeability. They may be activated by an electric current in either direction. The resulting magnetic field interacts with the earths magnetic field to produce a torque. The CDMU makes use of the measurements from the magnetometers (see above) to determine the appropriate current drives. There will always be one direction, around the local geomagnetic field vector, in which it is impossible to generate a torque in this way. This direction changes, in the satellite reference frame, all around the orbit.
- **Reaction Control Subsystem**: this is a cold gas propulsion system for auxiliary attitude control (in which it provide dead-band protection around the axis defined by the instantaneous geomagnetic field) and for orbit transfer and maintenance manoeuvres. It has 16 attitude control thrusters of 10 mN each and 4 orbit control thrusters of 40 mN each. The propellant is gaseous nitrogen, which is stored in a 132 l tank at a maximum expected operating pressure of 276 bar. The thrusters are not operated at this high pressure; a high pressure regulator maintains the pressure in the low-pressure feed system to the thrusters at a constant 1.5 bar.

The attitude control in the normal operating mode, the Fine Pointing Mode (FPM) is, as noted above, primarily based on the use of magnetotorquer although dead-band protection requires the use of small cold-gas thrusters. In principle, each pair of thrusters produces precisely matched pulses (thrusts) that produce a torque around one of the three principle axes of the satellite and no net force along these axes. In reality, due to imperfections of the thruster activation times and duration, misalignment of the thrusters or asymmetry of the exhaust gases, *etc.*, the thruster pulses may not exactly balance and net forces are introduced. Such a net force, even a tiny one, will anomalously accelerate the satellite in that direction and hence, in the long run, will also change the position of the satellite. This may degrade the Precise Orbit Determination.

This effect has been studied by *Scharroo and Visser* [Ref. 5] and by *Shum* [Ref. 6]. The overall conclusions are that the effect of thruster forces is marginal if the thruster pairs are arranged such that no pair is aligned with the flight direction. This is the case, as shown in Figure 4.8–1.

4.8.1 Experimental Rate Sensor

CryoSat-2 will carry a small technology experiment as a passenger. This device is an attitude rate sensor based on Micro-Electro-Mechanical-Systems (MEMS) technology in which microelectronics and mechanical devices (in this case a sensor) are fabricated on the

Figure 4.8–1 Direction of thrust of the attitude control thrusters. None of them acts in the along-track direction, yet combinations of 2 or 4 thrusters are able to provide pure torques about each axis. For example the pair y1 and y2 provide a torque in yaw, while the quad p1 and p2 provide a torque in pitch.

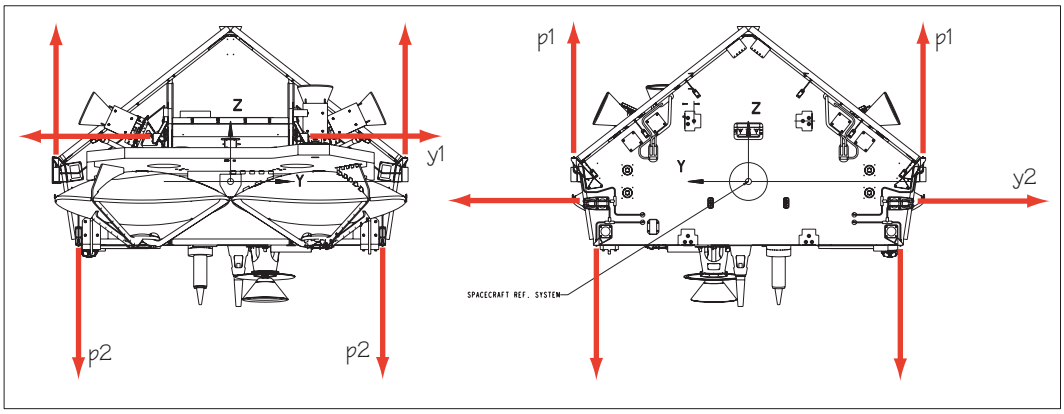

same substrate. The MEMS sensor detects attitude rate to provide the same function as a more traditional gyro and is based on a device widely used in in-car navigation systems.

Three orthogonal MEMS sensors are mounted in the experiment, to measure 3-axis attitude rates. The unit is called MEMS Rate Sensor (MRS) in the CryoSat context[7] and it is under development within the technology directorate of ESA with the goal of providing a low-cost rate-sensor or gyro. The device is provided free of charge to CryoSat-2 in exchange for the flight opportunity.

The measurement data are not used on-board and only sent in housekeeping telemetry to the flight control centre. Here they will be used as an additional data type in monitoring satellite dynamics during attitude transitions.

The CryoSat MRS has some operating limitations due to the constraints of fitting it into an existing design. In particular it will use analog outputs instead of the intended 16-bit digital outputs, since CryoSat has 3 spare analog channels available. These are digitised as 8-bit values so the MRS has to apply gain-switching to these analog outputs. Two such gains are available: in Mode 1 the dynamic range is 20°/s with a resolution of 70 arcsec/s, while in Mode 2 the range is 1°/s with a resolution of 3.5 arcsec/s. In Mode 1 the MRS will be able to measure the attitude dynamics during the launch while Mode 2 is sized for the expected rates after separation from the launcher.

4.9 Electrical Power

CryoSat will spend many periods during its 3.5 year mission undergoing eclipses, of varying duration. It needs a source of primary power (a solar array), a means of energy storage (a battery) and a unit to control the generation and storage of power, and its distribution on board (the power control and distribution unit, PCDU). Due to the nodal regression of the orbit the illumination conditions change significantly, and the satellite must maintain its orientation with respect to the flight direction to keep its interferometric baseline across track. The satellite configuration, and particularly the orientation of the two solar array

7. In the context of the technology programme in which the MRS has been developed it is called SiREUS-FExp, for European Silicon Rate Sensor Flight Experiment.

panels, has been designed to cope with these conditions, without any rotation or moving parts being needed.

Since the arrays have no moving parts, and also no parts deployed after launch, there is a constraint on the physical size of the array panels due to the size of the launcher fairing. The satellite equipment and its payload are relatively power consuming so, in order to maintain the full operations even in the times of the worst overall solar illumination around the orbit, it is necessary to use solar cells with a very high efficiency in converting sunlight to electricity. The cells chosen are advanced triple-junction gallium-arsenide (GaAs) with an efficiency of 27.5%.

The solar array can generate >850 W per panel at end of life, assuming normal solar incidence. Power control of the array is provided by a sequential switching shunt regulator.

The secondary power source, the battery, is a set of Lithium-Ion cells. This type of battery has many advantages compared to nickel-cadmium (NiCd), including better (and more tolerant) recharge performance and easier handling during pre-launch activities. The CryoSat-2 battery has a 78 Ah capacity at launch, increased to ensure >53Ah after 5.5 years in orbit.

The on-board power bus is unregulated; this allows an efficient power system which avoids over-sizing of the solar array, and power management electronics.In this configuration the battery provides its energy directly onto the power bus during eclipse and also during sunlight periods where the solar array cannot cover the peak load. The nominal voltage is 28 V, but can range between 22 V and 34 V.

The overall power demand, in nominal conditions, is given in Table 4.9–1.

Table 4.9–1 CryoSat power demand in nominal conditions, not including margin nor the power required for battery charging. The Satellite value includes the dissipation in the wiring harness. All values are in watts.

Item	SIRAL Standby	SIRAL LRM	SIRAL SARIn	SIRAL SAR	SIRAL SAR + X-band
SIRAL	61.9	95.6	124.1	127.1	127.1
DORIS	30.0	30.0	30.0	30.0	30.0
Platform	188.5	189.7	191,4	182.6	264.4
Satellite	281.9	317.5	348.3	342.4	425.9

4.10 Thermal Control

The Thermal Control system is relatively conventional, in that it relies on a mixture of passive radiators and insulating blankets, in combination with controlled heaters. However, there are a number of critical points:

- the use of the earth facing side as the radiator;
- the temperature extremes of the solar array;
- adequate heat radiation from the SIRAL electronics units;
- thermal stability requirements of the SIRAL electronics;
- stringent thermal stability requirements for the SIRAL antenna bench.

These points will be addressed in the following paragraphs.

The only surface which does not, at some time, point towards the sun for significant periods is the earth-facing side. Therefore CryoSat exploits the nominal earth-pointing atti-

tude: all of the dissipating units of the platform are mounted on the nadir-facing panel, which is equipped with appropriate radiators. The earth is warmer than cold space, the normal sink temperature for spacecraft radiators, but this is compensated by appropriate sizing of the radiators. These radiators, together with thermistors, thermostats and heaters keep the units and instruments within the required temperature range. In nominal operation the thermistor / heater systems are controlled by the CDMU. For failure cases thermostats protect the units against extreme low or high temperatures. The consequence of this design approach is that the satellite has to maintain the nominal earth pointing even in Safe Mode.

The satellite configuration has been described in Section 4.5, in which the tent-like form of the solar arrays was shown. Depending on the local solar time these may be both illuminated, or one or the other may be in permanent shadow. The ability of the array to generate power is also variable, depending on the solar aspect angle, and the instantaneous power demand is also fluctuating due to the mix of payload operating modes. Some array sections may be switched off by the power control system at times; the 21% of incident solar energy which would otherwise be transported into the electrical power subsystem then remains as absorbed heat in the panels. This gives rise to extreme temperature variations over the long term. In order to try to reduce these variations the solar array panels are not insulated from the satellite body, which can radiate to the inner compartment of the satellite. Areas of the solar array with no possibility of cooling by radiation from the backside are always kept in operational mode to prevent the absorbed solar flux heating them up.

The SIRAL electronic boxes are located on the nose structure holding the SIRAL antennas. The radiator for these electronic boxes is located at the top of the satellite. The main radiating side of the radiator points towards the earth although the zenith side radiates 50% to space. The dissipated heat of the boxes is conducted by 4 identical one-dimensional heat pipes to the radiator.

5 Operations

5.1 Operations Concept

The overall operational planning of the CryoSat mission is performed according to a small set of rules assigning priority to different types of operations. These are summarised, as a function of mission phase, in Table 5.1–1. This priority list will be reviewed prior to the launch of CryoSat-2.

Table 5.1–1 Operations priorities as a function of mission phase.

Commissioning Phase	Science Phase
Satellite safety	Satellite safety
Support to validation campaigns	Support to validation campaigns
System and payload calibration	Nominal mission (cryosphere)
Validation time-series	Accepted AO acquisitions
Nominal mission (cryosphere)	Validation time-series
	System calibration
	Ocean altimetry

Within these rules the operations of CryoSat will be conducted according to very few principles, in order to avoid unnecessary complexity. While the simplification afforded to the control system by this approach is significant, it does not impose any constraint on the full exploitation of the system. The principles for the operations are:

- Command and Control as well as downlink of scientific telemetry is performed using a single ground station;
- the payload is continuously on, and SIRAL is the only instrument which needs mode switching commands;
- the SIRAL mode switching is mostly based on a geographical mask;
- SIRAL operations not included in the mask (such as calibration or validation) will be manually inserted into the operations time-line;
- operations are automated as far as possible – the satellite itself is autonomous for up to 72 hours, including in emergency conditions, thus eliminating the need for operator shifts outside normal working hours;
- after the acquisition of the nominal Science Phase orbit it is not foreseen to change to the Validation Phase orbit (2-day repeat) during the mission.

5.2 Geographical Mask

Switching sequences between SIRAL modes will generally be derived from a geographical mask. The geographical mask will be updated regularly, to allow for the changing extent of sea-ice (at least). The system can tolerate updates every month. In Figure 5.2–1 we show an example of such a mask – this is a composite of the one supplied to the satellite manufacturer in order to dimension the CryoSat subsystems, such as data storage, together with the results of the initial CryoSat Data AO. This mask shows the winter extent of sea-ice in both hemispheres and is therefore a “worst-case” for resource sizing.

Figure 5.2–1 Extent of the regions defining the reference mission, to be used during the Science Phase. In addition to the cryospheric mission a number of regions have been added in response to the Data AO.

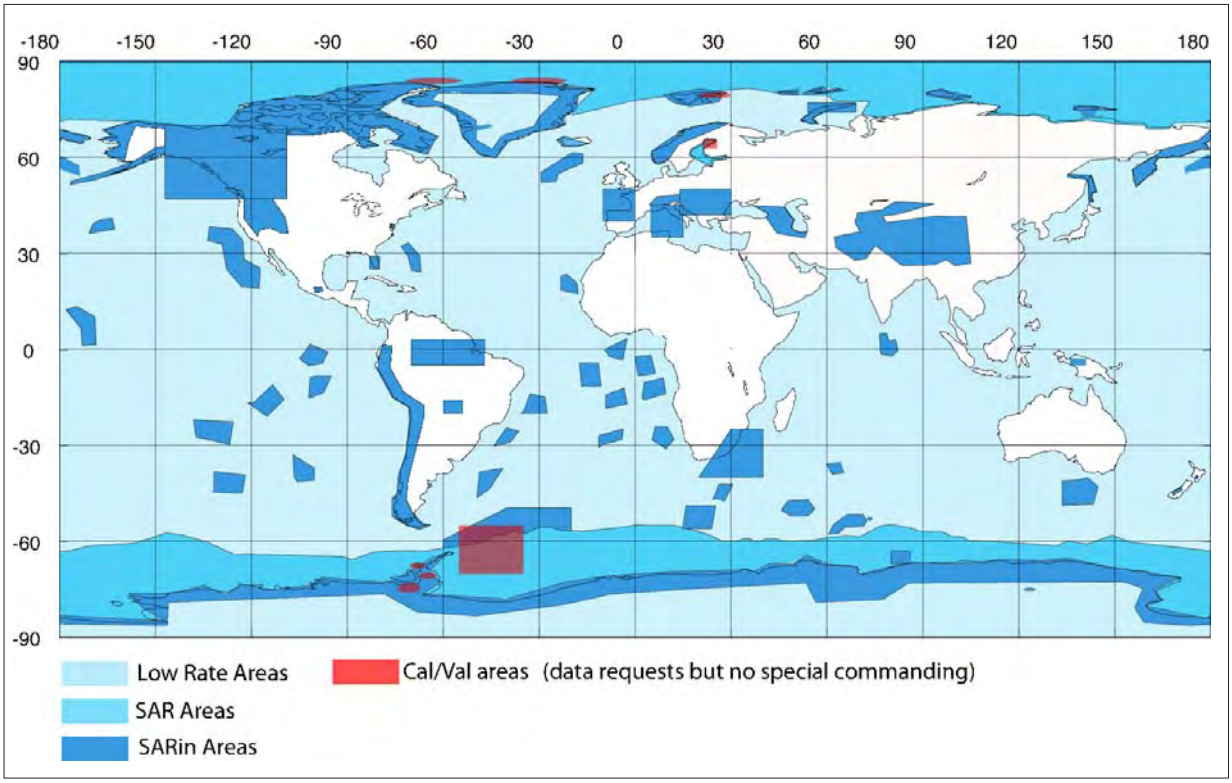

The geographical mask will be converted into a weekly timeline of instrument commands, by means of a dedicated software tool, taking into account the CryoSat reference orbit. It will be combined with commands for regular satellite activities, such as activation of the science data downlink over the ground station. This weekly timeline will be uploaded to the satellite one week in advance. The timeline (on-board and on-ground) may be updated after generation or uplink, with some constraints.

In addition to the SIRAL mode switching defined by the geographical mask, the Low Resolution mode will be operated over the major ocean basins, within the resource capabilities of the satellite. The key resources are power and data storage, and both of these will have a varying margin through the life, due to the rather irregular operations of the satellite. Nevertheless we expect to be able to provide substantial coverage of ocean basins most of the time.

A further possibility is operation over land. It is not foreseen to operate the SIRAL over ice-free land, but, within the limited resources available, it is possible.

5.3 Operations Planning

The overall procedures for the CryoSat mission operations, including the means and authority for the updates to the geographical mask, will be reviewed prior to launch. However we can identify some principles:

- the authority for all CryoSat operations will be the *Mission Manager*;

- the operations of CryoSat shall principally provide the measurements required to satisfy the mission requirements as defined in [Ref. 1]. Requests for measurements in support of other objectives shall only be granted within the resources remaining;
- the geographical mask will be updated regularly in order to track the sea-ice boundaries;
- specific operations, in which the SIRAL will be commanded into a mode other than that defined by the geographical mask at that time or place, in support of calibration and/or validation activities will be coordinated by the CVRT[8];
- specific operations for other purposes specified in those AO proposals already accepted for the original CryoSat mission are authorised within the resource capabilities. A further AO for the exploitation of CryoSat data will provide a mechanism for any additional requests.

8. the establishment of the CryoSat Calibration, Validation and Retrieval Team (CVRT) was a consequence of the first CryoSat AO, for Calibration, Validation and Retrieval. The formation of the CVRT, and its scope, is defined in the AO text.

6 CryoSat Ground Segment

The Ground Segment for the CryoSat mission, like the Space Segment, makes use of existing infrastructure and the reuse of existing designs, wherever this is possible. This offers savings in both development and operational costs.

The Ground Segment implements the following main functions:

- *mission planning*: the spacecraft maintenance activities and the radar altimeter mode changes have to be planned – we described this in Chapter 5, "Operations";
- *data processing, archiving and distribution:* all data products are generated and archived at Kiruna during the mission, Level-1b and Level-2 are distributed to the scientific community – we describe this in Section 6.2. Note that limited amounts of other, intermediate data products will be distributed to dedicated validation teams, in order to support products validation;
- *satellite command and control:* instrument and spacecraft commands are uplinked and recorded telemetry acquired by the Kiruna ground station – we describe this is Section 6.4.

Further activities are needed in order to fully exploit the CryoSat data, and these are performed outside of the project itself. We describe these in Section 6.3.

6.1 Architecture

The CryoSat mission is very focused both in its objectives and in its implementation. Therefore the architecture of the CryoSat Ground Segment is relatively simple, although the principle of re-use and sharing with other missions, which we mentioned above, does lead to some complexities. However the benefits to the programme of such re-use outweigh the additional interfaces introduced.

We show the architectural breakdown and major data flows of the CryoSat Ground Segment in Figure 6.1–1. The major elements are:

- A *Reference Planning Facility* (RPF): responsible for the planning of the payload and the satellite resources verification.
- A *Flight Operations Segment* (FOS): responsible for the telecommand scheduling, satellite command and control, and telemetry acquisition.
- A *Payload Data Segment* (PDS): responsible of scientific data processing, archiving and distribution.
- A *Monitoring Facility* (MF): responsible for providing measures of the performance of the system, and in particular of the instruments.
- Complementary supporting ESA elements, shared with other missions:
  - the *User Services Facility* (USF);
  - the *Long-Term Archive* (LTA).
- Other elements outside ESA:
  - SSALTO, the DORIS control and processing centre which provides precise orbits;
  - auxiliary data providers (*e.g.* meteorological data);
  - Satellite Laser Ranging (SLR) stations.
- We also include the User Community and the Calibration, Validation and Retrieval Team in this Figure.

Although the ground segment makes use of a single ground station its functions are nevertheless distributed among several locations, and these are implemented under several

Figure 6.1–1 Functional breakdown of the CryoSat system, including the major data flows. See the main text for a description of the elements.

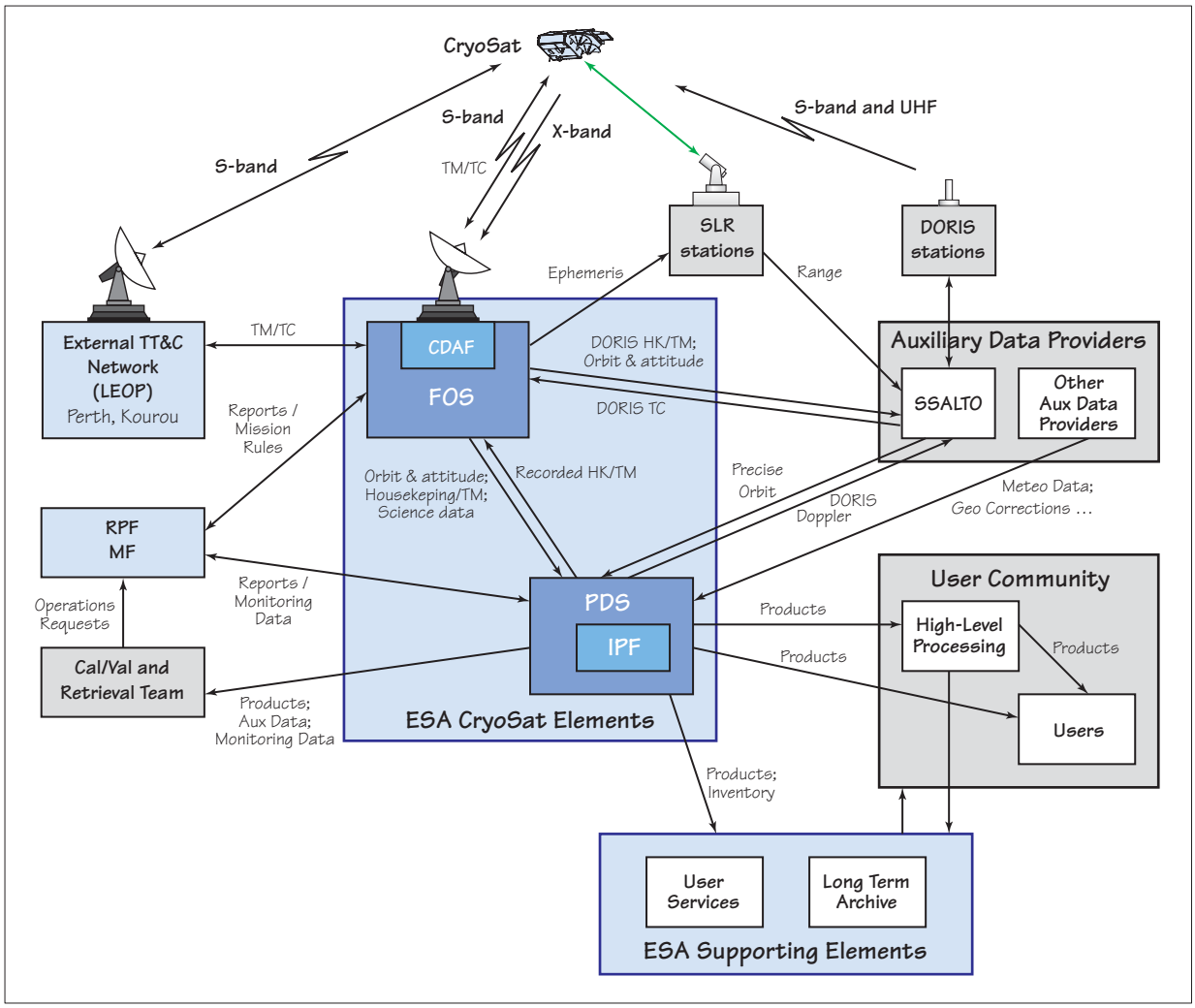

responsibilities. In Figure 6.1–1 we have shown ESA facilities in blue colours, while non-ESA facilities are grey.

6.2 Payload Data Segment

As we stated above, the PDS is responsible of scientific data processing, archiving and distribution. In this Section we will describe the functions and configuration of the PDS. Data processing may be categorised according to the time when it is performed; we take this approach in the following Sections. We will describe the data products themselves in Chapter 7, "Data Products".

6.2.1 Functions

The Payload Data Segment (PDS) is located at the ESA ground station at Salmijärvi, near Kiruna in northern Sweden. It is collocated with the FOS Command and Data Acquisition

Facility (CDAF), used for the command and control of the mission (see Section 6.4) and for the reception of the downlinked science telemetry. The Kiruna ground station also hosts facilities used for other ESA Earth observations missions, ERS and EnviSat. Unlike these other missions, Kiruna is the only data downlink station for CryoSat, allowing the single PDS to process the data without the need to consolidate data dumps from different sites.

The PDS is required to perform the following functions within the overall CryoSat Ground Segment:

- ingest the stream of raw data directly from the demodulators of the CDAF, in real-time during the downlink data dump;
- process this data stream to files containing level 0 data, by decoding the telemetry frames, separating virtual channels[9] and generating files sorted by Application ID (APID)[10];
- distribute the level 0 housekeeping telemetry (HK/TM) files to the FOS shortly after the end of the satellite pass;
- distribute the files containing DORIS level 0 data to SSALTO;
- archive the level 0 data locally;
- process data required in near real time (see Section 6.2.5);
- distribute and archive near real time data products;
- ingest precision orbit data from SSALTO, and geophysical correction data files from other sources;
- process archived level 0 data files to produce the full range of products (see Chapter 7, "Data Products");
- distribute and archive processed data products;
- distribute product inventory information.

Additionally the PDS has to have a command and control function, able to monitor its internal processes and to respond to commands. It must also maintain a database of processing parameters, many derived from instrument characterisation, and it must correctly associate these parameters with the data being processed.

6.2.2 Configuration

The PDS operates as a pipeline process, and is data-driven. It is triggered by the arrival of data, during the satellite pass: ingestion and level 0 processing are performed in real-time. Other than a few near real time tasks (transfer of HK/TM and any near real time processing required for calibration or validation), handling of all acquired data is performed in deferred time. This avoids the transfer of the very large amount of raw scientific data (more than 400 Gbits per day) over a wide area network. All of the processing steps (full bit rate, level 1b and level 2) are concatenated in order to maximise system efficiency.

The PDS includes an element called the *Instrument Processing Facility* (IPF) which implements the algorithms required for the processing of the payload data from level 0 to generate data products. This is a scalable sub-system which is developed independently. The remainder of the PDS performs the other functions identified in the previous Section.

9. all science data share a single virtual channel, and recorded housekeeping telemetry has another.

10. each different type of source packet has a unique APID, and source packets from each SIRAL mode has a separate APID (and interferometric channels have one for each channel).

6.2.3 Real-Time Processing

As we have described, only level 0 processing, of all the telemetry, is performed in real-time, since it uses real-time demodulated downlink signal as input. The result is level 0 data products, including instrument data and raw house-keeping telemetry data.

6.2.4 Routine Processing

The bulk of the processing performed by the PDS will be data driven, and systematic, *i.e.* when SIRAL data, and all required auxiliary data, are available they have to be processed. The main driver is the delay before the precise orbit information will be available, which will take one month.

All available SIRAL data will be systematically processed, and all results will be systematically distributed to registered users.

6.2.5 Near Real Time (NRT) Processing

Near Real Time (NRT) processing will be required to generate the monitoring data used for the verification of payload health and status, beyond what can be detected by housekeeping telemetry. Such monitoring of basic instrument characteristics derived from the science data stream has proved to be vital in detecting problems in previous altimeters, such as ERS and Poseidon. Such data will typically be produced within about 4 hours.

Near Real Time processing will also be needed to generate, on-request, the data products needed to provide rapid feedback during calibration or validation campaigns. Specific commands will be issued to the PDS to generate these data, and due to constraints on the processing capacity and on the on-line distribution means, there will be constraints applied to the volume of data produced. The particular constraints will be dependent on the level of data product which is required. These campaign support data will typically be available within one day.

This NRT processing cannot wait for the precise orbit and so the DORIS Navigator orbit, computed on-board and available as a result of the real-time level 0 processing, will be used.

6.2.6 Re-Processing

The PDS has been designed to support re-processing of the data.

There are two classes of re-processing and both are foreseen in the PDS. Firstly it may be necessary to re-process data due to updates in auxiliary data or other causes (such as spurious errors in the processing chain). Such re-processing is often limited in scale and uses the same versions of the processing software. Re-processing of this type may be performed within the capacity margins of the system.

The second class of re-processing is much more extensive and results from significant upgrades to the processing software itself. A major upgrade is inevitable at least once during the CryoSat mission as the SIRAL is a new sensor and the needs of the programme development have meant that the design of the processor has been several years prior to launch.

Improvement of the processing software will be partially based on the calibration and validation activities. New software will be developed in a suitable development environment, making use of CryoSat measurement data and other validation data. After verification and acceptance of the new software in the IPF it will be installed in the PDS, replacing the obsolete processing software. Furthermore it will trigger the need to perform a systematic re-processing of all accumulated data, in parallel to the on-going

processing of the newly acquired data. Such re-processing will put a significant load on the processing capacity of the PDS, and in particular, the IPF. However the design of the IPF is scalable so that this extra power may be added when it is needed.

Note, however, that in order to simplify operations and avoid perturbations to the routine PDS operations, re-processing will likely be performed off-line in the Long-Term Archive Facility (see below).

6.3 Other Elements

In this Section we will provide some information about some of the other elements of the ground segment which appear in Figure 6.1–1.

6.3.1 Mission Management

We described some of the responsibilities of the Mission Manager in Section 5.3. In addition to these responsibilities the Mission Manager is the point of contact between the PDS and the user community, including the Calibration, Validation and Retrieval Team. He will receive requests and issue the corresponding instructions to the PDS (and the FOS) and he will receive reports on the fulfilment of these instructions. The Mission Management will also monitor the performance of the overall system, by means of reports from the PDS and the FOS, and will inform the User Community.

6.3.2 *Segment Sol Altimetrie et Orbitographie* (SSALTO)

Within the scope of the CryoSat Ground Segment the role of SSALTO is to:

- operate and maintain the network of DORIS beacons;
- monitor the status of the CryoSat DORIS receiver (by means of the HK/TM provided by the PDS) and generate telecommands for DORIS – these telecommands will be sent to the FOS for uplink to the satellite;
- generate, and provide to the PDS, the CryoSat precise orbit from DORIS data, augmented by data from the Satellite Laser Ranging (SLR) network;
- generate estimations of the ionospheric Total Electron Content (TEC) from DORIS measurements and provide these to the PDS for the correction of the SIRAL data.

The (level 1b) Doppler measurements from DORIS will also be provided to end-users.

In addition to these CryoSat activities, SSALTO performs other functions within the domain of other ESA and bi-lateral altimetry missions and is also an important part of the *International DORIS Service* (IDS).

6.3.3 Satellite Laser Ranging

The global network of Satellite Laser Ranging (SLR) stations consists of many independent entities. In addition to the stations themselves there are a number of data centres which generate the orbit predictions in a standardised format (*Inter-Range Vectors*, IRV's) and which collect the ranging measurements from the lasers for general distribution. The most common form is *normal point* data, which are calibrated range measurements accumulated into data points at regular intervals, typically 15 s for satellites such as CryoSat.

The FOS will provide the CryoSat predicted ephemeris to a data centre which will use this to generate CryoSat IRV's. The CryoSat normal points will be available from the data centre to SSALTO and to other orbit determination centres.

6.3.4 Long Term Archive

The CryoSat Ground Segment will maintain a local archive of all its data products for the duration of the mission in order to service user requests and to provide the data-set needed for re-processing. The PDS has also been designed to enable the addition of transcription equipment so that copies of all the data may be made in parallel, for transfer to other archive or processing facilities outside the project.

At regular intervals, the PDS data archive will be synchronized to a multi-mission long-term archive, by performing bulk transfers of the newly archived data at the PDS.

6.3.5 User Services

The CryoSat Ground Segment will provide products catalogue information to the Multi-Mission User Service, in order to allow regular ESA users to enquire about and order archived CryoSat data products.

6.4 Flight Operations Segment

The Flight Operations Segment (FOS) is responsible for the mission planning, command and control, and telemetry acquisition. It may be broken down into two main elements:

- the *Command and Data Acquisition Facility* (CDAF) at Kiruna. The FOS will use a 13 m S and X-band antenna (this is the current EnviSat backup antenna, originally installed to support ERS operations). It shares the 13 m and 15 m Kiruna antennas with other missions, notably ERS-2 and EnviSat;
- the *Flight Operations Control Centre* (FOCC) at ESOC Darmstadt, in Germany.

Although preparations and rehearsals will take place during a long pre-launch period, the Mission operations proper commence at the separation of the satellite from the launcher and continue until the end of the mission, when ground contact to the spacecraft is aborted. In more detail, mission operations comprise the tasks we describe in the following Section.

6.4.1 Operations Tasks

Mission planning is implemented as a long term *Flight Operations Plan*, which plans the spacecraft and payload activities. It is realised as a series of incremental updates to the mission timeline, typically covering a one week period. These will be converted into the detailed command schedule needed to implement the spacecraft operations over the coming 72 hours. It will be possible to insert extra commands, or to delete commands, from this schedule at short notice – the limiting (and obvious) requirement is that there must be an available contact from the ground station prior to a change in the on-board schedule being implemented.

Spacecraft status monitoring by means of processing the housekeeping telemetry such that the status of all spacecraft sub-systems, and the attitude, can be monitored. This function uses the real-time downlink on the S-band link during the ground station pass, and uses, off-line, the telemetry recorded on-board and dumped along with the science data.

The *spacecraft control* task is performed by taking control actions, by telecommand, based on the monitoring of housekeeping data. Such actions follow the Flight Operations Plan; actions which must be taken in anomalous situations will follow procedures defined in the *Satellite Users Manual*.

Operational orbit determination and control will be performed using tracking data (range and range-rate) from the S-band transponder while over the Kiruna ground station. This operational orbit will be used in the planning of and monitoring of orbit manoeuvres to change the spacecraft velocity such that required orbital conditions are achieved.

Attitude determination and control based on the processed attitude sensor data in the spacecraft monitoring and by commanded updates of control parameters in the on-board attitude control system. Note that this is separate from the determination of interferometer baseline orientation which is part of the scientific data processing.

On-board software maintenance, integrating software images received from the spacecraft manufacturer (pre-launch and post-launch), including the instruments, into the telecommand process.

These are all tasks which are common to any low-earth orbit mission like CryoSat. In addition to these, the FOS will provide orbit ephemeris data to the laser community to enable the generation of predictions for the global network of Satellite Laser Ranging (SLR) stations. The highly precise range measurements from these SLR stations will support the precise orbit localisation performed by the DORIS processing centre, SSALTO, and will also be used in the SIRAL range calibration.

6.4.2 Operational Scenario

As we have described throughout this document, the CryoSat mission will be controlled from the operations centre at ESOC, by means of the ESA ground station at Salmijärvi, near Kiruna. The operational scenario is designed to minimise the operations costs and therefore shares many elements, including some staff, with other ESA missions, particularly the other missions in the Earth Explorer series.

Kiruna will be the only ground station used during routine operations and therefore coverage of every orbit will not be possible, as Kiruna can acquire an average of 11 orbits out of the 14 orbits per day. CryoSat has been designed to take this into account, especially in the sizing of its on-board data storage, which is able to cope with the 3 blind orbits without losing data.

This capacity will be used both to enable efficient scheduling of the ground station operations, and to resolve possible conflicts in antenna access between missions. The CryoSat and EnviSat missions will nominally have separate antennas at the ground station so the only case of conflict occurs when they are close in the sky. This is a rare event, and the relative orbital speed and inclination difference means that the satellite alignment only lasts for a few seconds. CryoSat will share the ground station antenna with GOCE. Analysis has shown that conflicts will occur relatively rarely, and they may be solved by skipping a CryoSat pass as we describe above.

The scheduling of the ground station passes with other Earth Explorer missions, in order to optimally resolve such conflicts, will be coordinated by ESOC.

7 Data Products

In this Chapter we present information about the general nature and content of the data products which will be delivered from the CryoSat mission, as well as some other details relating to product delivery. However we shall not present detailed specifications of the products here. Instead they may be found in [Ref. 8] for the Level 1b data and [Ref. 9] for Level 2 data.

We will describe the character, general contents and delivery means in the following Sections, but first we provide a product list and a tabular summary, Table 7.0–1. We also present a set of simulated examples of data which would be available in the products in Chapter 8, "Simulated Results".

Table 7.0–1 Summary of the characteristics of CryoSat data products

Data Product	Characteristics	Main Use	Data Volume
SIRAL Level 0	Raw telemetry source packets: • filtered for errors; • time ordered; • time and telemetry quality information.	input for higher level processing	430 Gbit/ day
SIRAL Level 1b Full Bit Rate	Level 0 data with • housekeeping and non-science data removed; • instrument corrections and geophysical corrections added • precise orbit	• Detailed scattering behaviour • Beam forming • Calibration • Instrument trouble-shooting	430 Gbit/ day
SIRAL Level 1b	• Beam formation • Waveform power data are averaged ("multi-looked") • SARIn data contains multi-looked phase • Full engineering and geophysical corrections applied	• Scattering behaviour • Elevation retrieval methods over land and sea ice • Calibration & Validation • Instrument trouble-shooting	3 Gbit/ day
DORIS Level 1b[1]	Doppler (range rate) data from DORIS	• independent precise orbit determination	
SIRAL Level 2	elevations and waveform power and profile information (e.g. backscattering coefficient, etc.) along the orbit track	• ice fluxes and other geophysical phenomena • Validation	20 Mbit/ day
Monitoring data	Temporally sub-sampled continuously around the orbit: • instrument data • acquisition data; • radar tracking information	• Instrument health • Instrument long-term monitoring	5 Mbit/ day
On-request data	• A subset of the FBR, level 1b and level 2 data; • limited period of SIRAL operation • real-time DORIS Navigator orbit	• rapid, detailed analysis of the scientific data • assessing acquisition of calibration and validation measurement; • investigation of instrument anomalies	

1. DORIS data are provided by SSALTO directly, as for EnviSat

Further information about the processing concept and the means by which these products will be generated may be found in the CryoSat Data Processing Concept, [Ref. 4].

All data products will have a full set of geophysical corrections appended.

The CryoSat DORIS Level 1b doppler data are available but are not provided by the PDS. They will be supplied directly from SSALTO (where they are produced), under an arrangement with ESA similar to the implementation for EnviSat. We will not describe these data further.

7.1 Level 1: Full Bit Rate Data

In the Low Resolution Mode (LRM), which is a pulse-limited mode of operation, the SIRAL echoes are incoherently multi-looked on-board the satellite prior to altimetry (as with, for example, the SeaSat or ERS satellite radar altimeters). In this mode, the Full Bit Rate (FBR) data consist of the multi-looked echoes at a rate of ~20 Hz.

In SAR and SARIn modes, the radar echoes must first be synthetic aperture processed before incoherent multi-looking, and, in SARIn mode, phase multi-looking will also be applied. This synthetic aperture processing is performed on ground, and the data telemetered from the satellite is taken from earlier in the receiver chain than is the case in the pulse-limited LRM. The FBR data in the SAR and SARIn modes consists of the individual, complex (I and Q) echoes. In SARIn mode, there are two such echoes, one for each antenna of the interferometer.

The main purpose of these data is to permit independent investigation of the synthetic aperture processor (beam-formation and direction, slant range correction and multi-looking). To support such investigations, the data will have instrument and geophysical corrections appended, together with a precise orbit. Not all these corrections will be applied however. In conventional pulse-limited altimetry, as part of the radar pulse-compression technique, echoes are fast-Fourier transformed into the 'spectral domain' prior to multi-looking. In SAR and SARIn modes the data are telemetered in the 'time domain' prior to the on-board FFT. Some corrections (such as those for the IF antialias filter) can only be performed once this transformation is performed. The user will have to apply these corrections.

7.2 Level 1b: Multi-looked Waveform Data

Level 1b data consist, essentially, of an echo for each point along the ground track of the satellite. In all three modes, the data consist of multi-looked echoes at a rate of, approximately, 20 Hz. (In pulse limited mode, the contents of the level 1b data are the same as that of the FBR data.) In SARIn mode, the multi-looked echo is complex, consisting of the echo power and interferometer phase. As with the FBR data, the data will have instrument and geophysical corrections appended, and will have a precise orbit added. In pulse-limited mode, these data are similar to the "SDR" data of Seasat altimeter, or the "WAP" data of the ERS-1 and ERS-2 altimeters.

In the SAR and SARIn modes, there are additional information in the level 1b data, derived as part of the multi-looking. An important source of geophysical information is the variation in echo power as a function of the incidence angle of each Doppler beam. (This information may also help determine Doppler beam ambiguity). This information is parameterised prior to multi-looking and included as part of the level 1b data. In addition, in SARIn mode, the coherence of the interferometer phase is also estimated as part of the

phase multi-looking. In SARIn mode, the phase coherence is also added to the level 1b waveform.

7.3 Level 2: Elevation and other Surface Characteristics

Level 2 data consists, essentially, of individual estimates of the surface elevation and other surface parameters (such as the radar backscattering coefficient) determined from each echo in the level 1b data. Their rate in all three modes is approximately 20 Hz. For data derived from the pulse-limited mode of operation, these data are similar to the "GDR" data of the Seasat altimeter or the "OPR" data of the ERS altimeters.

Over sea-ice covered water, the data will also include an estimate of ice thickness and other information derived from the echo power and its behaviour as a function of delay time and incidence angle. Over land ice, the data will be "slope-corrected". Where the data are derived from SARIn mode echoes, the correction will be determined from the interferometer phase. For elevations derived from LRM echoes, the correction will be obtained from a digital elevation model (DEM) of the ice sheet surface.

7.4 Monitoring Data

Monitoring data will provide information on the health of the payload. It consists of a set of parameters whose values are routinely monitored around each orbit. Examples are the satellite altitude, radar power gain, echo delay time, the internal range, gain and phase corrections, *etc.* In addition, it contains the information telemetered by the SIRAL radar describing the acquisition and control of the radar tracking system. (Unlike previous altimeters, in SARIn mode, the echoes used by the SIRAL for radar tracking are different from those of the measurement data.) The monitoring data is mainly to provide early warning of instrument anomalies, and to investigate their cause and possible solution. It is likely to be intensively used during the commissioning phase of the mission.

7.5 On-Request Data

The CryoSat PDS will be "data-driven" in its normal operation. The instrument operation (and in particular the selection of SIRAL modes) will be automated through the use of the geographical mode mask. Data arriving at the PDS in any mode will automatically trigger its processing. This will not occur until all the data that are required to generate a data product are available, and, in particular, until the precise orbit is available. There will be occasions when it will be necessary to augment the automated operation to provide rapidly an assessment of the scientific data stream. This will support for example rapid analysis of campaign data to check, for example, the successful acquisition of transponder signals, or rapid detailed investigations associated with instrument anomalies.

Instruction from Mission Management will trigger the production of the on-request data. The data comprise a set of FBR, level 1b and level 2 data corresponding to a few minutes of instrument operation, provided in "near real time". Because the data are near real time, they use the real-time DORIS Navigator orbit, which has a degraded precision in comparison with the precise orbit.

7.6 Data Distribution

The distribution of CryoSat data is summarised in Table 7.6–1. This table identifies for each product:

- *Data Latency:* the time delay between data acquisition and data distribution.
- *Minimum Duration:* the smallest interval of continuous satellite operation for which a data product is available.
- *Maximum Duration:* the largest interval of continuous operation for which a data product is available.
- *Users:* this distinguishes those data whose distribution is restricted to the CryoSat Calibration, Validation and Retrieval Team (CVRT). The selection of the CVRT was through the *Announcement of Opportunity for Calibration, Validation and Retrieval*, which closed in April 2002. However the CVRT may be augmented by any suitable proposals under later AO's.

Table 7.6–1 CryoSat data distribution

Data Product	Latency	Minimum Duration	Maximum Duration	Users
Full Bit Rate data	1 month	10 minutes	10 min	CVRT members (within resource limitations)
Level 1b	1 month	10 min	none	CVRT members. Requests from Data Exploitation AO
Level 2	1 month	1 orbit	none	CVRT members. Requests from Data Exploitation AO
Monitoring data	< 4 hours	1 orbit	none	CVRT members
On-Request data	< 1 day	10 minutes	10 minutes	CVRT members

Tailored software for data access and conversion will be provided to the user. Data distribution will be handled by CD and/or DVD discs and FTP transfers where this is practicable.

8 Simulated Results

In order to provide an illustration of the nature of the results to be expected from the SIRAL instrument, in its SARIn mode, we have prepared some examples using the CryoSat Mission and Performance Simulator (CRYMPS). This is a software tool able to simulate the echoes which would be received by the SIRAL over surfaces and to process the echoes. It is being used as a test bed for the development of the processing algorithms.

We have used two different target scenarios: one with an array of point targets and one with an ocean-like surface. The point targets are arranged in a row along the sub-satellite track, with a second and third row offset to the side. In the plotted results which follow we show four panels. On the left are the results over the point targets while the ocean-like echoes are on the right. In the upper panels we plot the power response, while in the lower panel we plot the angle to the surface which produced the instantaneous echo, inferred from the interferometric phase.

In interpreting the results it will be useful to review some properties of the radar echoes over a flat surface, shown in Figure 8.0–1[11]. Range rings are familiar from pulse-width

Figure 8.0–1 Properties of the radar echo over a flat surface.

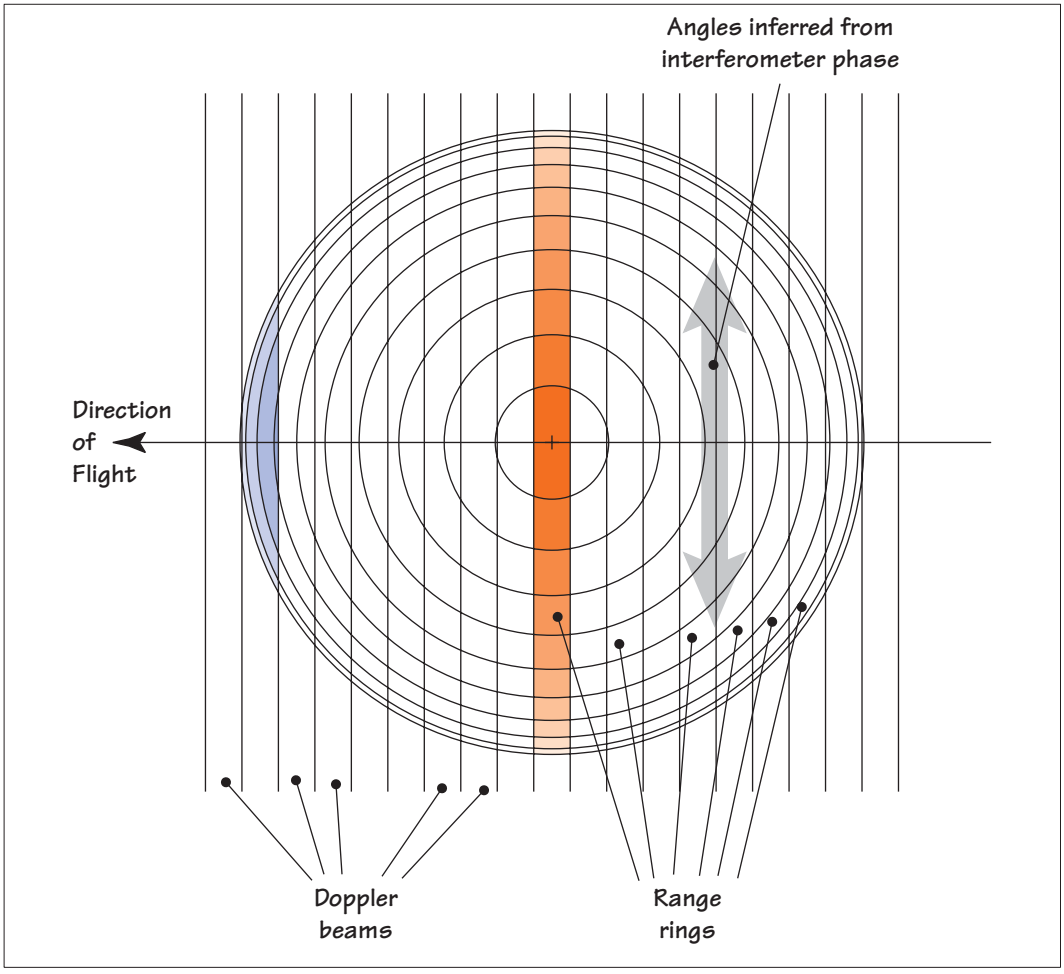

11. some graphical elements of the CryoSat logo may be seen in this Figure.

limited altimetry and are the series of concentric circles marked by the range resolution increments of the instrument. In the SARIn (and SAR) modes the Doppler beams discriminate in the along-track direction. Beams at the centre of the pattern sample a full span of range rings, from the sub-satellite point to the edge of the region observed by the range window (*i.e.* the full set of range rings). Doppler beams at the edge can only sample a limited set of range rings; the closest point is at greater range and the spread of ranges is smaller than in central beams. Finally, the angles inferred from the interferometric phase are in the plane parallel to the interferometric baseline, which is aligned cross-track.

Over a topographic surface the relationship between range rings, Doppler beams and arrival angle is more complex, and surface-dependent. We will only show one set of results from such a surface, in the final part, Section 8.4, where we will show some results from a topographic surface.

The results which we will show illustrate various levels of data products to which we refer in Section 7. However they are not presented in precisely the same way and usually have had some additional processing applied for display purposes. The equivalence is:

- in Section 8.1 we describe the characteristics of a *single burst*, which represents the contents of the Full Bit Rate (FBR) data, but with a 2-D Fourier transform applied for display purposes;
- in Section 8.2 we describe a *single stack* of Doppler beams – data are handled at this level inside the processor but do not appear externally in this form;
- in Section 8.3 we show the *level 1b* data.

In all cases we have applied some processing to the phase data to prepare plots of the inferred angle between the normal to the interferometric baseline (which is pointing towards the nadir) and the direction to the reflection point of the radar signal.

8.1 Single Burst

In the first set of simulated data we show, in Figure 8.1–1, a single burst of echoes. The echoes have had a 2-D Fourier transform applied to perform range compression and to form the Doppler beams. Note that the data volume after this 2-D Fourier transform is conserved: it is the same as the raw data. The "horizontal" plane of the plots represent the result of this process: the beams are formed from the "front" to the "back" (the axis marked "Time [ms]") while the range compression is formed "left" to "right".

The labelling on both these axes is slightly confusing. The time span of the plots is 3 ms, the duration of the burst, during which the satellite moves a horizontal distance of 20 m. Yet this axis is really showing the Doppler beams, each of which covers about 250 m on the ground. The other axis, plotted as the "Range Bin", shows the echo delay time (effectively the range to the target). The range bin units are the inverse of the transmitted chirp bandwidth, being about 3 ns. The range scale on this plot therefore spans about 100 m.

The signature of the target in the echo is most clearly seen in the power from the point targets in the upper left panel. A set of three point targets across-track is visible: at the closest range is the point target on the sub-satellite track. It in not at the centre of the burst – it is viewed by a beam looking slightly backwards. At a slightly later delay time (*i.e.* greater range) is the next point target with smaller radar cross-section. Further still is a weak echo from the last, small point target.

The strong echo signal from the first point target spreads over several range bins; this is the effect of the sidelobes of the 2-D FFT.

The radar cross-section of each of the point targets is the same so the differences in echo power are due to the effect of the antenna pattern, which attenuates echoes as they move

Figure 8.1–1 Simulated results for a single echo burst. See the text for explanation.

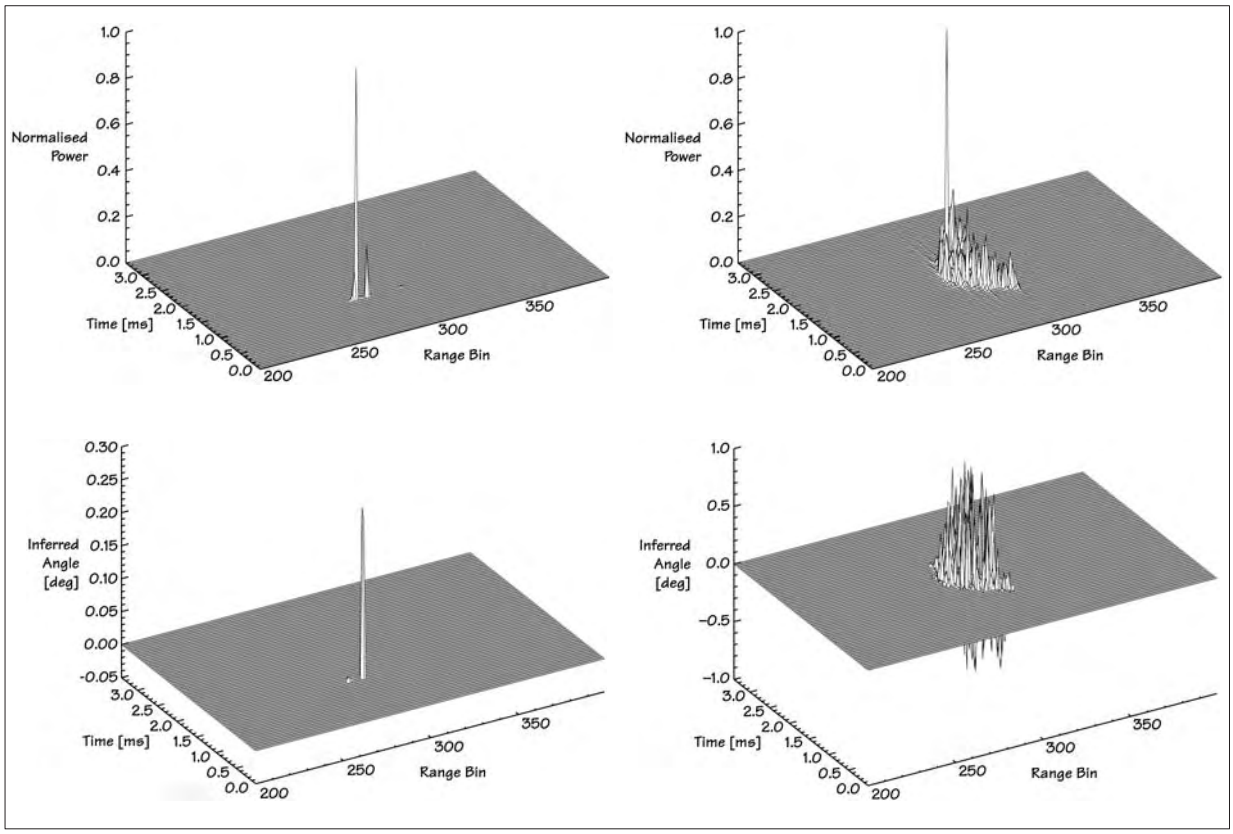

further away from the antenna boresight, *i.e.* the nadir. This effect will become obvious later.

The point targets only appear in one of the along-track Doppler beams as they are infinitesimally small while the Doppler beams each cover about 250 m along-track.

In the plot in the lower left panel the inferred angle, derived from the interferometric phase, is plotted. The first, strong echo actually has an inferred angle of zero, as it is on the sub-satellite track. The small inferred angle which is visible in the plot at this position is, on closer examination, actually coming from the sidelobes of the FFT, as mentioned above. The next point target is further away, and has a larger inferred angle. The third point target is very small and is not registered in this plot, because *we have fixed the inferred angle to zero for all samples with power less than 0.05 of the maximum power*. This is true for all the plots.

We may now interpret the ocean-like echoes, based on this understanding of the point target echoes. Unlike the former, ocean surfaces are an extended target and they are diffuse, so echoes are detectable over a range of angles. They are also formed of many small facets so the overall radar echoes exhibit "speckle", a statistical irregularity due to interference effects.

The geometry of the observation of this surface by the Doppler beams is shown in Figure 8.1–2. Each of the Doppler cells identified in the Figure, which is actually a cross-track strip, returns power in the case of the diffuse surface. So the power in the burst will be distributed among the Doppler beams.

Figure 8.1–2 Geometry of measurement for a single burst, viewed from the "side" compared to Figure 8.0–1. Only 10 Doppler beams are shown, for clarity, instead of the 64 which will be generated. Additionally the divergence angle between them is exaggerated.

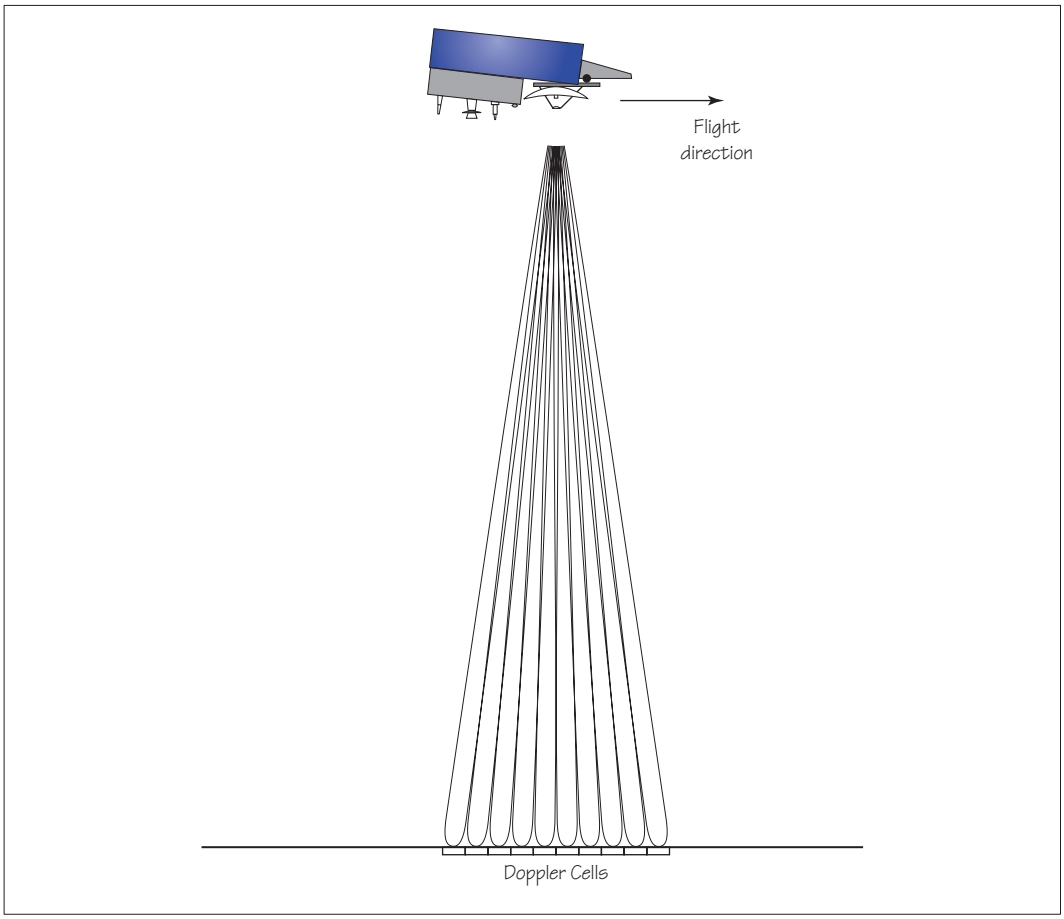

In the upper right panel of Figure 8.1–1 we show the echo power in the Doppler beams from the ocean-like surface for a single burst. In the central beams the echoes are strongest and have minimum range. They sample the full spread of range rings and they arrive from a relatively wide range of cross-track angles.

Doppler beams towards the edges of the set are viewing the surface at (along-track) angles which are off-nadir. The echo reflections have a greater range (they are displaced to later range bins) and they have reduced power compared to the nadir echoes because of the antenna pattern effects mentioned earlier. They also have a reduced spread of ranges (only the range bins at the edge of the pattern are observed) and a reduced range of cross-track angles. All these features may be deduced from Figure 8.0–1.

In the plot of inferred angle, at the lower right, the echoes in the central beams have a small off-nadir angle at the closest range. As the range in these echoes increases the range of arrival angles also increases and, over this flat surface, becomes ambiguous as both sides of the track are sampled (note that this is not always true over topographic surfaces). In fact the only non-ambiguous arrival angle, in this case, is at the leading edge of the echo.

8.2 Single Stack of Doppler Beams

The second set of simulated results which we will present, shown in Figure 8.2–2, is the result of *stacking* the Doppler beams. In this process, which again conserves the full data volume, the data are re-sorted so that all of the Doppler beams pointing towards a particular strip of the surface are collected together[12]: this set is called a *stack*. We show the geometry of this process in Figure 8.2–1, which illustrates how successive bursts illuminate a given Doppler cell.

Figure 8.2–1 Geometry of measurement for a stack, viewed from the "side" compared to Figure 8.0–1. Again only 10 Doppler beams, and 10 bursts are shown for clarity. One beam from each burst illuminates a particular area on the surface; these are collected together to form the stack.

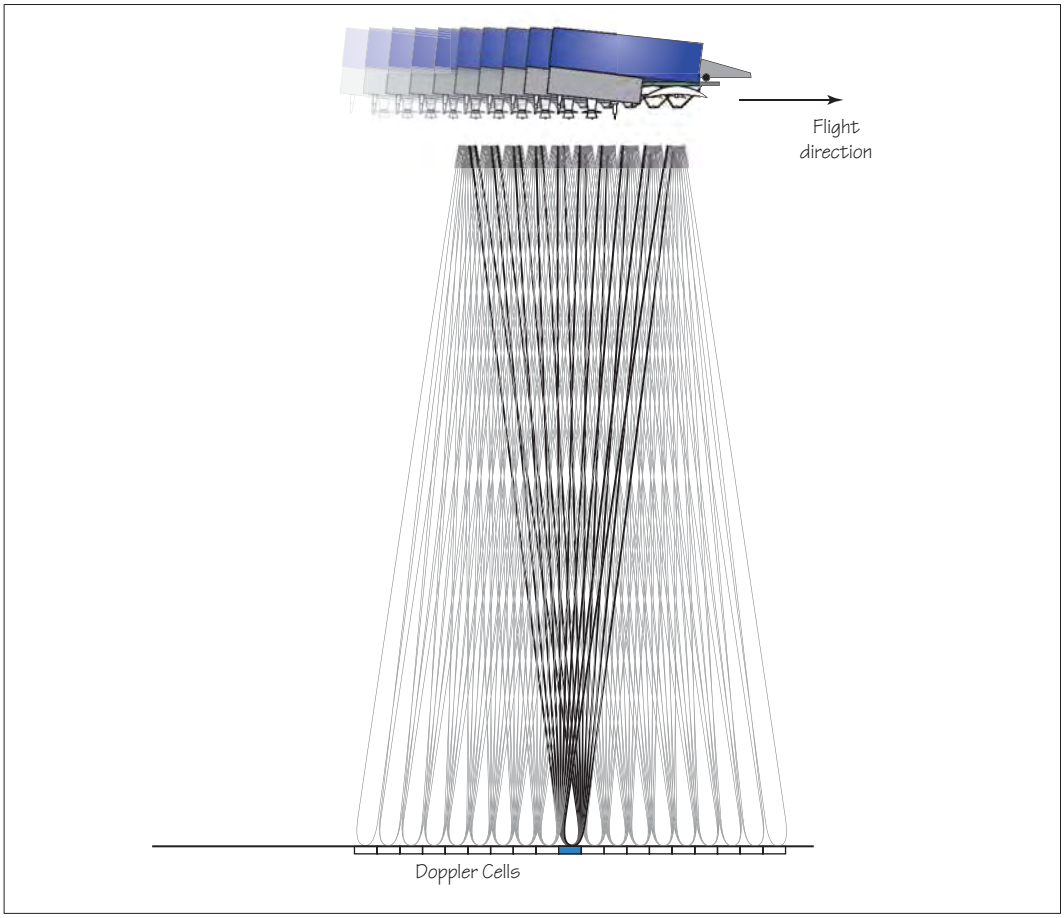

During stacking a process called *slant-range correction* is applied, as we will describe now.

We showed in Figure 8.0–1, and demonstrated in the plot of echo power for ocean-like surfaces, in the upper right panel of Figure 8.1–1, that the Doppler beams at the edges were observing elements of the surface at a greater range (called *slant-range*) than the nadir-looking beams, with the result that the echoes were displaced on the range scale. If

12. in fact the processing is, in general, more elaborate than a simple sorting, and is designed to ensure that beams from successive bursts do indeed illuminate the same ground strip, regardless of topographic effects, by steering the beam formation using a phase rotation prior to the Fourier transform.

Figure 8.2–2 Simulated results for a stack of echoes. See the text for more explanation.

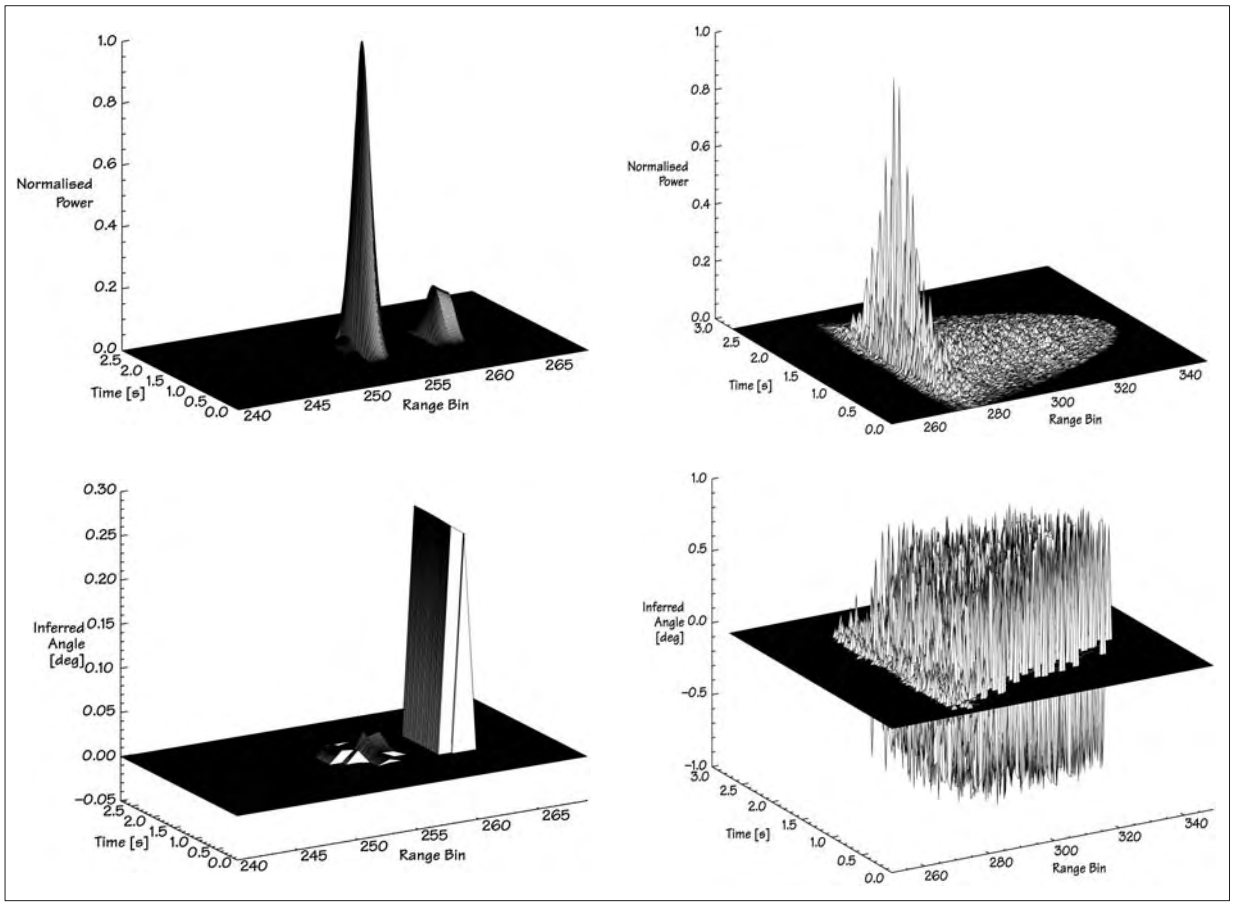

we wish to combine the looks from the individual Doppler beams this geometrical effect must be removed. We must compensate the slant-range of beams viewing off-nadir (along-track) to the equivalent range at nadir. This process is called slant-range correction.

In the upper left panel of Figure 8.2–2 we show the stack of Doppler beams, one per burst, which have observed the set of point targets; one such beam was shown in Figure 8.1–1. Note that the Range Bin scale has been enlarged compared to the previous Figure. Now the time axis has a clear meaning: it refers to the time, as the satellite flies along-track, during which the point targets are visible. Each successive strip of Figure 8.2–2 shows one Doppler beam from a given burst, and the next strip shows the next Doppler beam from the next burst. The echoes from the point targets remain within the antenna beamwidth for about 2 s. At the start of this period the power measured in the extreme forward-looking Doppler beams is virtually zero. As the satellite moves forwards so that the point targets increase in reflected power until they are at nadir. Subsequent bursts see the point target echoes in ever-more backward looking Doppler beams, and the echoes become weaker.

The first point target, on the sub-satellite track, is almost centred in a range bin, and has a clear peak with energy in adjacent range bins due to the weighted FFT sidelobes. The second point target is in between two range bins and has significant energy in the two.

The lower left panel shows the inferred echo arrival angle over the same span of range bins. The inferred angle of the point target on the sub-satellite track is actually zero at the position of the point target. Small angles are registered in the surrounding range bins and

Doppler beams due to the sidelobe effect mentioned above; these sidelobes are higher than the 0.05 threshold (see Section 8.1). The second point target has a slightly different inferred angle in each of the two range bins in which echo power is recorded, constant over the Doppler beams which have power. Sidelobes are below the 0.05 threshold and so do not appear.

We now address the ocean-like echoes, shown in the panels on the right. Again the stack shows beams from successive bursts after slant-range correction. The plot of echo power, at the top-right, may be interpreted with the aid of Figure 8.0–1, Figure 8.2–1 and the single burst at the top-right of Figure 8.1–1. Note that the "Range Bin" scale is not the same in these Figures. The Doppler beams have been slant-range corrected so that the stack may later be accumulated to provide a composite waveform with a consistent range-scale (see Section 8.3). The off-nadir Doppler beams, at the edges of the stack, have a reduced spread of range, and reduced power, compared to the central beams.

It is also evident, from this Figure, that the power in the stack falls off more sharply with range than in the conventional, pulse-width limited case as described by *Brown* [Ref. 7]. The power in the trailing edge of the pulse-width limited echo is integrated around all azimuth angles while in the SAR or SARIn mode this energy in distant range bins is confined to the central Doppler beams only; the edge beams have been slant-range corrected and have no energy in the more distant (after correction) range bins.

The plot of inferred angle, at the lower right, also shows the characteristic reduction in span of the edge beams compared to the central ones. As in the single burst, the ambiguity in the inferred arrival angle for the echo power after the leading edge is quite large.

8.3 Level1b

The third set of simulated results, shown in Figure 8.3–1, show the nature of the data in the level 1b product, after *multi-looking* the stacks of Doppler beams. Multi-looking does not conserve data volume and results in a significant reduction in the size of the data-set. Each stack of 64 separate Doppler beams is accumulated into one composite waveform in this process.

During multi-looking a weighting function may be applied across the beams in the stack such that the central beams are more heavily weighted than those near the edges. Such weighting is likely to be especially useful over surfaces like sea-ice, where the echoes are highly specular and only the central beams have any significant echo power. In such a situation a simple window function may be sufficient.

In the upper left panel of Figure 8.3–1 we present the multi-looked waveform stacks over the set of point targets. Each stack has been accumulated into a single waveform and these have all been plotted for a simulation run covering 20 s, or about 140 km along-track. The three rows of 8 point targets clearly appear in a few of the multi-looked stacks. The majority of stacks have no signal.

The spill-over from the main echo of the point target into adjacent range bins is clearly visible, for both the larger point targets. The third one is visible but only registers a low signal level in a single range bin.

In the plot of inferred angle, at the lower left, a regular pattern emerges. The central range bin of the first point target has an inferred angle of zero; it is on the sub-satellite track. The spill-over of power into adjacent range bins, on both sides of the peak, shows up with a small non-zero inferred angle. The second point target shows the same response already observed in the stack and the third remains below the threshold for plotting.

Figure 8.3–1 Simulated level 1b data, after multi-looking stacks of Doppler beams.

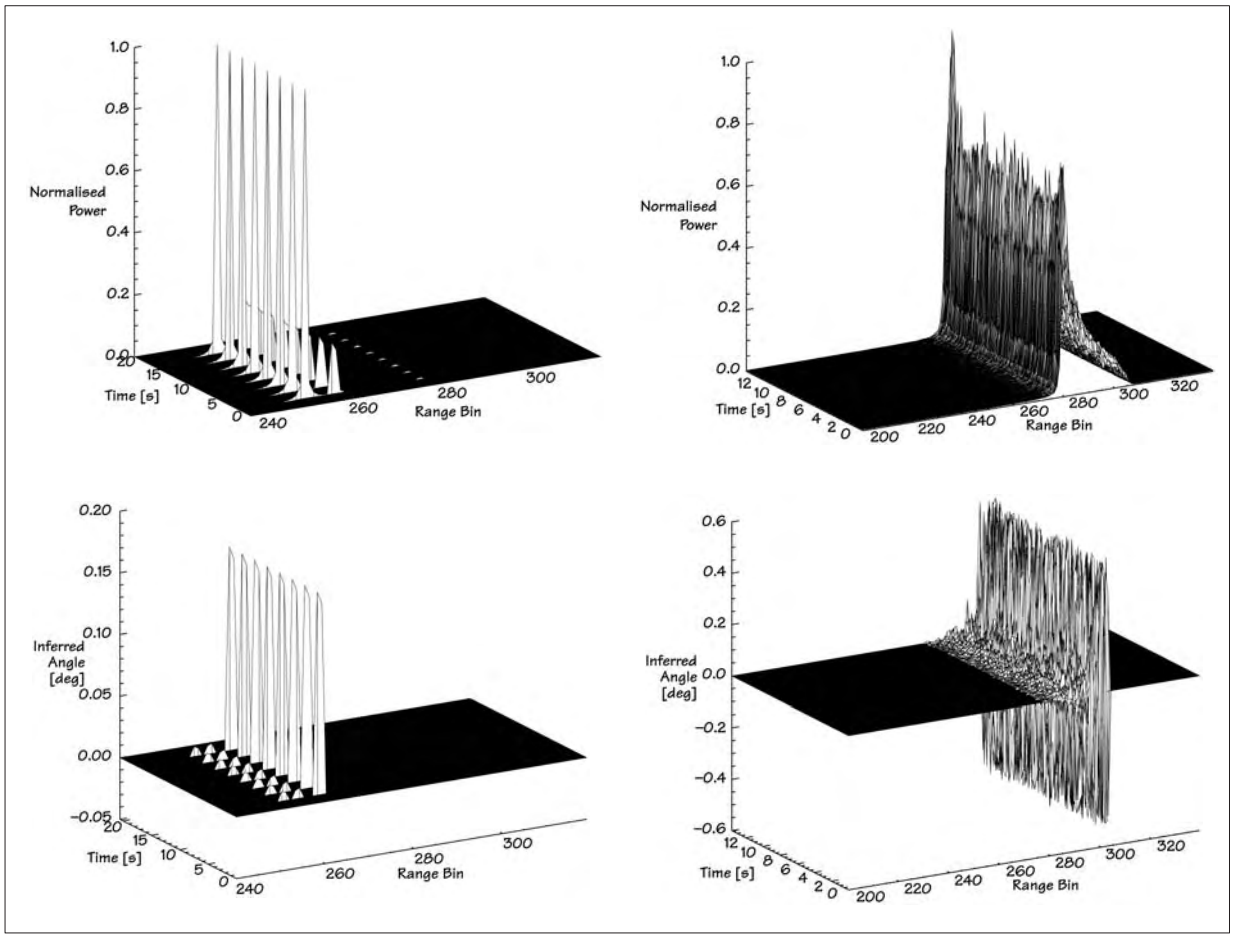

The plot of the power in the multi-looked stacks over ocean appears to be very similar to a conventional altimeters waveform product over ocean. The principle difference is the sharper fall-off in power, as explained above. However we note that the normalised power increases at each end of the processing run. This is due to the variation in the number of beams in the stack at the start and end of processing, and the particular normalisation which was applied. The stack takes one beam from each of a large number of bursts. As the processing is necessarily based on a certain period of instrument operation, and therefore a fixed number of bursts, there will always be this transient effect at the ends.

The plot of inferred angle, at the lower right, may be clearly understood. At the leading edge of the echo the echo comes from the nadir, so the inferred angle is zero. In the trailing edge of the echo the reflecting facets in the across-track parts of the Doppler beams are contributing progressively more, and the inferred arrival angle becomes increasingly ambiguous.

8.4 Topographic Surfaces

The results presented in the previous Sections have been based on point targets, which are a very specific artificial target, and over an flat, ocean-like surface. This is typical of the

Figure 8.4–1 Part of the Totten Glacier in East Antarctica, displayed as a map of surface slope. Superimposed on this is the simulated satellite track and the locations of the multi-looked stacks of SARIn echoes.

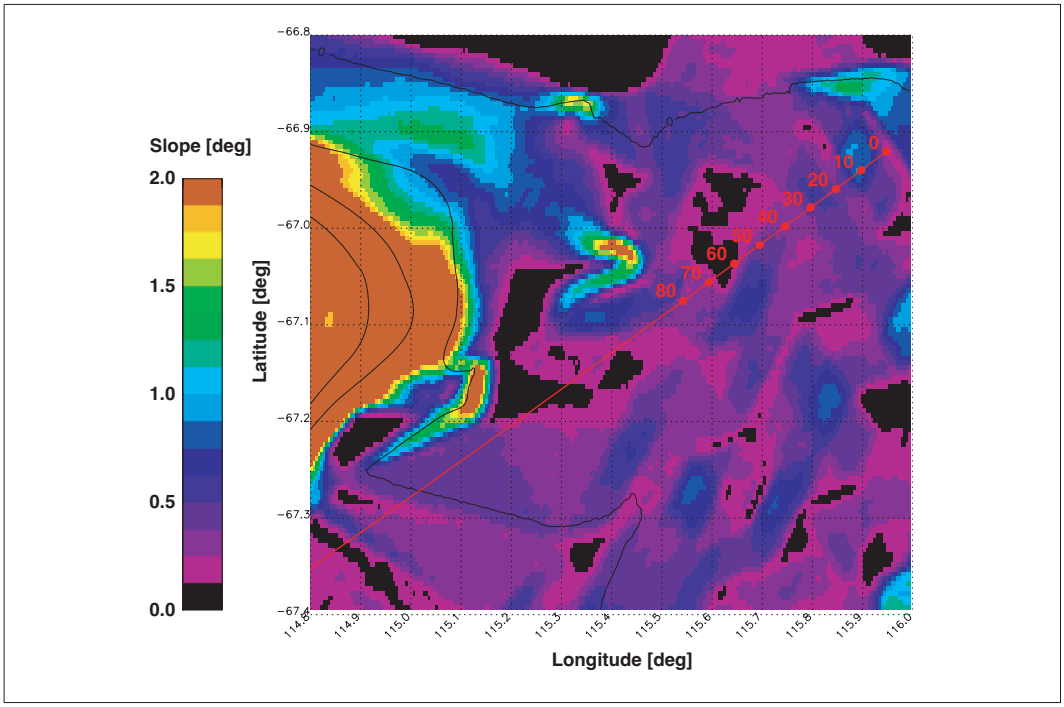

type of flat surface for which the SAR mode will be used in its measurements of sea-ice thickness. However the we have been illustrating the behaviour of the SARIn mode, with its additional measurement of interferometric phase, and hence inferred angle.

The SARIn mode is designed to be used over topographic surfaces where the measure of the arrival angle of the echo will be crucial for the determination of the surface elevation of the reflector, rather than simply its range from the radar. We have limited examples of this type of surface, but one scenario has been prepared.

We present it in a different format from the previous examples. In Figure 8.4–1 we show the scenario, part of the Totten Glacier. This has been extracted from a digital elevation model of Antarctica and we display it as a colour coded map of overall surface slope (both along and across-track), with some superimposed elevation contours. The simulated satellite ground track is shown as a red line, and there are nine locations marked corresponding to the localisation of the multi-looked stacks of Doppler beams, equivalent to the level 1b data products described in Section 8.3.

We present the simulated data in Figure 8.4–2. We show them as simple one-dimensional plots, showing echo power and inferred arrival angle as a function of range bin, at each of the nine locations identified in Figure 8.4–1. In these plots we also show the coherence, which has not appeared in the earlier results. This parameter quantifies the coherence of the wavefront arriving at the two antennas of the interferometer, and it may be used as a proxy for the validity of the inferred arrival angle. The initial rise in coherence, coincident with the leading edge in the power trace, indicates that the corresponding inferred angle is unambiguous and valid.

In these nine plots it is clear that the inferred arrival angle is providing useful information. As an illustration consider locations 0, 10 and 20, in which the total surface slope (and, we assume, the across-track component as measured here) is, qualitatively speaking, respec-

tively low, high and medium. We clearly see that the arrival angle of the leading edge in the corresponding echoes of Figure 8.4–2 shows the same relative behaviour.

Figure 8.4–2 Simulated echoes from the Level 1b product at the measurement points shown in the previous Figure. The black line indicates the echo power, the blue line the inferred arrival angle and the red line the coherence – the magnitude of this value at the echo leading edge indicates where the inferred arrival angle is valid.

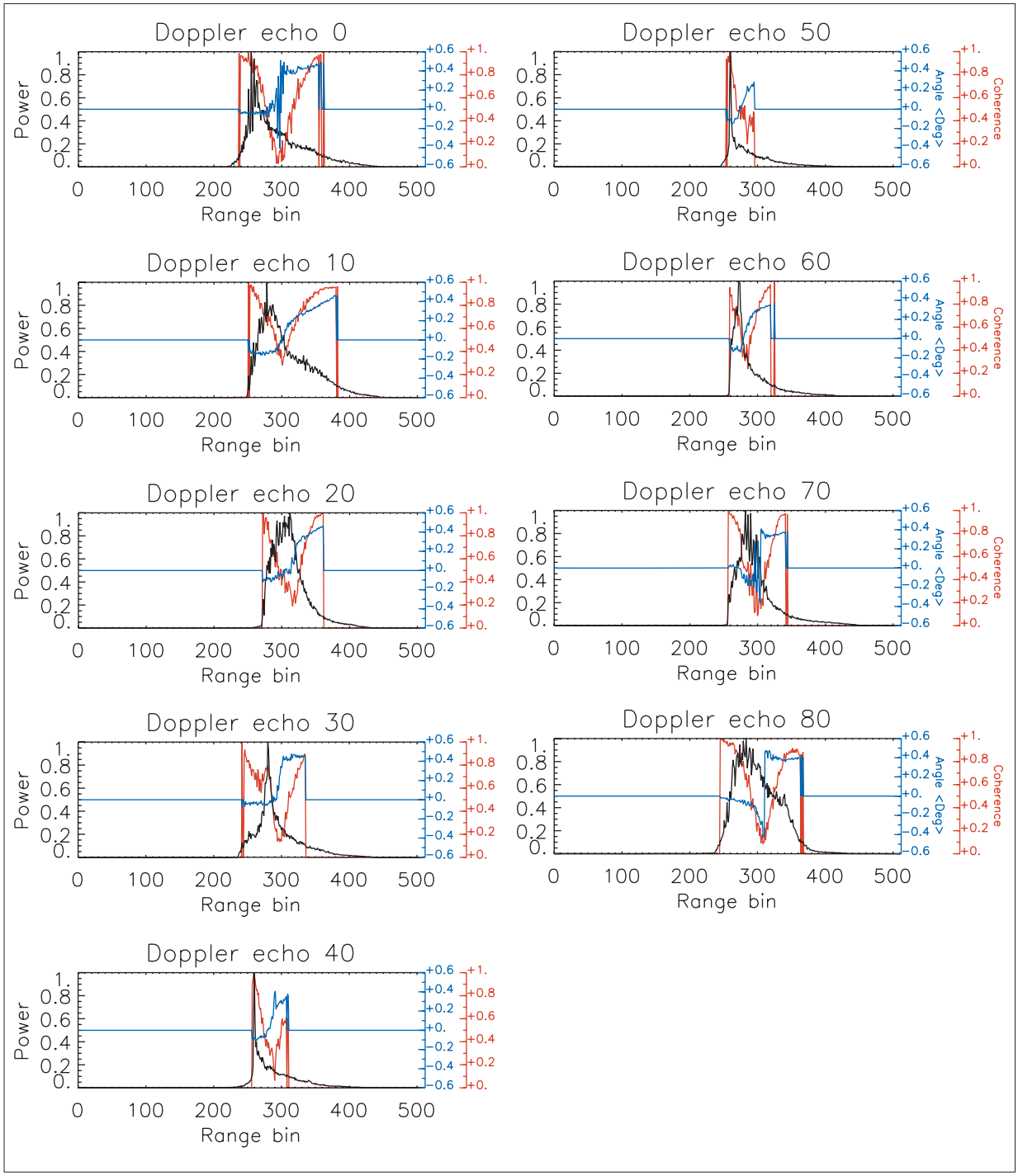

ANNEX A References

Ref. 1 CryoSat Mission Requirements Document, CS-RS-UCL-SY-0001

Ref. 2 CryoSat Calibration and Validation Concept, CS-RP-UCL-SY-0003

Ref. 3 CryoSat: a mission to determine the fluctuations in Earth's land and marine ice fields, Wingham, D. J., C. R. Francis, S. Baker, C. Bouzinac, D. Brockley, R. Cullen, P. de Chateau-Thierry, S.W. Laxon, U. Mallow, C. Mavrocordatos, L. Phalippou, G. Ratier, L. Rey, F. Rostan, P. Viau and D.W. Willis, *Adv. Space Res.* **37**, pp 841-871, 2006.

Ref. 4 CryoSat Data Processing Concept, CS-PL-UCL-SY-0005

Ref. 5 Scharroo, R. and Visser P, *The Effect of AOCS Thrusters on the Orbit Determination Accuracy of CryoSat*, ESA/ESTEC Consultancy Contract Report, 24 May 2000

Ref. 6 Shum, C. K., *The Effect of AOCS Thrusters on Orbit Accuracy of CryoSat*, ESA/ESTEC Consultancy Contract Report, 12 July 2000

Ref. 7 The Average Impulse Response of a Rough Surface and its Applications, G.S. Brown, *IEEE Trans. Ant. Prop.*, **AP-25**, 1, p.67, 1977.

Ref. 8 Instrument Processing Facility L1b Products Format Specification, CS-RS-ACS-GS-5106

Ref. 9 Instrument Processing Facility L1b Products Format Specification, CS-RS-ACS-GS-5213

Intentionally Blank

ANNEX B Acronyms and Abbreviations

Please note: this list of acronyms and abbreviations is in general use within the CryoSat project and contains entries not used within the current document.

ACN	Attitude Control and Navigation
ACSYS	Arctic Climate System Study
ADC	Analog to Digital Converter
ADD	Architectural Design Document
ADR	Architectural Design Review
AGC	Automatic Gain Control
AI	Action Item
AIT	Assembly, Integration and Test
AIV	Assembly, Integration and Verification
ANX	Ascending Node Crossing
AOCS	Attitude and Orbit Control Subsystem
AOS	Acquisition of Signal
AP	Application Process
APID	Application ID
ASIC	Application Specific Integrated Circuit
ATP	Authorisation to Proceed
AUT	Autonomy
BER	Bit Error Rate
BPSK	Binary Phase Shift Keying
BOL	Beginning of Life
CAD	Computer Assisted Design
CADU	Channel Access Data Unit
CBCP	Current Baseline Cost Plan
CCB	Configuration Control Board
CCN	Contract Change Notice
CCS	Command and Control Subsystem
CCSDS	Consultative Committee for Space Data Systems
CDMU	Control and Data Management Unit
CDPU	Central Data Processing Unit
CDR	Critical Design Review
CETeF	Coordinated European Test Facilities

CFE	Customer Furnished Equipment
CFI	Customer Furnished Item
CFRP	Carbon Fibre Reinforced Plastic
CIDL	Configured Items Data List
CIL	Critical Items List
CLIVAR	Climate Variability and Predictability Program
CM	Configuration Management
COG	Centre of Gravity
CPS	Company Project Structure
CPU	Central Processor Unit
CR	Change Request; Cost Reimbursement
CRB	Change Review Board
CRR	Commissioning Results Review
C-SAG	CryoSat Science Advisory Group
CTR	Control
CVCDU	Coded Virtual Channel Data Unit
CVRT	Calibration, Validation and Retrieval Team
DCN	Document Change Notice
DCR	Document Change Request
DDD	Detailed Design Document
DEM	Digital Elevation Model
DIL	Deliverable Items List
DM	Documentation Management
DMA	Defense Mapping Agency; Direct Memory Access
DML	Declared Materials List
DMS	Data Management Subsystem
DOD	Depth of Discharge
DORIS	Doppler Orbitography and Radio-Positioning Integrated by Satellite
DRD	Documents Requirements Description
DRL	Documents Requirements List
DVC	Device Commanding
ECP	Engineering Change Proposal
ECMWF	European Centre for Medium-term Weather Forecasting
ECSS	European Co-operation for Space Standardisation
EDAC	Error Detection and Correction
EEE	Electronic, Electrical and Electromagnetic parts
EEPROM	Electrically Erasable Programmable Read Only Memory
EGSE	Electrical Ground Support Equipment

EIDP	End Item Data Package
EIRP	Effective Isotropic Radiated Power
EOEP	Earth Observation Envelope Programme
EOPP	Earth Observation Preparatory Programme
EMC	Electromagnetic Compatibility
EMI	Electromagnetic Interference
EPC	Electrical Power Conditioner
EPS	Electrical Power Subsystem
EOL	End of Life
ERS	European Remote Sensing Satellite
ESA	European Space Agency
ESO	European Southern Observatory
ESOC	European Space Operations Centre
ESTEC	European Space Technology Centre
ET	Ephemeris Time
EVRP	Event Reporting
FA	Functional Analysis
FAR	Flight Acceptance Review
FD	Flight Dynamics
FDDB	Flight Dynamics Data Base
FDDC	Flight Dynamics Database Content
FDDD	Flight Dynamics Database Delivery
FEC	Forward Error Correction
FFP	Firm Fixed Price
FFT	Fast Fourier Transform
FID	Function Identifier
FIFO	First In, First Out
FMECA	Failure Mode and Effects Criticality Analysis
FOM	Flight Operations Manual
FOP	Flight Operations Procedure
FOV	Field of View
FTA	Fault Tree Analysis
FTP	File Transfer Protocol
FTS	in-Flight Testing
GCM	Global Circulation Model
GDR	Geophysical Data Record
GOCE	Gravity Field and Steady-state Ocean Circulation Explorer
GPS	Global Positioning System

G/S	Ground Station
GSE	Ground Support Equipment
HA	Hazard Analysis
HPA	High Power Amplifier
HSRRA	High Spatial Resolution Radar Altimeter
IAG	International Association of Geodesy
IAU	International Astronomical Union
ICBM	Intercontinental Ballistic Missile
ICD	Interface Control Document
ICU	Instrument Control Unit
ID	Identification
ie	ice equivalent
IERS	International Earth Rotation Service
IF	Interface, Intermediate Frequency
I/F	Interface
IGBP	International Geosphere-Biosphere Program
INFT	In-Flight Testing
IOS	Industrial Organisation Structure
IPCC	Intergovernmental Panel on Climate Change
IRI	International Reference Ionosphere
IRM	IERS Reference Meridian
IRP	IERS Reference Pole
IRV	Inter-Range Vector
ISP	Instrument Source Packet
ITT	Invitation to Tender
ITU	International Telecommunications Union
ITRF	IERS Terrestrial Reference Frame
JD	Julian Day
JGM-3	Joint Geopotential Model, version 3
LCL	Latching Current Limiter
LEOP	Launch and Early Orbit Phase
LFM	Linear Frequency Modulation
LHCP	Left Handed Circular Polarisation
LI	Lead Investigator
LLI	Long Lead Item
LOL	Limit of Liability

LOS	Line of Sight; Loss of Signal
LRR	Laser Retro Reflector
LSB	Least Significant Bit
LVA	Launch Vehicle Adaptor
MDD	Mission and Data Description
MGSE	Mechanical Ground Support Equipment
MLI	Multi Layer Insulation
MLST	Mean Local Solar Time
MJD	Modified Julian Day
MM	Memory Management
MNEM	Mnemonic
MPP	Milestone Payments Plan
MRD	Mission Requirement Document
MSB	Most Significant Bit
MSIS	Mass Spectrometer, Incoherent Scatter atmospheric model
MTL	Master Timeline
NA	Not Applicable
NCR	Non Conformance Report
NEOS	National Earth Orientation Service
NSSDC	National Space Science Data Centre
OBC	On Board Computer
OBCP	Original Baseline Cost Plan
OBCP	On-Board Control Procedure
OBMF	On-Board Monitoring Function
OBMT	On-Board Mission Timeline
OBSM	On-Board Software Management
OBSR	On-Board Storage and Retrieval
OBT	On Board Time
OBTM	On-Board Time Management
OGSE	Optical Ground Support Equipment
OTS	Off-the-Shelf
PA	Product Assurance
PACK	Packet (Telecommand or Telemetry)
PAD	Part Approval Document
PCR	Preliminary Concept Review
PDF	Portable Document Format

PERP	Periodic Reporting
PFC	Parameter Format Code
PFM	Proto Flight Model (of spacecraft)
PDHS	Payload Data Handling Subsystem
PI	Principal Investigator
PID	Parameter Identification Number
PMP	Project Management Plan
POD	Precise Orbit Determination
PPL	Preferred Parts List
PREF	Parameter Reference Number
PRF	Pulse Repetition Frequency
PROM	Programmable Read Only Memory
PRT	Packet Routing Table
PSK	Phase Shift Keying
PSS	Procedures, Specifications and Standards
PT	Product Tree
PTC	Parameter Type Code
PTXC	Packet Transmission Control
QPL	Qualified Parts List
QPSK	Quadrature Phase Shift Keying
RA-2	Second generation Radar Altimeter
RAM	Random Access Memory
RCS	Reaction Control System (of spacecraft)
RF	Radio Frequency
RFA	Request for Approval
RFC	Radio Frequency Compatibility
RFD	Request for Deviation
RFI	Radio Frequency Interference
RFQ	Request for Quotation
RFW	Request for Waiver
RHCP	Right Hand Circular Polarisation
RMS	Root Mean Square
ROM	Read Only Memory; Rough Order of Magnitude
RSS	Return Signal Simulator; Root Sum of Squares
R-S	Reed-Solomon encoding
RTU	Remote Terminal Unit
RX	Receive

SAR	Synthetic Aperture Radar
SARIn	SAR/Interferometry
SBT	Satellite Binary Time
S/C	Spacecraft
SCC	Stress Corrosion Cracking
SDBC	Spacecraft Reference Data Base Content
SDBD	Spacecraft Reference Data Base Delivery
SDE	Software Development Environment
SDR	System Design Review; Sensor Data Record
SEL	Single Event Latch-up
SEU	Single Event Upset
SFP	Single Failure Point
SI	International System of Units
SID	Structure ID
SIRAL	SAR/Interferometric Altimeter
SLR	Satellite Laser Ranging
SMF	Software Maintenance Facility
SMTP	Simple Mail Transfer Protocol
SOW	Statement of Work
SPF	Single Point Failure
SRD	System Requirement Document
SRDB	Spacecraft Reference Data Base
SSALTO	*Segment Sol Altimetrie et Orbitographie*
SSP	Sub Satellite Point
SSR	Solid State Recorder
STR	Star Tracker
STRP	Statistic Reporting
SUM	Software Users Manual, Satellite User Manual
SUMC	Satellite User Manual Content
SUMD	Satellite User Manual Delivery
SVF	Software Verification Facility
TAI	*Temps Atomique International*
TBC	To Be Confirmed
TBD	To Be Defined
TB/TV	Thermal Balance, Thermal Vacuum
TC	Telecommand
TCS	Thermal Control Subsystem
TCV	TeleCommand Verification
TEB	Tender Evaluation Board

TIM	Timing
TM	Telemetry
TPN	Telemetry Packet Number
TRP	Technology Research Programme
TTC	Telemetry, Telecommand and Control
TWT	Travelling Wave Tube
TX	Transmit
UCL	University College London
ULS	Upward Looking Sonar
UQPSK	Unsymmetrical Quadrature Phase Shift Keying
URD	User Requirements Document
URL	Universal Resource Location
USO	Ultra Stable Oscillator
UT1	Universal Time UT1
UTC	Coordinated Universal Time
UV	Ultra Violet
VCDU	Virtual Channel Data Unit
WBS	Work Breakdown Structure
WCRP	World Climate Research Program
WGS-84	World Geodetic System 1984
WOCE	World Ocean Circulation Experiment
WPD	Work Package Description